Pontificia Universidad Católica de Chile

Facultad de Ciencias Biológicas

Programa Doctorado en Ciencias Biológicas

Mención Biología Celular y Molecular

TESIS DOCTORAL

Mecanosensibilidad en linfocitos B:

rol en la dinámica y funcionalidad de lisosomas durante la sinapsis inmunológica

Por: Felipe Andrés Del Valle Batalla

Directora de Tesis: Dra. María Isabel Yuseff

Comisión de Tesis: Dra. Cristina Bertocchi

Dr. Hugo Olguin

Dr. Andrés Tittarelli

2023

‘‘πάντες ἄνθρωποι τοῦ εἰδέναι ὀρέγονται φύσει.’’

“Todos los hombres desean por naturaleza, el saber”

Aristóteles, Metafísica.

Dedicatoria y Agradecimientos

El trabajo que presento acá realmente no es solo el reflejo de los últimos 5 años, en que he buscado descubrir y explicar una parte infinitesimalmente pequeña del conocimiento que existe sobre los linfocitos B. Es una parte de mi vida, que con mucho amor y dedicación le presento a la comunidad.

Agradezco en primer lugar, a mis padres. Mamá, Papá. Ustedes me motivaron desde que tengo memoria a buscar las respuestas por mi cuenta, a tener hambre de conocimiento, a no quedarme con lo primero. Siempre desde el amor y la responsabilidad. Les doy las gracias por la paciencia y por darme la oportunidad de estudiar sin problemas una carrera que me permitió llenar el corazón de alegría y el cerebro, de más dudas.

A mi hermana, Lucía, a quién admiro. También te agradezco, por todo el apoyo y las risas. El amor incondicional y la increíble experiencia que es poder pasar de hablar de mecánica cuántica en las células hasta los chistes más malos. Se suma a esto el respeto gigante que te tengo como profesional y científica. Es un orgullo compartir esta parte de la vida contigo.

A mi esposa, Antonia. Anto, me conoces desde el principio del doctorado. Tomaste el camino de acompañar a una persona con una agenda extraña, con un futuro laboral impredecible y me siento increíblemente afortunado que pueda mirarte cuando explico lo que hago con una sonrisa. Gracias por estar ahí y seguir estando. Te amo a ti y a nuestros gatos.

A mis amigos, compañeros de laboratorio y familia de ciencias. A Martina, Juan Pablo, Isidora, Jheimmy, Romina, Fernanda, Oreste, Andrés y Pablo. Son los que más me han visto caer y estar en la cima. Gracias por estar codo a codo, en experimentos, análisis, risas, locuras y cafés. Sobre todo, cafés. Es increíble haber compartido con ustedes la felicidad de hacer ciencia. Sé que cada una y uno de ustedes logrará todos sus propósitos personales y académicos. A los que no estuvieron en gran parte de esta tesis, les agradezco también: Jonathan, Danitza, Juan José y Jorge. Jamás olvidaré todas las risas y consejos. Sobre todo, muchas gracias a Jorge Ibañez, quien me dio la temprana oportunidad para aprender junto a él.

Finalmente, quiero agradecer el incondicional apoyo y eterna disposición de mi tutora de tesis, la Dra. María Isabel Yuseff. "Profe", usted se ha convertido en un modelo a seguir que tengo para hacer ciencia y es para mí un orgullo haber sido formado en su laboratorio. Las enseñanzas que me deja son mucho más que el método científico. Termino esta etapa siendo mejor persona, más paciente y maduro. Gracias por todo.

INDEX

FIGURE INDEX

ABBREVIATIONS

Ab: Antibody

Ag: Antigen

Ag-Beads: Antigen coated beads

Ag-coverslips: Antigen coated coverslips

APC: Antigen presenting cell

BCR: B cell receptor

BCR-Ligand-: Negative B cell receptor ligand

BCR-Ligand+: Positive B cell receptor ligand

BM: Bone marrow

cSMAC: Central supramolecular activation complex

dSMAC: Distal supramolecular activation complex

GEF: Guanine exchanger factor

GC: Germinal center

IL- : Interleukin – (character)

IgX : Immunoglobulin (character)

IS: Immune synapse

ITAMs: Immunoreceptor tyrosine activation motifs

MHC-II: Major histocompatibility complex II

MZ: Marginal Zone

pSMAC: Peripheral supramolecular activation complex

SC: Subcapsular sinus

siATAT1: Small interference RNA against ATAT1

siCTL: Small interference RNA control

SLO: Secondary lymphoid organs

SMAC: Supramolecular activation complex

TIRFM: Total internal reflection fluorescence microscopy

TLO: Tertiary lymphoid organs

Th: T helper lymphocyte

TLR: Toll-like receptor

Tregs: T regulator lymphocyte

RESUMEN

El estudio de la mecanosensibilidad celular representa una rama de la biología que recientemente ha ganado mucho interés, reflejado en el premio Nobel de fisiología y medicina de 2021 otorgado a Ardem Patapoutian por el descubrimiento y caracterización del mecano-receptor PIEZO1. Sin embargo, poco se ha estudiado sobre cómo las señales mecánicas provenientes del entorno extracelular pueden dictar el funcionamiento del sistema inmune, y en particular, de los linfocitos B: las únicas células capaces de producir anticuerpos. En este trabajo se estudió cómo las propiedades físicas de la superficie presentadora de antígenos influyen en la capacidad de las células B para extraer antígenos inmovilizados y cómo estos procesos están conectados.

Se encontró que, al interactuar con sustratos más rígidos, las células B experimentan respuestas de estiramiento celular aumentadas y mayor acetilación de tubulina, específicamente en el centro de la sinapsis inmunológica. En sustratos rígidos, los lisosomas se ubican en el centro de la sinapsis, lo que reduce su movilidad en comparación con sustratos más blandos. Los lisosomas además muestran una preferencia por asociarse con tubulina acetilada en contextos de mayor rigidez. Mecanísticamente, esto implica la translocación de ATAT1, una enzima acetilasa de microtúbulos, del núcleo al citoplasma de las células B, actuando como señal mecánica durante la estimulación del BCR.

El silenciamiento de ATAT1 en células B disminuye su capacidad para estabilizar los lisosomas en la interfaz sináptica, lo que resulta en una extracción y presentación reducidas de antígenos inmovilizados a las células T. Estos hallazgos sugieren una vía que conecta la extracción de antígenos con señales mecánicas provenientes de células presentadoras de antígenos. En resumen, esta investigación aporta nuevos conocimientos y ofrece una base para comprender mejor las respuestas inmunológicas, con posibles implicaciones en terapias y trastornos inmunológicos.

ABSTRACT

This thesis aims to explain the intricate interplay between B cells, mechanosensing, and antigen extraction within the context of immune synapse formation. The capacity of B cells to extract immobilized antigens is influenced by the physical properties of the surface in which antigens are found. Despite its significance, the underlying mechanisms that connect B cell mechanosensing to antigen processing remain insufficiently understood.

The results demonstrate that B cells engaging with antigens on stiffer substrates exhibit a significant increase in spreading responses and upregulation in tubulin acetylation specifically at the immune synapse's center. B cells activated over stiffer substrates prompt a concentration of lysosomes, resulting in reduced lysosome mobility compared to interactions on softer substrates. Notably, lysosomes exhibit a preference for association with acetylated tubulin tracks under stiffer conditions. Mechanistically, this process involves the translocation of ATAT1, a microtubule acetylase, from the nucleus to the cytoplasm of B cells. As a novel finding, this translocation acts as a mechanoresponsive event during BCR stimulation. In support of these observations, B cells in which ATAT1 is silenced display an impaired ability to stabilize lysosomes at the synaptic interface, resulting in diminished extraction and presentation of immobilized antigens to T cells.

Collectively, these findings underscore the existence of a pathway that links antigen-extraction mechanisms to mechanical cues originating from antigen-presenting cells, a regulation governed by BCR-mediated mechanosensing. In conclusion, this thesis not only presents new knowledge about the intricate mechanisms underlying these processes but also paves the way for deeper insights into immunological responses, with potential implications for therapeutic interventions and immune-related disorders.

1. INTRODUCTION

1. B cell function and maturation

B cells are a type of lymphocyte that play a critical role in the adaptive immune response. They are the only cells capable of producing high-affinity antibodies (Ab) against new and recurrent infections (1). B cells originate from hematopoietic stem cells in the bone marrow, where they undergo a series of maturation steps (2). Upon activation, naïve B cells can exhibit two potential outcomes: firstly, they can generate and release Ab, which play a vital role in the humoral immune response and protect the body against pathogens via long term memory B cells or Ab producing plasma cells. Secondly, they can secrete cytokines, such as IL-1β, IL-6, IL-10, IL-12, and TGF-β, which regulate and coordinate the differentiation of T helper (Th) cells into Th1, Th17, or T regulatory (Tregs) cells, thereby modulating the overall immune response (3). Consequently, B cells portray a crucial role in mounting an effective immune response against pathogens, while perturbations in B cell homeostasis are associated with conditions such as autoimmunity, allergies, immunodeficiencies, and cancer (4–6).

Before their activation, the first step in B cell maturation is rearranging the genes that encode the B cell receptor (BCR), which occurs in the bone marrow (BM). This process, called V(D)J recombination, generates a diverse repertoire of BCRs capable of recognizing a wide range of antigens (2). Following gene rearrangement, developing B cells undergo selection stages to ensure they are functional and non-self-reactive (7). The first of these, called positive selection, occurs when B cells encounter self-antigens presented by bone marrow stromal cells (8).

B cells that recognize self-antigens with low affinity receive survival signals and continue to mature, while those that recognize self-antigens with high affinity undergo apoptosis. The second selection process, called negative selection, occurs when B cells encounter self-antigens outside the bone marrow (9). B cells reacting to self-antigens with high affinity are removed or go through receptor editing, a process in which the B cell receptor is modified to reduce its affinity for self-antigens (10).

2. Immune synapse formation

Once they have completed gene rearrangement and selection, B cells leave the bone marrow and migrate to secondary lymphoid organs (SLOs) (Fig.1). B cells may encounter antigens in two formats: Soluble immune-complexes or presented by antigen-presenting cells (APCs) such as follicular dendritic cells or subcapsular sinus macrophages (11).

Upon encountering an antigen in secondary lymphoid organs, B cells form a specialized structure known as the immune synapse (IS) termed synapse I, which, after internalization and processing of the Ag allows a second interaction (synapse II) between B cells and T-helper cells, termed B-T cooperation, that promotes the next steps of maturation of B cells (12). Following activation at the B cell-T cell boundary, B cells undergo robust proliferation in the outer B cell follicle. Within a few days after encountering antigens, some B cells differentiate into plasmablasts and migrate to locations outside the follicles, while others form clusters in the follicle center, giving rise to germinal centers.

Germinal centers are specialized microanatomical structures where B cells undergo somatic hypermutation in the variable regions of immunoglobulin genes that determine antigen-binding specificity. Mutated B cells are subsequently selected based on their affinity for antigens, leading to the gradual dominance of B cells with higher-affinity BCRs over those with lower-affinity BCRs.

Mature germinal centers exhibit a compartmentalized structure consisting of two zones: the dark zone, characterized by densely proliferating B cells, is considered the site where somatic hypermutation generates clonal variants with varying antigen affinities; the light zone, which is less dense and more diverse, contains not only B cells but also T follicular helper cells and follicular dendritic cells (FDCs). After this, some B cells will differentiate into plasma cells, which produce large amounts of antibodies to neutralize pathogens, while others may well become memory B cells, providing long-term protection against future infections. This thesis will focus on the first synapse between B cells and APCs.

The formation of an IS begins when the B cell receptor on the surface of the B cell recognizes and binds to the antigen presented by an APC (Fig. 2). The B cell receptor is comprised by a membrane-bound immunoglobulin and a non-covalently associated Igα/β heterodimer, which contains immunoreceptor tyrosine activation motifs (ITAMs) that are key for further steps in signaling and maturation (4) . This dynamic and highly regulated structure facilitates the recognition and processing of antigens by B cells. The IS is characterized by the recruitment and activation of several signaling molecules, developing a polarized signaling phenotype, which involves the localization and activation of polarity proteins such as Par3, Cdc42, and aPKC at the IS (12).

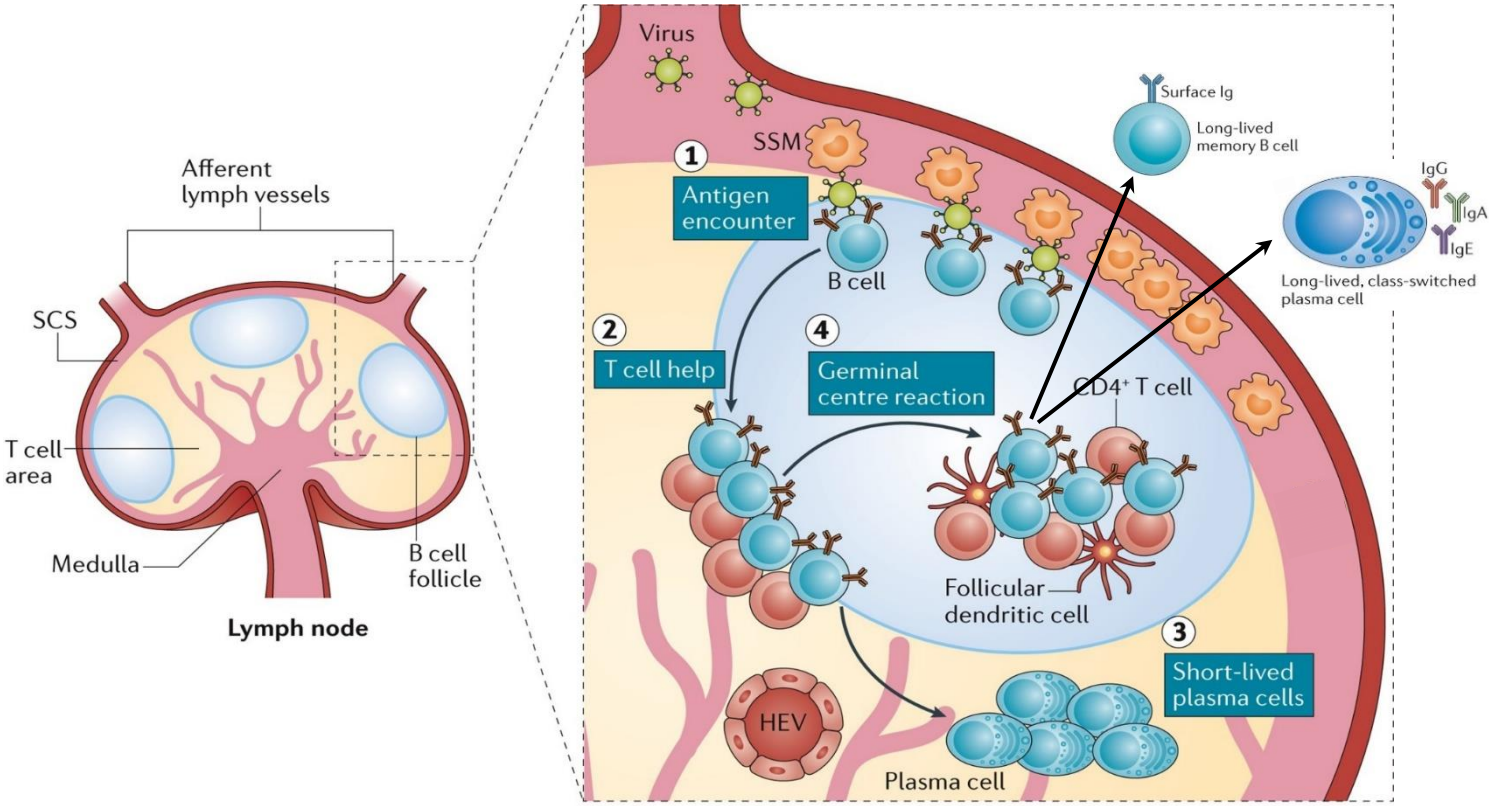

Figure 1: Acquisition of antigens by B cells and B-T cooperation at secondary lymph nodes.

Scheme of a lymph node, depicting the subcapsular sinus (SCS), T cell area and B cell follicle (left). Viruses and other immune-complexes are drained by afferent lymph (right) are captured and retained by SCS macrophages (SSMs), which shuttle the virus across their surface towards naive B cells in the underlying follicle (step 1). B cells can recognize soluble antigen from the lymph or obtain it from Follicular dendritic cells (FDC) situated in the GC. Upon recognizing the antigen, B cells extract and process it into peptides, eventually presenting it within an MHC-II complexes to T helper cells (step 2).

Interaction with cognate CD4+ T cells leads antigen-specific B cells either to differentiate into short-lived plasma cells secreting low-affinity antibodies (step 3) or to localize back to the follicle and enter a germinal center reaction (step 4). During germinal center reactions, antigen-specific B cells engage in interactions with T follicular helper cells and antigens (retained by follicular dendritic cells) and undergo an affinity maturation process, which ultimately results in the production of high-affinity neutralizing antibodies. HEV, high endothelial venule. Modified from Kuka et al, Nature reviews immunology, 2018.

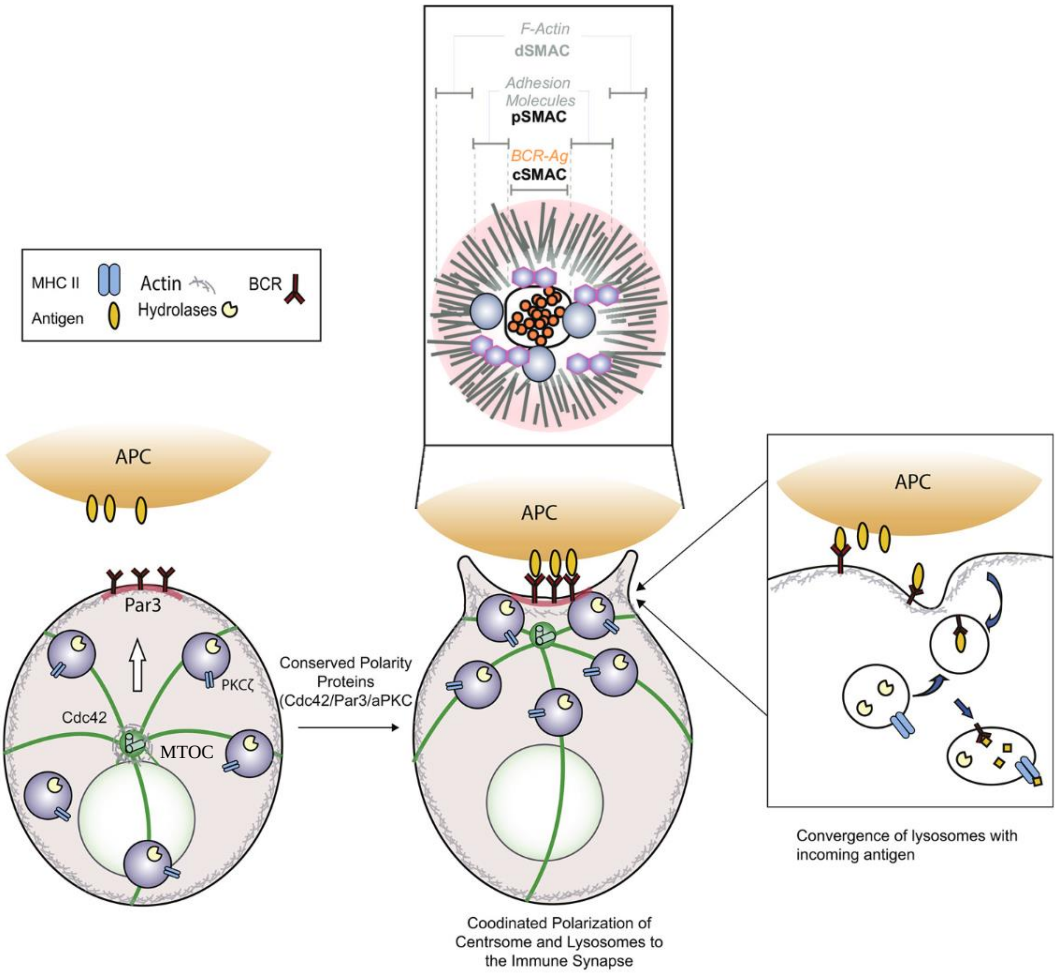

Figure 2: Immune synapse formation, organelles recruited and polarity phenotype

Polarity proteins such as Par3, Cdc42 and PKCz are recruited to the immune synapse upon BCR stimulation along with organelles that help with antigen extraction and internalization. Acting as a scaffold for signaling proteins and other organelles, the MTOC is repositioned to the contact site with the APC.

Lysosomes are found in a central cluster around the MTOC and fuse with the plasma membrane to release their acidic content and promote more efficient antigen extraction and internalization. Modified from Del Valle et al, Molecular immunology, 2018.

Upon encountering an antigen, the BCR undergoes clustering and conformational changes that facilitate antigen binding and downstream signaling, followed by the recruitment of coreceptor molecules such as CD19 and CD81 (13). One of the key molecules recruited to the synapse is the protein tyrosine kinase Syk, which is activated by phosphorylation upon binding to ITAMs of the BCR (14–16). Syk then recruits several downstream signaling molecules, including the adapter protein BLNK and the phospholipase C gamma (PLCγ). This initiates a signaling cascade that leads to the mobilization of intracellular calcium and the activation of protein kinase C (PKC) together with AKT and ERK kinases that are also phosphorylated. Importantly, these early signaling events lead to a rearrangement of the actin cytoskeleton, structured by various actin-binding proteins, including members of the WASP-Arp2/3 complex (17), Rho GTPases such as Rac1 and Cdc42 (18) and cofilin (19). This remodelling of actin interrupts the maintenance of the B cell resting state by loosening actin-based diffusion barriers (20).

After this rapid actin-dependent spatial reorganization, BCRs increase their mobility at the plasma membrane (fig.3) enabling the formation of BCR microclusters at the B cell-APC contact site leading to amplified BCR signaling (19,21). Spatially, BCR microclusters and co-receptors are distributed at the IS in multiple layers and domains characterized by three distinct supramolecular activation clusters (SMACs) (12,13,22); The central supramolecular activation cluster (cSMAC) contains the BCR and signaling molecules such as CD19 and CD81. The peripheral SMAC (pSMAC) comprises adhesion molecules such as the integrin LFA-1 and its ligand ICAM-1 at the APC, and the distal SMAC (dSMAC) which displays molecules that regulate signaling, such as CD45.

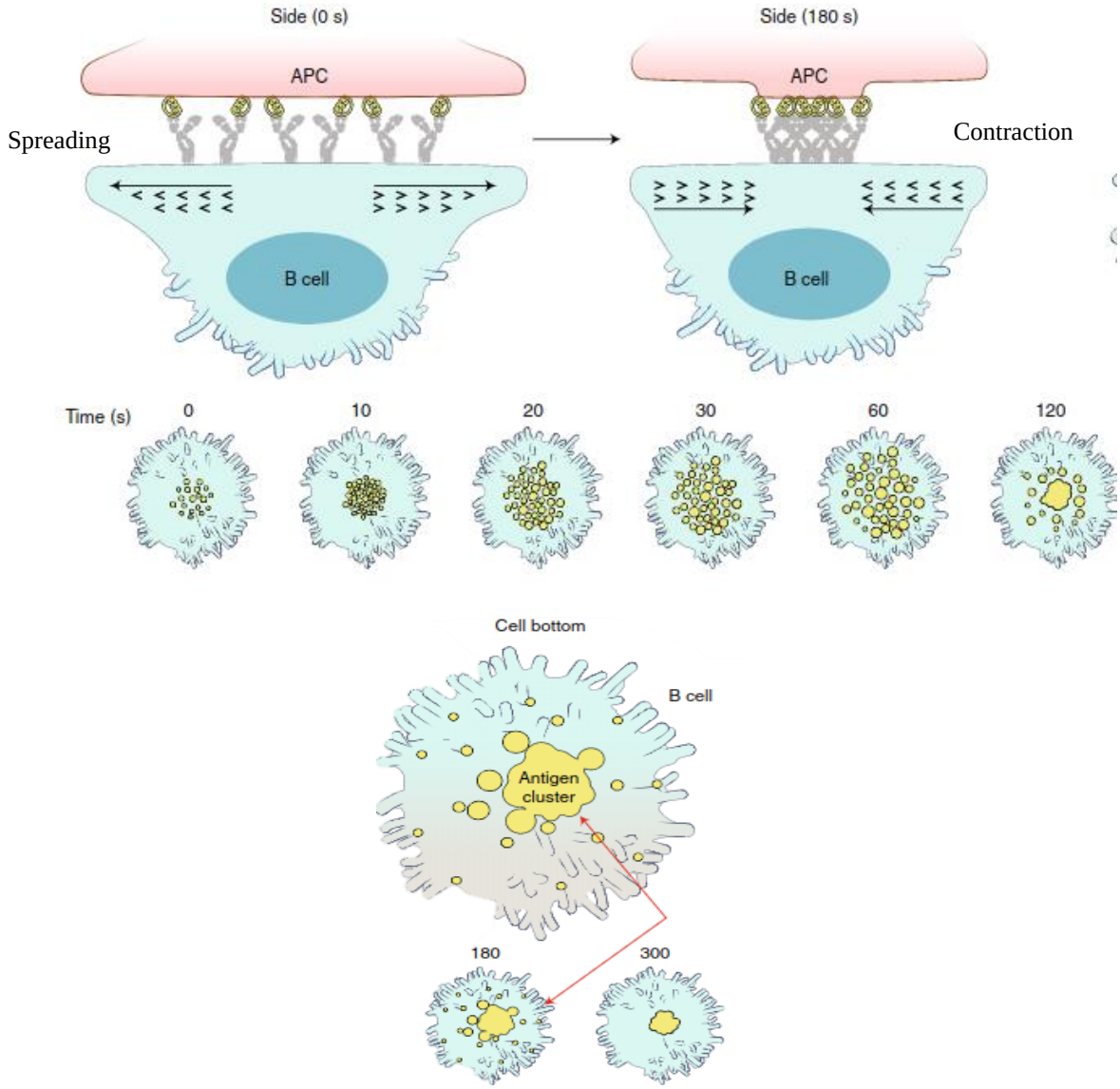

Figure 3: Actin cytoskeleton remodelling, lysosome and BCR clustering at the IS

After the spreading response upon BCR stimulation, B cells use contractility forces and remodel their actin cytoskeleton to generate retrograde actin flow allowing for the accumulation of BCR-Antigen complexes to the center of the IS. Lysosomes are also preferentially located in this region. Modified from Kwak, Nature Immunology, 2019.

After the spreading phase, B cells experience a contraction step, where all the membrane antigen-bound BCR complexes gather at the center of the IS. The accumulation of BCRs in the central region is facilitated by the microtubule-associated motor dynein, which is recruited to the IS through the involvement of the polarity protein Par3 (23). Concomitantly to actin remodelling, the centrosome, acting as the microtubule-organizing center (MTOC) is polarized to the IS (12,24,25). This relies on its successful detachment from the perinuclear region, promoted by the depolymerization of the surrounding actin cloud. Recent work has provided evidence that this is mediated by the correct functioning of the ubiquitin-proteasome system, specifically tuned by the ECM29 proteasome regulator subunit (26,27). After BCR stimulation, lysosomes are recruited to the IS to promote efficient antigen internalization and processing into multivesicular bodies (12).

3. Lysosomes and their role in antigen capture, processing and presentation

Lysosomes are commonly characterized as intracellular vesicles containing degradative acid hydrolases. Recent research suggests a diverse array of vesicles within this category, varying in subcellular localization, acidity, contents, and signaling functions. Additionally, hybrid lysosomal-related organelles (LROs) form through fusion and fission events, as well as "kiss and run" processes (28). Lysosomes exist as numerous vesicles in all mammalian cells, exhibiting sizes that can range from approximately 50 to 1000 nm. To date, nearly 200 distinct proteins have been identified on the lysosomal membrane, each serving different structural or signaling roles (29).

Endolysosomes in various immune cells exhibit distinct characteristics, primarily their role in intracellular processing of extracellular antigens for peptide-MHCII presentation, which is essential for activating B and T effector cells in the adaptive immune response. This process occurs in specialized lysosomal Ag processing compartments containing controlled proteolytic enzymes.

Although the Ag processing compartments exhibit a distinct lysosomal character due to their acidic and proteolytic environment, their primary function is to generate essential protein complexes for presentation, rather than solely degrading cargo. Recent studies indicate that BCR-mediated antigen processing initiates along the entire endosomal pathway. This includes the rapid fusion of internalized antigens with peripheral acidic compartments, concurrent with plasma membrane-derived MHCII (30).

Lysosomes are transported along the microtubule network towards the centrosome in a centripetal fashion by the motor protein dynein (31). In parallel, as the previous events take place, at the MTOC vicinity the GTP exchange factor H1 (GEF-H1) dissociates from microtubules and promotes the correct exocyst assembly at the synaptic membrane, enabling lysosome tethering and fusion with the plasma membrane at the synaptic interface (32) facilitating the degradation of the antigen bound to the APC into peptides. Lysosomal exocytosis, typically associated with LAMP-1, facilitates the release of vesicular contents, including hydrolases, into the extracellular space. This phenomenon can be identified by the exposure of the luminal epitope of LAMP-1 on the outer side of the plasma membrane, a location where this epitope is typically not found (33).

Lysosome exocytosis in B cells has also been shown to involve permeabilization of the PM to facilitate efficient Ag extraction in a mechanism that requires BCR signaling and non-muscle myosin II activity (34). in brief, the higher the affinity of antigen to the BCR, the more permeable the PM becomes and the higher the rates of lysosomal exocytosis are, measured by LIMP-2 at the cell surface. Antigens are then endocytosed, cleaved and mounted onto the Major-Histocompatibility-Complex-II (MHC-II) molecules (31) to establish the aforementioned B-T cooperation.

In vitro models to study antigen presentation and immune synapse formation in B cells consist in using antigen-coated beads or coverslips (35). Additionally, other models of activation such as, synthetic lipid bilayers or plasma membrane sheets can be used (36). Artificial planar lipid bilayers have demonstrated that during the spreading phase, B cells sense the affinity and avidity of the antigen (37). In contrast to synthetic bilayers supported by glass, the lipid bilayers in the PMSs (plasma membrane sheets) are only loosely and indirectly connected to the coverslip through transmembrane proteins and remnants of the extracellular matrix (38). The benefit of this arrangement is that the PMSs mimic the viscoelastic flexibility of the actual plasma membrane. Consequently, interacting cells can exert force on the PMSs, enabling the pinching off of vesicles for endocytosis, a phenomenon observed in live antigen-presenting cells (APCs). These different surfaces used to immobilize antigens for presentation to B cells have helped to uncover a role for physical properties in the activation of B cells.

B cells exhibit two distinct, yet compatible molecular pathways for extracting the antigen at the IS: (a) lysosome secretion, also referred to as the proteolytic pathway, which is preferred when the B cells recognize antigens associated to membrane with high stiffness, or (b) mechanical forces, which are activated under low membrane stiffness conditions (39). Additionally, extracellular cues, including Galectin-8, a glycan-binding protein located in the extracellular environment, responsible for controlling interactions between cells and matrix proteins, can enhance B cell arrest phases when these cells encounter antigens in living organisms. (40). Considering these external factors, studying how B cells interpret extracellular cues is crucial to have a better understanding of their activation in increasingly complex systems that resemble physiological conditions.

4. B cell mechanosensing

Mechanosensing is a fundamental cellular response that enables cells to perceive and react to physical environmental cues (41). This ability allows various cell types to adapt to tissue geometry and stiffness, which in turn can influence genetic reprogramming, cell adhesion, migration, and organelle function (42) (Fig. 4).

The mechanical properties of the extracellular environment play a critical role in regulating the behavior of B cells. For instance, substrate stiffness, shear stress, and compression forces can influence B-cell mechanosensing (43). B cells can sense the stiffness of the substrate through integrin-mediated adhesion to the extracellular matrix, which leads to cytoskeletal rearrangements and changes in gene expression. The adhesion of B cells to stiffer substrates enhances B-cell activation and proliferation, while softer substrates promote B cell differentiation and antibody production.

Surface receptors such as integrins are crucial in this process serving as the main link between the extracellular matrix and the cytoskeleton. Talin and vinculin, two cytoskeletal proteins, bind to integrins and help mediate this linkage (44). Actin and myosin form the basis of the contractile machinery and generates the forces required for cell movement and deformation in response to mechanical cues. Finally, the Rho family of GTPases regulate actin and myosin activity and help mediate the response to mechanical cues (45).

Together, these components work to orchestrate B cell mechanosensing and allow the appropriate response to mechanical cues such as substrate stiffness, shear stress, and compression forces.

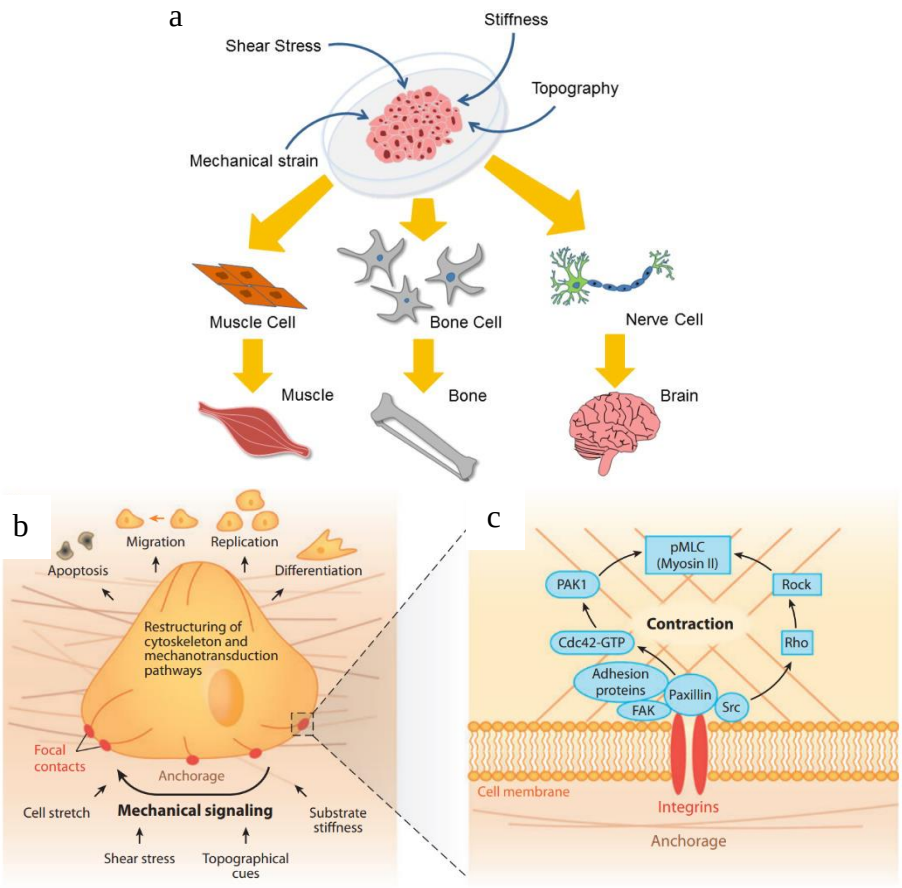

Figure 4: Mechanosensing directs tissue fate and orchestrates cell signaling

(a) Illustration depicting biomechanical control over stem cell actions. Mechanical cues, encompassing mechanical strain, substrate rigidity, shear stress, and surface topography, collectively influence stem cell characteristics.

(b) Various extracellular cues, such as substrate rigidity, cell elongation, shear stress, and surface topography regulate cellular signaling and functionality in the microenvironment. These factors cause shifts in mechanical forces across the ECM, cells, and cytoskeleton, leading to cellular perception of mechanical stimuli. Subsequently, these signals prompt biological responses, triggering reorganization of the cytoskeletal structure and intracellular signaling pathways (e.g., FAK and Src). These pathways are sensed through transmembrane adhesion receptors, specifically integrins, and mechanosensitive ion channels. As a result, mechanotransduction pathways activate to control gene expression, cell contractility, and diverse cellular processes, including apoptosis, migration, proliferation, differentiation, and growth.

(c) For instance, manipulating ECM mechanics or adjusting cytoskeletal tension generation via small Rho GTPases effectively governs stem cell differentiation (notably, 13 and 15). Moreover, cells dynamically remodel the ECM by secreting proteins and reconfiguring the cytoskeleton. This ECM remodeling consequently reshapes the array of cues that cells receive from their environment, creating a feedback loop of mechanical stimuli (as referenced by 213 and 226). Modified from Kshitiz et al, Integrative biology, 2012 and Kim et al, Annual Review of Biomedical Engineering, 2009.

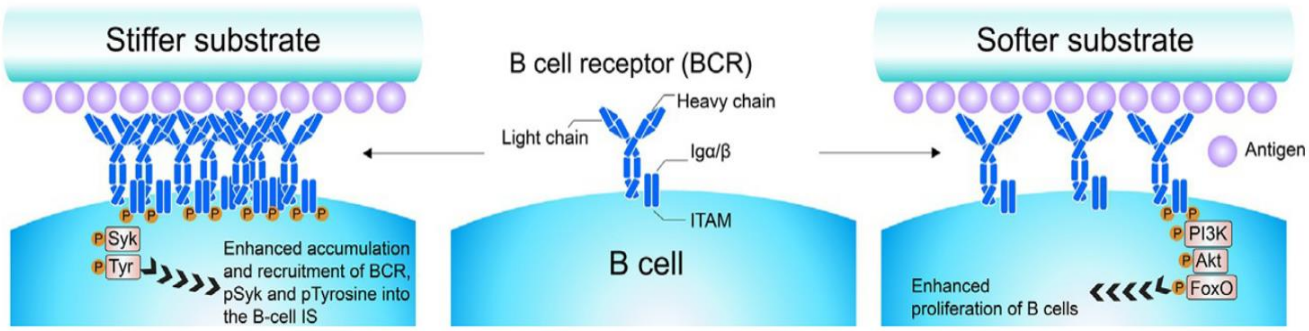

Figure 5: BCR-mediated mechanosensing

In B cells, mechanosensing responses through BCR signaling are sensitive to increasing substrate stiffness of antigen presenting surfaces. In softer substrates, less BCR-Ag complexes are formed than in stiffer substrates, where ITAM residues of BCR tails are phosphorylated in a higher extent thus promoting accumulation and activation of kinases such as SYK. These kinases are crucial for early B cell activation responses. Modified from Shaheen et al, Advances in immunology, 2019.

Importantly, the BCR itself acts as a mechanosensor (Fig. 5). It has been studied and compared with the T cell receptor (TCR), as they share similarities in activation and structure (46). To fulfill this function, the BCR employs a force testing mechanism with contracting movements known as "mechanical proofreading" (47), establishing a slip bond-like mechanical linkage (48) until it reaches the required force threshold for activation. This is known as affinity discrimination (20), and it is a key determinant for antigen extraction.

The APCs encountered by B cells can exhibit a range of stiffness dictated by their origin and composition (43). Stiffness, measured in Pascals (Pa) with the modulus E (elasticity), is one of the parameters that must be considered for mechanosensing. In physical terms, this measurement refers to the amount of force per unit length applied to a section of the plasma membrane area (49). Physiologically, antigens that can be obtained from the extracellular matrix (ECM) and APCs exhibit a range of stiffness from 0.012 kPa to 20 kPa, while soluble antigen particles have a stiffness of 100 Pa (43), highlighting the wide range of stiffnesses with which B cells can interact (Fig. 6).

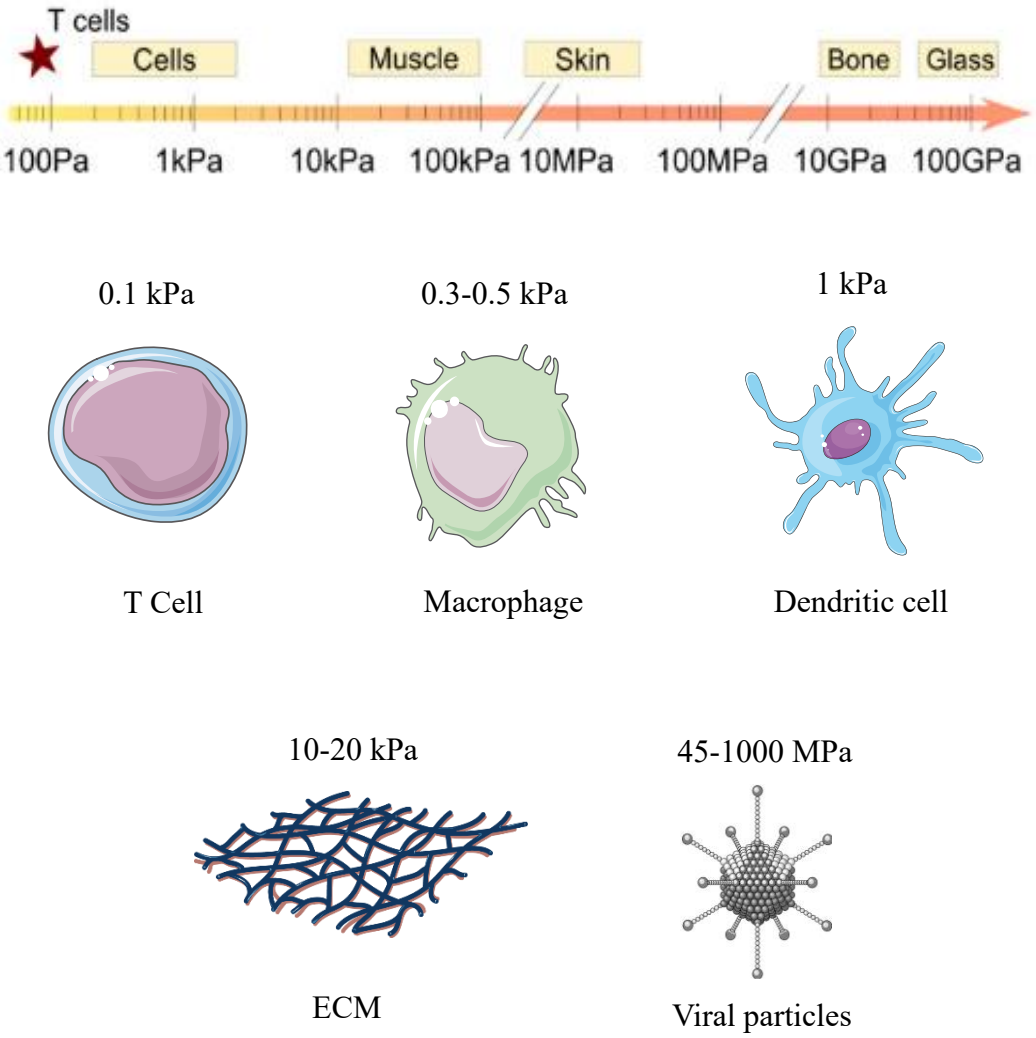

Figure 6: Ranges of stiffness associated with different antigen-presenting surfaces that can trigger BCR activation

A scale of stiffnesses present in different biological substrates, from cells to stiffer substrates such as glass. Scheme of different surfaces where tethered antigens can be found with their respective values of rigidity. All the previous are considered APCs. Modified from Bufi et al, Biophysical Journal, 2015.

Interestingly, it has been shown that APCs modify the stiffness of their membranes in inflammatory environments. In the case of macrophages, when exposed to β-adrenergic receptor agonists, their stiffness increases by 30%, as well as their migration time indicating less deformability capacity. This, by demonstrating that inflammatory signals promote actin polymerization in its branched form, through nucleating factors like the ARP2/3 complex (50).

Other signals produced in inflammatory sites such as INFγ increase the stiffness of dendritic cells and macrophages by enhancing signaling in cellular pathways that stimulate actin polymerization and the action of proteins including myosin IIA (51). Similarly, there is evidence showing that, on rigid surfaces, T lymphocytes which are actively involved in B cell maturation increase cytokine secretion (52).

In a relevant physiological context, it has been observed that tertiary lymphoid organs (TLOs) with functional germinal centers can originate at sites of chronic inflammation (53). These TLOs give origin to populations of immune cells, such as memory B cells, that encounter maturation conditions such as those described earlier, contributing in some cases to the exacerbation of rheumatoid diseases like arthritis (54). In this way, it can be asserted that both B cells and their APCs encounter different ranges of substrate stiffness that have effects on their interactions through the formation of immune synapses. Among the effects of different substrate stiffnesses, the impact on BCR microclustering and downstream signaling molecules, such as enhanced phosphorylation of Syk (pSyk) (55) under conditions of higher stiffness is noteworthy.

This behavior is also replicated in the signaling of protein kinases PKCβ and Focal Adhesion Kinase (FAK) (56), orchestrating changes in the cytoskeleton in response to mechanical substrate differences. Thus, B cell activation is affected by the variability of stiffness of the surface where antigen is encountered, their potential to become autoreactive (53) and

ultimately influencing their cellular lineage, as shown in activation conditions of higher stiffness that affect class switching, a process where a mature B cell changes the class of antibodies it produces while retaining the same antigen specificity. This allows B cells to produce different antibody classes (e.g., IgM to IgG),

Considering the evidence that mechanical stimuli regulate BCR activation, there is a knowledge gap when explaining the role of lysosomal function as a response to mechanical changes in the environment and how these translate into functional outcomes related to antigen capture and presentation. Interestingly, components of the cytoskeleton directly associated with the immunological synapse, such as microtubules, have been shown to be mechanosensitive (57), exhibiting higher affinity for dynein binding when subjected to contractile forces or deformation. Furthermore, posttranslational modifications, such as acetylation of microtubules (58) modify the affinity of motor protein binding to vesicles. As mentioned before, results from our laboratory (32) have shown that, under conditions of B cell activation using a high-stiffness substrate model (Ag-coupled glass coverslips), the MTOC and its closest microtubules increase their acetylation state.

In other cell types, the positioning and function of VAMP7+ lysosomes can respond to mechanical stimuli, regulating their association with kinesins and dyneins and, therefore, their subcellular distribution (59). Importantly, upon B cell activation, VAMP7 facilitates the fusion of lysosomes with the B cell's plasma membrane, releasing the lysosomal contents into the immune synapse (60). The previous could suggest a mechanosensory response of lysosome mobilization in a centripetal manner towards the MTOC at the IS.

Since vesicular trafficking in polarized cells such as neurons profoundly relies on microtubule availability to transport lysosomes to the synapse site (61,62), it becomes intriguing to evaluate how the distribution of these organelles may vary related to the mechanosensitive responses of microtubules. This leads to the question of whether mechanical stimuli from APCs with different rigidity can influence the positioning and functional dynamics of lysosomes in B lymphocytes, ultimately modulating their capacity for antigen extraction and presentation.

5. Tubulin acetylation: regulation and mechanosensing

Microtubules (MTs) are dynamic structures comprised of α/β-tubulin dimers that polymerize into tubular assemblies. They represent fundamental constituents of the cytoskeleton in most eukaryotic cells. Post-translational modifications (PTMs) play a pivotal role in modulating the properties and functions of MTs (63). Notably, acetylation of the lysine 40 residue (K40) on α-tubulin is a prominent PTM, catalyzed by the enzyme α-tubulin acetyltransferase (ATAT1). This acetylation event occurs within the lumen of the microtubules and substantially influences their stability and persistence.

Acetylation of microtubules stabilizes and promotes the formation of long-lived microtubule networks, that are fundamental for the polarization and migration of cells (64). Studies have shown that inhibition of tubulin acetylation leads to impaired cell migration and altered cytoskeletal dynamics.

However, the regulation of tubulin acetylation is not exclusively governed by ATAT1. Other enzymes, such as the deacetylases HDAC6 and SIRT2, are implicated in this process as well (Fig. 7). Particularly, the NAD-Independent deacetylase HDAC6 associates with microtubules and localizes with the microtubule motor complex containing p150(glued) to remove acetylated subunits of a-tubulin (65). Additionally, the NAD-Dependent enzyme SIRT2 cooperates with HDAC6 to promote tubulin deacetylation. These additional enzymatic players add a layer of complexity to the acetylation dynamics, impacting the behavior and functionality of MTs (66). The balance between these modifications and enzymatic regulations is essential for the precise organization of MTs, which, in turn, is critical for diverse cellular events such as intracellular transport, cell division, and maintenance of cellular morphology (63,66,67).

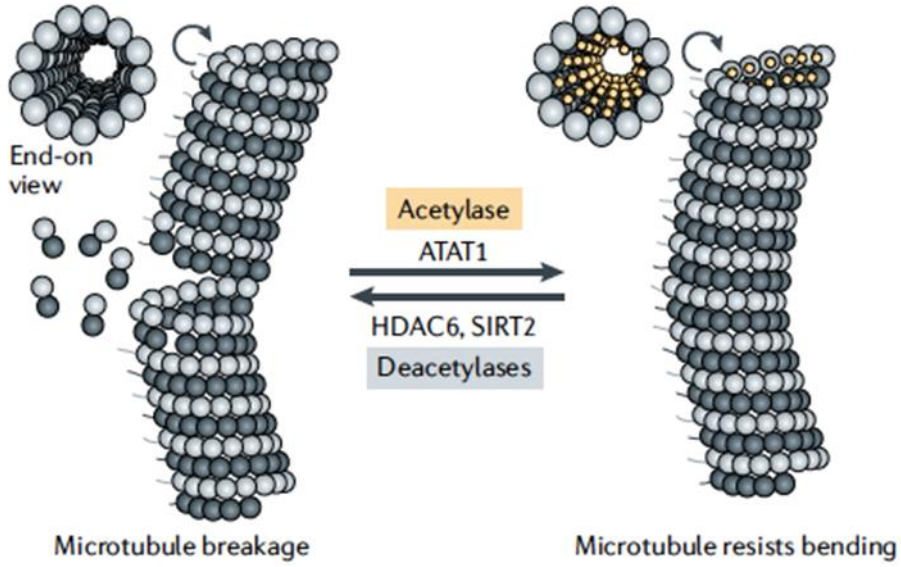

Figure 7: Control of tubulin acetylation

Tubulin acetylation is controlled by the acetylase ATAT1, which catalyzes the acetylation of lysine 40 in the interior of the microtubule lattice. HDAC6 and SIRT2 enzymes remove acetylation and balance the overall ratio of acetylated to non-acetylated tubulin. Modified from Janke et al, Nat. Rev. Molecular cell biology, 2020.

The regulation of tubulin acetylation is complex and involves various signaling pathways. For example, the Rho GTPase pathway regulates tubulin acetylation through the kinase ROCK by phosphorylating TPPP (tubulin polymerization-promoting protein 1), leading to the inhibition of the TPPP1-HDAC6 interaction and subsequent enhancement of HDAC6 activity. The net effect is a reduction in microtubule acetylation, which can impact various cellular processes related to microtubules and cytoskeletal dynamics (68). In addition to its effects on cell migration and vesicle/lysosome trafficking, tubulin acetylation has been implicated in various other cellular processes such as mitosis and cilia formation (65,69). For instance, acetylation of microtubules is required for the formation and maintenance of primary cilia, which are sensory organelles present on the surface of many cells. Tubulin acetylation has also been implicated in regulating the trafficking of vesicles and lysosomes: acetylated microtubules are preferentially used for vesicle and lysosome transport (Fig. 8) , as they provide a stable and efficient transport network (58,62,70).

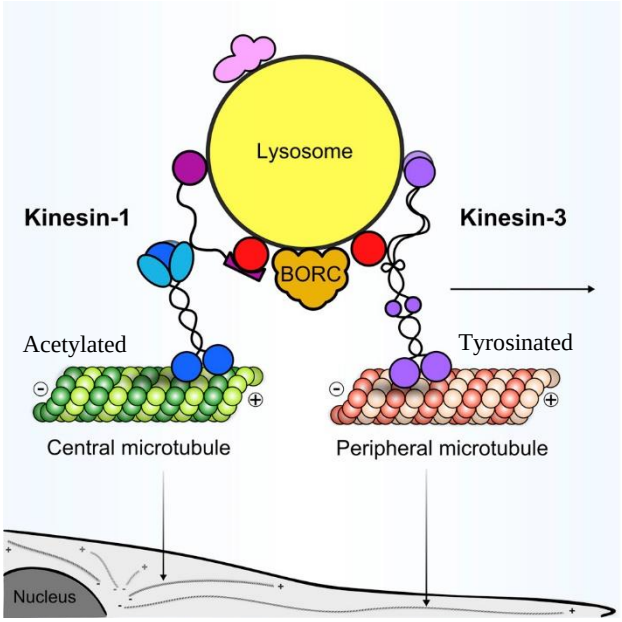

Figure 8: Lysosome accumulation at different microtubule tracks

In other cell models, lysosomes adapt their transport on microtubules with different PTM. Kinesin-1 and kinesin-3 are shown to mediate centrifugal lysosome transport in perinuclear and peripheral regions of the cytoplasm, respectively, through association with different microtubule tracks. Modified from Guardia et al, Cell Reports, 2016.

for astrocytes, a mechanism relying on talin and actomyosin plays a significant role in controlling microtubule acetylation (71). This is achieved by the recruitment of ATAT1 to focal adhesions. Interestingly, in B cells, Ag capture is increased on focal adhesions formed at the synaptic membrane (72). The process of microtubule acetylation finely tunes the mechanosensing of focal adhesions and impacts the translocation of Yes-associated protein (YAP) to the nucleus (73). This mechanism could be relevant in the context of B cell mechanosensing, as contractile forces related to focal adhesion formation are key for the stabilization of the immune synapse. Furthermore, microtubule acetylation, in a reciprocal manner, leads to the release of the guanine nucleotide exchange factor GEF-H1 from microtubules. Similarly, to what was previously illustrated for B cells. After GEF-H1 release, RhoA is activated, resulting in increased actomyosin contractility and traction forces (Fig. 9). These findings shed light on the essential interplay between microtubules and actin in mechanotransduction.

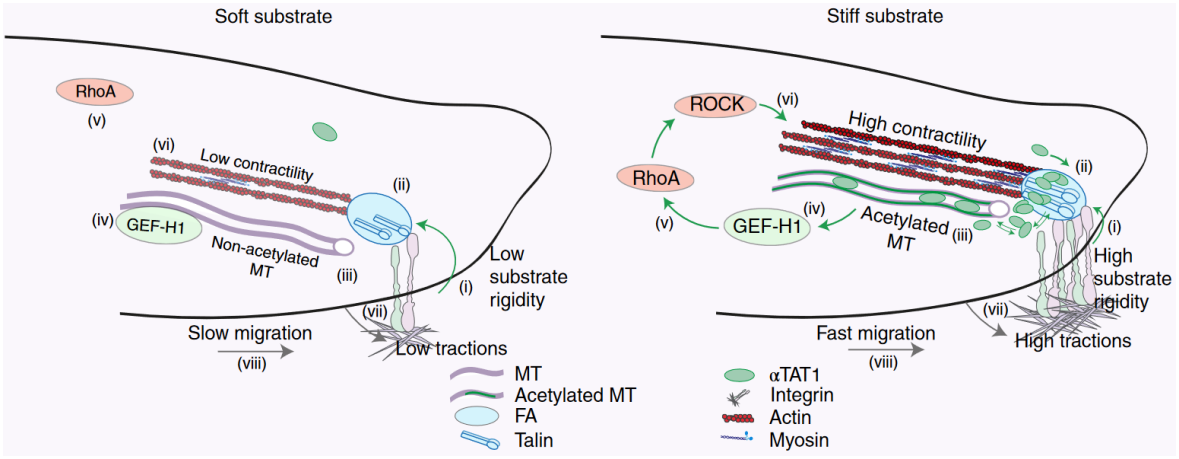

Figure 9: Interplay between microtubule acetylation, focal adhesions and GEF-H1

Cells perceiving a soft substrate (i) in conjunction with altered integrin-signaling (ii) manifest reduced microtubule acetylation (iii). This outcome leads to the attachment of GEF-H1 to MTs (iv) and consequently hampers the initiation of RhoA (v), thereby diminishing cellular contractility (vi). Under such circumstances, cells generate diminished adhesive forces (vii) and exhibit decelerated migratory behavior (viii). Conversely, on rigid substrates, the sensing of rigidity through integrin and talin interactions (i) facilitates the tension-responsive recruitment of αTAT1 to FAs (ii) and amplifies microtubule acetylation (iii).

The mechanism by which αTAT1 infiltrates the luminal space of microtubules remains enigmatic; however, it could be speculated that the recruitment of αTAT1 to FAs augments the localized cytosolic reservoir of the protein, enabling its subsequent penetration into microtubules through lattice imperfections or the exposed termini of microtubules in proximity to FAs.

The acetylation of microtubules triggers the liberation of GEF-H1 from MTs (iv), instigating the activation of the RhoA–ROCK–myosin IIA pathway (v) to foster actomyosin-generated contractile forces (vi), adhesive forces (vii), and cellular migration (viii). Modified from Seetharaman et al, Nature materials, 2022.

2. HYPOTHESIS AND OBJECTIVES

Considering the following evidence illustrated in the introduction section:

1) BCR signaling is regulated by substrate stiffness during antigen recognition
2) Microtubule acetylation is enhanced at the IS during activation on stiff substrates.
3) Mechanosensing pathways are coupled to actin dynamics and tubulin acetylation.
4) Tubulin acetylation modulates lysosome trafficking in several cell models.
5) Mechanical constrains modulate lysosome trafficking and exocytosis.

This work proposes the next hypothesis.

1. Hypothesis

"The distribution and positioning of lysosomes depend on the stiffness of the substrate where the immune synapse of B cells is formed, affecting their capacity to extract and present antigens."

2. Objectives

Specific Objective 1: To demonstrate that the positioning and dynamics of lysosomes at the immune synapse are modulated by the stiffness of an antigen-presenting interface.

Specific Objective 2: To determine whether the interaction of B lymphocytes with substrates of different stiffnesses regulates post-translational modifications of microtubules.

Specific Objective 3: To show that B cell activation and their capacity to capture and present antigens is regulated by the stiffness of the surface where antigens are encountered.

3. MATERIALS AND METHODS

All materials and methods related to this thesis are detailed in manuscripts 1 and 2.

In summary, manuscript 1 contains all the information sufficient to replicate the experiments performed: cell lines and cell culture, treatments with drugs, preparation of tunable-stiffness poly-acrylamide (PAA) gels, activation and immunofluorescence of B cells on PAA gels, immunoblotting, atomic force microscopy (AFM), primary and secondary antibodies, cell electroporation, silencing and transfection of constructs (expression vectors and siRNAs), antigen presentation assay and imaging configuration.

Manuscript 2, as a methodology report, focuses on image analysis of the B cell immune synapse in different experimental approaches. For this thesis, I have actively developed new image analysis workflows that are included in said manuscript. In particular, and related to manuscript 1, image analysis of 2D distribution of organelles is extensively explained in manuscript 2.

4. RESULTS

The following section contains 3 manuscripts, submitted for peer reviewing. These aim to cover the major results obtained from the specific aims 1 to 3. Considering the restrictions of the manuscript format, the results presented here will be discussed with more detail in the "Discussion" section. Before each manuscript, a summary or abstract on how it relates to each objective is stated.

Aims 1, 2 and 3 - Manuscript 1: Spatiotemporal control of microtubule acetylation by mechanical cues regulates lysosomes dynamics at the Immune synapse of B cells to promote antigen presentation

This is the main manuscript associated to aims 1, 2 and 3 as detailed in the following abstract:

The capacity of B cells to extract immobilized antigens through the formation of an immune synapse can be tuned by the mechanical properties of the surface where antigens are found. However, the underlying mechanisms that couple mechanosensing by B cells to the mode of antigen extraction remains poorly understood. We show here that B cells activated by BCR ligands associated to stiff substrates activate the focal adhesion kinase (pFAK), exhibit enhanced spreading responses, and upregulate the formation of actin foci at the synaptic membrane where antigen extraction occurs. Importantly, activation of B cells on stiff substrates also leads to enhanced tubulin acetylation at the center of immune synapse, where lysosomes preferentially localize and become less motile. We show that microtubule acetylation is coupled to the enrichment of the microtubule acetylase ATAT1 in the cytoplasm of B cells, which occurs in response to B cell activation on stiff substrates. Accordingly, B cells silenced for ATAT1 were unable to upregulate microtubule acetylation and focus their lysosomes at the synaptic interface, resulting in lower extraction and presentation of immobilized antigens to T cells. Overall, this work highlights how B cell mechano-responses coupled to changes in microtubule acetylation orchestrate the spatial-temporal distribution of lysosomes to promote antigen extraction and presentation.

Spatiotemporal control of microtubule acetylation by mechanical cues regulates lysosome dynamics at the immune synapse of B cells to promote antigen presentation

Felipe Del Valle Batalla [1], Isidora Riobó [1], Sara Hernández-Pérez [2,3,4], Pieta K Mattila [2,3,4], María Isabel Yuseff [1]*

[1] Laboratory of Immune Cell Biology, Department of Cellular and Molecular Biology, Pontificia Universidad Católica de Chile, Santiago, Chile

[2] Institute of Biomedicine, and MediCity Research Laboratories, University of Turku, Finland

[3] Turku Bioscience, University of Turku and Åbo Akademi University, Turku, Finland

[4] InFLAMES Research Flagship Center, University of Turku

* Corresponding author

Abstract

The capacity of B cells to extract immobilized antigens through the formation of an immune synapse can be tuned by the physical characteristics of the surface where antigens are encountered. However, the underlying mechanisms that couple mechanosensing by B cells to antigen extraction and processing remain poorly understood.

We show that B cells activated by antigens associated with stiffer substrates exhibit enhanced spreading responses and higher tubulin acetylation at the center of the immune synapse, where less motile lysosomes preferentially localize. This process is coupled to the translocation of the microtubule acetylase, ATAT1 to the cytoplasm of B cells, which occurs as a mechano-response during BCR stimulation. Accordingly, B cells silenced for ATAT1 are unable to stabilize lysosomes at the synaptic interface and display a lower capacity to extract and present immobilized antigens to T cells.

Overall, these findings highlight how BCR-dependent mechano-responses trigger microtubule network modifications to precisely orchestrate lysosome positioning to promote antigen extraction and presentation in B cell.

Introduction

Mechanosensing is a fundamental cellular process that enables cells to perceive and respond to physical environmental cues (Shaheen *et al.*, 2019). This ability allows cells to adapt to tissue geometry and stiffness (also referred to as rigidity, measured in kPa), which in turn can influence genetic reprogramming, cell adhesion, migration, and organelle function (Chen *et al.*, 2017). How mechanical cues associated with antigen recognition by B cells dictate their activation remains unresolved.

B lymphocytes interact with antigens that display diverse mechanical properties, ranging from less stiff immune complexes to highly rigid viral capsids (~100 MPa) (Shaheen *et al.*, 2019). Additionally, antigens can be recognized in a soluble form, considered to be in an environment with extremely low stiffness (0.01 kPa), or tethered to membranes of antigen-presenting cells (APC), which display stiffness values of approximately 0.1-0.5 kPa. B cells can also capture antigens associated with the extracellular matrix with rigidities of ~20 kPa (Ciechomska *et al.*, 2014). Moreover, the physical cues arising from membranes can change upon inflammatory conditions modifying the stiffness of the plasma membrane from the presenting cell (Bufi *et al.*, 2015; Kim *et al.*, 2019). Consequently, external physical cues emerge as an additional layer of information that B lymphocytes can sense and thereby impact their responses. Both B and T cells display membrane-bound immunoglobulin receptors, the BCR and T cell receptor (TCR), which possess the ability to sense the mechanical properties of their ligands (Zhu, Chen and Ju, 2019; Zhu *et al.*, 2019). Additionally, B cells activated on stiff surfaces exhibit augmented BCR clustering and downstream signaling (Wan *et al.*, 2013), leading to enhanced spreading responses and actin cytoskeletal rearrangements. Whether this has an impact on the capacity of B cells to extract and present antigens acquired at the immune synapse (IS) is unknown.

The mode of antigen extraction used by B cells depends on the physical properties of the substrate in which antigens are presented: antigens on flexible, softer surfaces are internalized into clathrin-coated pits by Myosin IIA-mediated pulling forces that trigger invagination of antigen-containing membranes (Hoogeboom and Tolar, 2016). During this process, the complexes formed by the B cell receptor and the antigen (BCR-Ag complexes) are internalized at regions enriched in actin foci (Roper *et al.*, 2019). On the other hand, antigens presented on more rigid surfaces require the local fusion of lysosomes at the synaptic membrane that release proteases and acidify the synaptic cleft, facilitating antigen extraction (Yuseff *et al.*, 2011). This proteolytic mode of antigen extraction relies on the precise positioning, tethering and secretion of lysosomes at the IS. Various factors regulate this process, including local actin cytoskeleton remodeling by proteasome activity (Ibañez-Vega, Del Valle Batalla, *et al.*, 2019), proper assembly of the exocyst complex (Sáez *et al.*, 2019), and the v-Snare VAMP7 to the plasma membrane (Obino *et al.*, 2017).

Both cytotoxic T lymphocytes and NK cells enhance perforin-mediated killing at the immune synapse when interacting with antigens associated to stiff substrates (Basu *et al.*, 2016), suggesting that lytic granule secretion is coupled to mechanosensing (Friedman *et al.*, 2021). However, the underlying mechanisms behind this process remain largely unknown. In other cell types, the rigidity of the environment regulates membrane trafficking through integrin and RhoA-dependent remodeling the actin cytoskeleton to promote docking of secretory vesicles (Lachowski *et al.*, 2022; Phuyal *et al.*, 2022). Notably, the role of mechanosensing in directing lysosome positioning has not been previously characterized and B cells emerge as a valuable model to study this process.

Vesicles move along microtubules (MT) by their association to motor proteins, which can be regulated by post-translational modifications (PTM) of the microtubule network (Pu *et al.*, 2016). In neurons, acetylation of microtubules fine-tunes the trafficking of lysosomes by modifying their affinity with kinesins (Morelli *et al.*, 2018). In T cells, upregulation of tubulin

acetylation by inhibition of the deacetylase HDAC6 leads to impaired transport of lytic granules to the synaptic membrane interacting with the target cell, highlighting how microtubule PTM, in particular acetylation, impact vesicle transport (Núñez-Andrade *et al.*, 2016).

Thus, mechano-responses can regulate MT posttranslational modifications of the microtubule network, resulting in differential trafficking of vesicles to sites where membrane exchange or exocytosis is required. Interestingly, acetylation of tubulin can also be coupled to mechano-responses and is significantly enhanced at the leading edge of migrating fibroblasts when traction forces occur, promoting the release of GEF-H1 and acto-myosin contractibility (Seetharaman *et al.*, 2022). In this work, we show that activation of B cells on stiffer substrates enhances the concentration of lysosomes at the center of the IS and ultimately improves their capacity to extract and present antigens. This process relies on increasing levels of tubulin acetylation in response to stiffness and the translocation of the acetylase ATAT1 from the nucleus to the cytoplasm. Elucidating how physical properties of antigen presenting surfaces are coupled to B cell effector responses that drive antigen extraction, processing and presentation, may provide valuable therapeutic tools for vaccine

design, drug delivery or treatment of autoimmune diseases.

Materials and methods

Cell lines, culture, and treatments

In this study we used the mouse A20 lymphoma cell line, an FcγR-defective B cell line with the phenotype of quiescent mature B-cells, and the LMR7.5 Lack T-cell hybridoma, which recognizes I-Ad-LACK156–173 complexes. Both cell lines were cultured as previously described (Sáez *et al.*, 2019) in CLICK medium (RPMI 1640, 10% fetal bovine serum, 100U/mL penicillin-streptomycin, 0.1% β-mercaptoethanol, and 2% sodium pyruvate).

For the induction of tubulin acetylation, cells were treated with 1 uM of the microtubule-stabilizing agent SAHA (TOCRIS bioscience Cat. No. 149647-78-9) for 30 minutes before activation or experimental procedures. For time-lapse acquisitions, lysosomes were labeled with Lysotracker DN-99 Red (Thermo Scientific, L7528).

Preparation of tunable-stiffness poly-acrylamide (PAA) gels

For preparing the tunable-stiffness PAA gels, two sets of coverslips are used: a silanized-bottom coverslip where the PAA gel is immobilized and an smaller impermeabilized coverslip on top to create a "sandwich" to allow for the polymerization of the PAA gel (Charrier *et al.*, 2020). Bottom coverslips are activated with a 2% 3-Aminopropyltrimethoxysilane (3-APTMS) (Sigma Aldrich 13822-56-5) in 96% ethanol solution for 5 minutes and washed with 70% ethanol. The top coverslips are siliconized or waterproofed with Rain-X. The coverslips are then washed with ultrapure water, dried well, and moved to the next stage.

The following reagents were used to prepare the PAA gels: 2% bis solution (Bio-Rad #1610142), 40% acrylamide (Bio-Rad #1610140), 10% APS in 10 mM HEPES solution, and TEMED (Table 1).

kPa	40% Acrylamide (µL)	2%Bis-Acrylamide (µL)	10% APS (µL)	TEMED (µL)	1X PBS (µL)	Total (uL)
0.3	75	30	10	1	895	1011
13	233,75	125	6,25	1,8	883	1249

Table 1: preparation of poly-acrylamide gels of 0.3 (soft) and 13 (stiff) kPa.

To prepare the gel, 9 uL of the gel solution was pipetted onto the center of the bottom coverslip. Then, it was well covered with the smaller cover and pressed gently until the mix spread outwards. After 30 minutes of polymerization, they were covered with aluminum foil. Next, 1X PBS was added to carefully remove the top

cover. The gel can be stored in fresh 1X PBS at 4°C overnight and used within 48 hours.

For conjugation with ligands a solution of 0.5 mg/mL SULFO-SANPAH (Pierce, Thermo-Scientific #A35395)-in HEPES buffer 10 mM was prepared. PBS was removed from the gels and immediately coated with SULFO-SANPAH at room temperature (RT). Gels were exposed to 365 nm UV light (Maestrogen UV illuminator MLB-16) for 10 minutes and washed with 1X PBS thrice. Finally, a BCR^+ ligand (F(ab')2 goat anti-mouse IgG) (Jackson ImmunoResearch, 115-006-146) was added to coat the gels at a concentration of 0.13 mg/mL and incubated overnight. This was followed by 3 washes with 1X PBS and immediately used for experiments or stored at 4°C protected from light for no more than 48 hr.

Activation and immunofluorescence of B cells on PAA gels

80 µL of B cells (1.0 x 10^6 cells/mL in CLICK medium with 5% FBS) were seeded onto an antigen ($BCR\ ligand^+$)-coated gel for different time points in a cell incubator at 37 °C / 5% CO_2. After each time point, the media was carefully aspirated off each PAA gel, and 100 µL of cold 1X PBS was added to stop the activation. PBS was removed, and each PAA gel was fixed with 50 µL of 3% PFA for 10 min at RT. PAA gels were washed three times with 1X PBS. The 1X PBS was removed, and 50 µL of blocking buffer (2% BSA and 0.3 M glycine in 1X PBS) was added to each coverslip.

Primary antibodies were diluted in permeabilization buffer (0.2% BSA and 0.05% saponin in 1X PBS) and incubated by adding 40 uL over the gels in a humid chamber at 4 °C overnight. The plate was sealed to avoid evaporation of the antigen solution. Gels were washed three times with permeabilization buffer. Secondary antibodies or dyes were diluted in permeabilization buffer, using 40 µL per PAA gel, and incubated for 1h at RT in dark and humid chambers. The PAA gels were washed twice with permeabilization buffer and once with 1X PBS. The PBS solution was removed from the coverslips. 8 µL of mounting reagent was added to a microscope slide. The PAA gels were mounted onto the slide with the cell side facing down. The slides were allowed to dry for 30 min at 37 °C or RT overnight protected from light.

Immunoblot

Cells were lysed with 40 uL of RIPA buffer, then supernatants of samples were collected and loaded onto gels and transferred onto polyvinylidene fluoride membrane (Trans-Blot Semi-Dry Transfer Cell; Bio-Rad). Membranes were blocked in 2%BSA/TBS + 0.05% Tween-20 and incubated overnight at 4 °C with primary antibodies, followed by 60-min incubation with secondary antibodies. Western blots were developed with Westar Supernova substrate (Cyanagen, Cat. No. XLS3,0100), and chemiluminescence was detected using the iBright imager (Thermo Fischer).

Atomic Force Microscopy (AFM)

The elastic modulus of the PAA gels (Young's modulus, E) was assessed using a JPK NanoWizard with a CellHesion module mounted on a Carl Zeiss confocal microscope, Zeiss LSM510 (AFM; JPK instruments), and silicon nitride cantilevers (spring constant: 1 Nm^{-1}, spherical 10 µm diameter tip; Novascan Technologies). The cantilever spring constant and deflection sensitivity were calibrated in fluid using the thermal noise method (Hutter and Bechhoefer, 1993).

Force measurements were then conducted at different locations (0.5 mm apart in x and y coordinates) within the region of interest. In each location, nine indentations distributed in a 3×3 point grid (30 µm × 30 µm) were performed. The elastic modulus for each force curve was calculated using JPK data processing software (JPK DP version 4.2), assuming a Hertz impact model.

Antibodies & dyes

For primary antibodies, we used Rat anti-mouse LAMP1 (BD Bioscience, #553792), Rabbit anti-mouse Acetyl-Tubulin (Lys40, D20G3) (Cell Signaling, #5335), Rabbit anti-mouse αTubulin (Abcam, #ab6160), Goat anti-mouse IgM Fab2 (Jackson ImmunoResearch), Rabbit anti mouse GEF-H1 (Abcam #ab155785), Rabbit anti-mouse

ATAT1 (Thermo Scientific, #PA5-114922), Rabbit anti-mouse YAP (D8H1X) XP (Cell Signaling #14074). For secondary antibodies: Donkey anti-rabbit IgG-Alexa 488/546/647 (Jackson Immunoresearch, 711-546-152), Donkey anti-rat IgG-Alexa 488/546/647 (Jackson Immunoresearch, 712-166-153), Phalloidin Rhodamine (Thermo Scientific, R415), Lysotracker-red DND 99 (Thermo Scientific, L7528) and Hoescht (Abcam, #ab228551).

Cell transfection and electroporation

The Nucleofector R T16 (Lonza, Gaithersburg, MD) was used to electroporate 4 x 10^6 A20 B cells with 3 µg of plasmid DNA using the LC-013 program. After transfection, cells were cultured for 18 ±2 hrs at 37 °C and 5% CO_2 before functional analysis. For ATAT1 silencing, cells were electroporated with 100 nM of siRNA (sc-108799-SH, Santa-cruz technology) or 100 nM of siRNA control (sc-37007, Santa-cruz technology).

Antigen presentation assay

Antigen presentation assays were performed as previously described on (Yuseff *et al.*, 2011) with modifications. Briefly, B cells were incubated with either Lack-BCR-Ligand or BCR Ligand coated PAA gels and PAA gels with different concentrations of Lack peptide (Lack 156-173) for 1h. Then cells were washed with PBS and incubated with Lack-specific LMR 24 7.5 T Cells in a 1:1 ratio for 4h in a cell incubator at 37ºC and 5% CO_2. Supernatants were collected, and interleukin-2 cytokine production was measured using BD optiEA Mouse IL-2 ELISA set following the manufacturer's instructions (BD Biosciences, Cat no. 555148).

Cell imaging and image analysis

For widefield imaging, all Z-stack images were obtained with 0.3 µm between slices. Images were acquired in a widefield - epifluorescence microscope (Nikon Ti Eclipse) with an X60/1.25NA objective. For confocal acquisition, images were obtained in a Zeiss LSM880 Confocal with Airyscan detection microscope using a 63X/1.4NA oil immersion lens, with a Z-stack configuration of 0.2 µm. All acquisition for experiment replicates were performed with same mW/cm^2 intensity for all illumination or equivalent exposition. The images were processed using Zeiss Black Zen software for Airyscan processing and analyzed with Fiji (ImageJ) (Schindelin *et al.*, 2012).

For image analysis, when quantifying cell spreading a threshold mask (Otsu) was used in parallel with manual segmentation in instances when automatic algorithms were not able to resolve general actin structures. For actin foci quantification, we performed analysis of particles that were found inside previously detected spreading cells. In this case, we took into account workflows that have been tested for determining such structures (Roper *et al.*, 2019). Other spot segmentation and cluster determination algorithms such as lysosome number at the IS, their size and pFAK counts were carried out with conservative algorithms of background subtraction and the same strategies of segmentation for each experimental set. Lysosome dynamics was studied with Fiji's TrackMate plugin using the LAP tracker in settings recommended for its unsupervised setting, always testing for quality score of tracks. Overlap coefficients for colocalization and fluorescence ratios were determined by quantification of the mean fluorescence intensity of segmented structures and for single planes of acquisition at the IS plane (closest z plane to the PAA gel surface). Specifically, for colocalization analysis only single planes and individual regions of interest of the single cells were used and quantified with JaCoP plugin for Fiji software following its instructions. Determination of the localization index for differential accumulation of lysosomes in central or peripheral zones of the cell, was adapted from previous publications (Ibañez-Vega, Fuentes, *et al.*, 2019). Nuclear and cytoplasmic accumulation was calculated following "Cyt/Nuc" plugin for Fiji (Grune *et al.*, 2018).

Statistical analysis

All data presented was tested for normality and homoscedasticity; accordingly, appropriate statistical tests were applied considering those factors. Data in plots and graphs are expressed as fold change of mean or mean ± SEM. If corresponding, experiments were analyzed by Student's t-test or Mann–Whitney test following Gaussian and non-Gaussian distribution, respectively after performing d'Agostino and Pearson omnibus normality test. In cases where two conditions are shown, two-way ANOVA with Sidak's multiple comparison test was performed if data followed normal distribution. When datasets followed non-gaussian distributions, Kruskal-Wallis tests were applied with Dunn's a-posteriori multi comparison examination. Experiments were carried out with a sum of $n \geq 30$ cells pooled from N = 3 biological replicates. Error bars shown are mean ± SEM. Statistical analysis was performed with Prism (GraphPad Software) and RStudio. For significance, p-values were calculated using different tests mentioned above and are illustrated in each figure.

Results and discussion

The rigidity of the antigen-associated surface regulates actin remodeling and spreading responses in B cells

Upon interaction with surface-tethered antigens, B cells trigger a spreading response to maximize antigen encounter and uptake (Yuseff *et al.*, 2013). In this study, we aimed to characterize cytoskeletal and vesicular responses coupled to mechanical cues sensed through the B cell receptor (BCR).

To examine this, B cells were activated for different time points on surfaces containing BCR ligands associated to polyacrylamide (PAA) gels of 0.3 and 13 kPa, hereafter referred to as "soft" and "stiff" gels, respectively (Fig. EV1 A). The stiffness of the gels was measured by atomic force microscopy (AFM) and values obtained for soft and stiff gels (Fig. EV1 B) were consistent with previous reports. These mimicked physiological and pathological mechanical cues (Wan *et al.*, 2013). BCR^+ ligands (F(ab')2 anti-IgG) coupled to both soft and stiff gels exhibited similar binding densities (Fig. EV1 C) and formed a continuous and homogeneous layer under all conditions.

B cells seeded onto gels of different stiffness, without BCR^+ ligands exhibited no alterations in cell spreading after 5 and 30 minutes (Fig. EV1 D-E). Conversely, B cells seeded over stiff substrates containing BCR^+ ligands, exhibited higher spreading responses after 15 and 30 minutes, in comparison with those seeded over softer substrates (Fig. 1A). Mean areas of B cells activated under stiff conditions were in the range of 300-400 μm^2 compared to an average of 100 μm^2 for B cells activated under soft conditions (Fig 1B). These observations suggest that B cells possess a BCR-dependent mechanosensing pathway that controls cell spreading in response to substrate rigidity coupled to BCR^+ ligands.

Additionally, when examining actin cytoskeleton organization in these cells, we observed an increase in the number of actin foci and lamellipodia area (Figs. 1C, D insets A and B respectively) in B cells activated on stiffer substrates compared to soft substrates. Actin foci structures are considered a hallmark of B cell mechano-responses by engaging on inward forces that facilitate antigen concentration and internalization (Roper *et al.*, 2019). These results support the idea that mechanical cues shape the activation of B cells, impacting the structure of the actin cytoskeleton, prompting us to explore how B cells couple the detection of physical cues during B cell activation to regulate antigen extraction and presentation.

B cells elict mechanotransduction pathways during activation as a response to variable substrate stiffness.

Until now, our results reveal that during activation, B cells remodel their actin cytoskeleton in response to external physical cues. The focal adhesion kinase (FAK) is involved in mechanosensitive responses, promoting the assembly of focal adhesions to support membrane protrusion during cell spreading and migration (Li *et al.*, 2023).

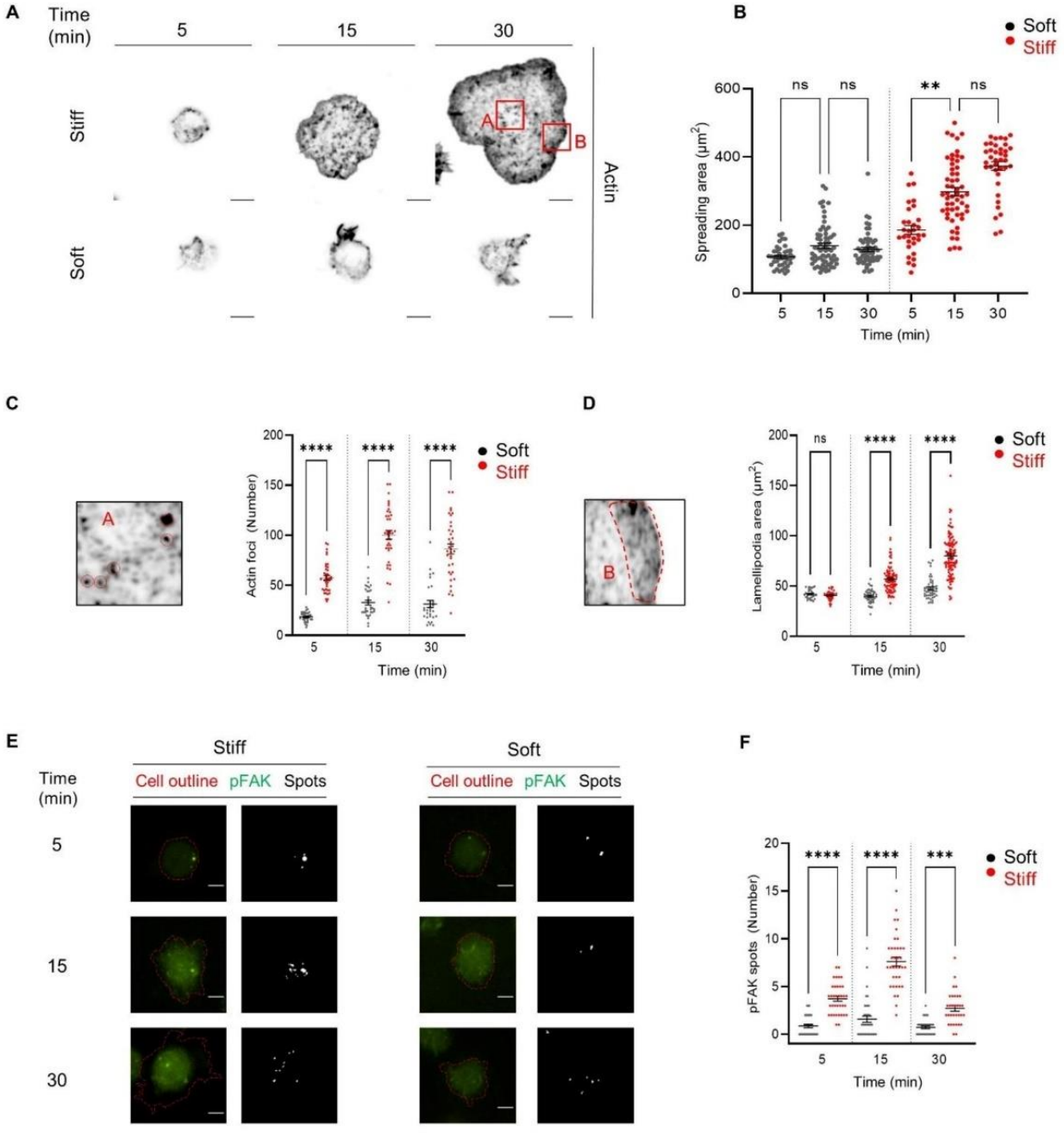

Fig 1. Substrate stiffness regulates cytoskeleton B cell responses upon BCR stimulation

(A) B cells seeded over stiff or soft substrates at different activation times. Actin (phalloidin) is shown in black. Red squares delimit actin foci and lamelipodia areas. (B) Quantification of cell spreading areas in (A) defined by actin staining. (C-D) Quantification of actin foci detected and lamellipodia area, respectively, for cells seeded on soft or stiff substrates. (E) Representative images of fixed cells interacting with soft or stiff substrates. pFAK in green and cell outline in red. pFAK is shown as segmented particles (spots). (F) count of pFAK spots from experiments performed in (E). For every experiment, shown data considers n ≥ 30 cells pooled from N = 3 biological replicates. All scale bars are 5 µm. P values illustrated with asterisks are ** < 0.01,*** <0.001, **** <0.0001. Error bars are mean ± SEM.

In B cells the phosphorylated active form of FAK (pFAK) is increased upon BCR stimulation in an integrin-independent manner known as "inside-out activation" through phosphorylation by PKCb (Shaheen *et al.*, 2017). Thus, we next sought to determine whether in our model B cells could promote FAK activation in response to substrate stiffness. Our results show that B cells activated on stiff surfaces display increased levels of pFAK, observed as individual spots, in comparison to soft conditions (Fig. 1E-F). pFAK spot number was upregulated at earlier time points of activation (5 to 15 minutes) and decreased after 30 minutes. We confirmed this by immunoblot analysis, which showed higher levels of pFAK in cell lysates from B cells activated on stiffer substrates at similar time points (Fig. EV1 F-G).

We also verified that B cells induce stronger BCR signaling responses when activated on stiffer versus soft substrates (Fig. EV2 A). After 15 minutes of activation, B cells activated on stiffer substrates displayed higher levels of phospho-AKT and phospho-ERK in comparison to softer conditions (Fig. EV2 B). Taken together, these findings show that BCR-mediated mechanosensing in response to substrate stiffness activates FAK and BCR downstream signaling molecules that regulate spreading and signaling pathways associated with enhanced states of B cell activation.

Tubulin acetylation is enhanced in a mechanosensory-dependent manner during B cell activation.

During engagement with antigens, B cells remodel their actin cytoskeleton according to external mechanical cues; however, the impact of such cues on lysosome trafficking have not been addressed.

Intracellular trafficking relies on the organization of the MT network, where posttranslational modifications of tubulin can tune MT dynamics and impact vesicle transport (Janke and Magiera, 2020). Acetylation of alpha tubulin at lysine 40 stabilizes the tubulin lattice, and ensures the accumulation of KIF proteins that promote synaptic vesicle transport in neurons (Bhuwania, Castro-Castro and Linder, 2014). Whether physical cues regulate lysosome transport at the IS by modifying microtubule PTMs remained to be determined.

Thus, we evaluated if acetylation of the MT network is regulated by physical cues sensed by B cells through their BCR. To this end, B cells were seeded over soft or stiff BCR^{+}-coupled PAA gels for 5, 15 and 30 minutes and stained for alpha tubulin (a-Tub) and acetylated tubulin (Ac-Tub). Noticeably, B cells activated on stiff surfaces displayed higher levels of Ac-Tub compared to cells activated on soft substrates (Fig. 2A), which was measured as the total amount of Ac-tubulin and as a ratio to total tubulin levels (Fig. 2 B-C). This result was confirmed by western blot analysis of cell lysates from B cells activated on stiff and soft substrates, showing that levels of Ac-Tub were upregulated in a time and stiffness-dependent manner (Fig EV2 C-D).

Mechano-responses to substrate rigidity by other cell types during adhesion and migration involve microtubule acetylation, which promotes the release of GEF-H1 from microtubules into the cytoplasm to increase Rho activity and cell contractility (Seetharaman *et al.*, 2022). We therefore evaluated levels and localization the Rho-GTPase GEF-H1, which is released from acetylated microtubules upon BCR activation and interacts with the exocyst complex to promote lysosome tethering at the immune synapse (Sáez *et al.*, 2019). By using the experimental setup described above, we observed that B cells interacting with stiffer substrates, displayed higher levels of GEF-H1 at the IS plane compared to cells activated on soft substrates (Fig EV2 E-F).

This result is consistent with B cells progressively enhancing the acetylation of tubulin at the IS interface upon stimulation with stiffer substrates. Collectively, these findings strongly support the notion that B cells respond to physical cues by enhancing tubulin acetylation, which is coupled to the accumulation of GEF-H1 at the synaptic membrane, previously shown to promote lysosome tethering at this interface. Therefore, we next evaluated whether this mechanosensory response directly impacts lysosome trafficking at the immune synapse of B cells.

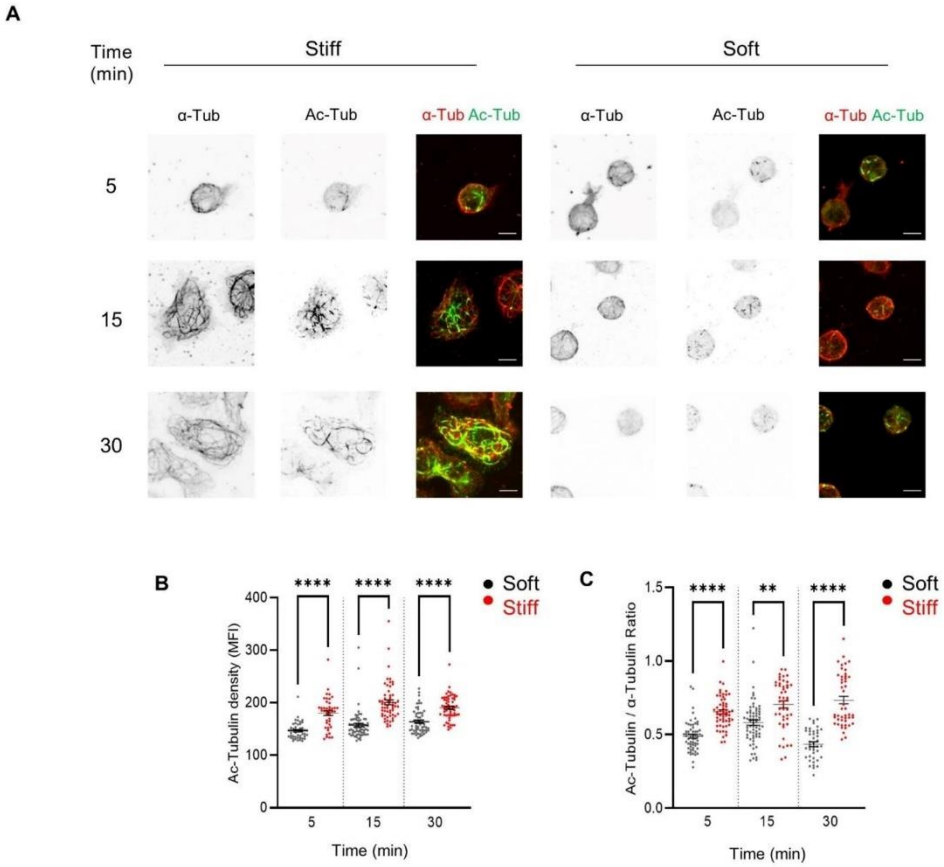

Fig. 2 Tubulin acetylation is enhanced during B cell activation on stiff substrates

(A) Representative images of fixed cells interacting with soft or stiff substrates at different time points. Alpha tubulin (a-Tub) and Acetylated tubulin (Ac-Tub) are shown separately and in composite format. (B) Ac-Tub density calculations based on MFI at the IS for images in (A). (C) Ac-Tubulin / α-Tubulin MFI ratios quantified at the IS for images in (A). For every experiment, shown data considers n ≥ 30 cells pooled from N = 3 biological replicates. All scale bars are 5 µm. P values illustrated with asterisks are ** < 0.01,*** <0.001, **** <0.0001. Error bars are mean ± SEM.

Substrate stiffness regulates lysosome positioning and dynamics at the IS

To assess whether physical cues sensed by B cells have an impact on lysosome positioning, we seeded B cells on soft or stiff substrates containing BCR^+ ligands, at increasing time points. Cells were then stained for the lysosomal marker LAMP1 together with an actin cytoskeleton marker and imaged using confocal microscopy (Fig. 3 A). The distribution of $LAMP1^+$ vesicles within the intracellular space, defined by cortical actin cytoskeleton was analyzed as follows: the total cell area was divided into 3 equally concentric sections (Fig. EV2 G) and raw intensity fluorescence values obtained were normalized with respect to the spreading area of each cell. As shown in Fig. 3B, cells stimulated on stiffer surfaces exhibited increased accumulation of lysosomes at the IS, after 15 minutes of activation compared to softer substrates. The amount of lysosomes at the center of the IS was comparable in both conditions after 30 minutes of activation. However, the number of lysosomes at the cell periphery was lower in B cells interacting with stiffer substrates, suggesting that the lysosomes are retained more efficiently at the center of the synaptic plane in B cells activated by antigens associated to surfaces with higher stiffness (Fig. 3B).

Additionally, we quantified the number of LAMP1$^+$ particles at the z-plane juxtaposed to the antigen-coated surface (Fig. EV3 A.) in B cells interacting with soft or stiff substrates. As expected, we found more lysosomes at the IS plane of B cells activated onto stiffer substrates. Interestingly, B cells on stiffer gels and increasing activation times displayed smaller lysosomes compared to cells activated on softer substrates (Fig. EV3 B). This could result from changes in lysosome fusion or fission dynamics mediated by mechanical cues that remain to be explored.

We next evaluated how substrate stiffness sensed by B cells regulates lysosome dynamics. To this end, B cells labelled with lysotracker were seeded on soft or stiff substrates coupled to BCR$^+$ ligands and live imaging was performed for 5-20 minutes, an adequate time frame to evaluate lysosome dynamics during the IS formation (Sáez *et al.*, 2019).

Consistent with results obtained in fixed cells, lysosomes preferentially accumulated to the cell center upon activation under stiff conditions, whereas in softer substrates, lysosomes were evenly dispersed (Fig. EV3 C). When comparing the mean speed and displacement of lysosomes at the IS, we found that in B cells seeded onto stiffer substrates, both values were lower compared to softer ones (Fig. EV3 D), confirming that lysosome motility and positioning are tuned by extracellular physical cues during B cell activation.

To investigate the functional impact of MT acetylation on lysosome dynamics, we first evaluated the co-localization of Ac-tubulin and LAMP1 in B cells activated on soft and stiff substrates.

Our results show that in B cells seeded on stiff substrates, lysosomes progressively increased their co-localization with Ac-tubulin (Fig.3 C-D), whereas this parameter remained constant in B cells activated on soft substrates. These results suggest that there is a functional link between microtubule acetylation during B cell mechano-responses and the positioning of lysosomes at the IS during B cell activation.

To precisely determine the effect of tubulin acetylation on lysosome dynamics in B cells, we evaluated the effect of SAHA, which enhances tubulin acetylation by inhibiting the deacetylase enzyme HDAC6 (Sáez *et al.*, 2019).

Treatment with 1 µM SAHA for 30 min effectively led to enhanced MT acetylation in B cells (Fig. EV3 E-F). Next, lysotracker-labeled cells were activated on stiff and soft surfaces for 15 min and imaged during 5 min at 3 seconds per frame. Lysosome trajectories from each cell under different conditions were acquired and analyzed. Our results show that lysosomes from SAHA-treated B cells activated on soft substrates, exhibited lower mean speed and were more confined compared to lysosomes from non-treated cells, displaying parameters similar to lysosomes from B cells activated on stiff substrates (Fig. 3 E-F).

Interestingly, treatment with SAHA had no significant effect on lysosome dynamics in B cells activated on stiff substrates, indicating that the level of tubulin acetylation or the threshold of tubulin acetylation to control lysosome mobility and positioning achieved by B cells activated on stiff substrates cannot be further increased by inhibiting HDAC6. Overall, this result suggests that tubulin acetylation directly impacts lysosome dynamics in B cells as a response to extracellular stiffness.

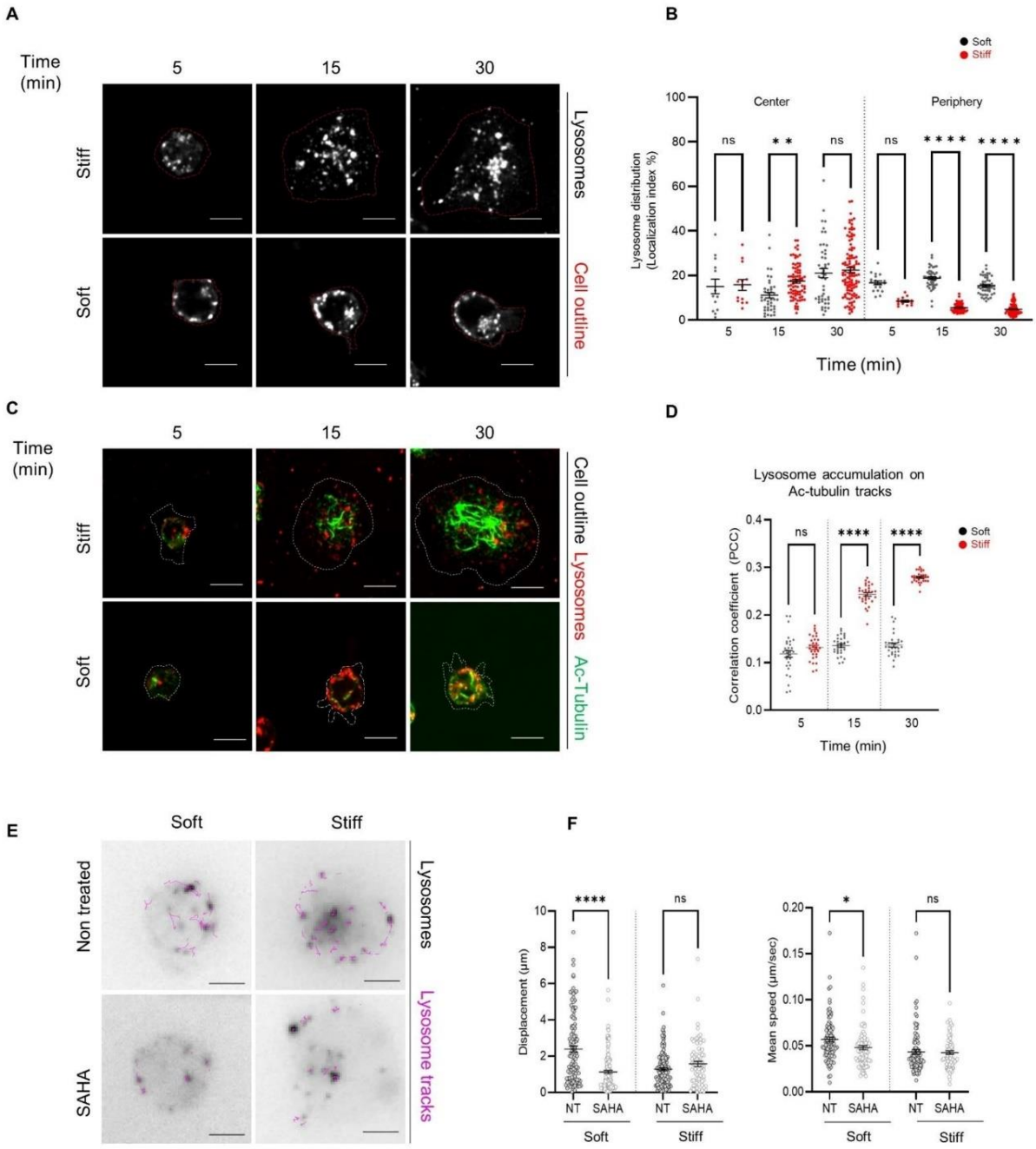

Fig.3: Lysosome localization and dynamics is dependent on tubulin acetylation as a mechano-response of B cell activation

(A) Representative confocal images of B cells seeded over stiff or soft substrates at different activation times. Cells were fixed and stained for LAMP1 and actin. The cell border (red outline) was defined by actin phalloidin staining. (B) Quantification of lysosome (LAMP1) accumulation either in the IS center or periphery for cells in (A). The localization index reflects the MFI in a defined area with respect to the total staining in the cell. (C) Representative images of cells seeded in stiff or soft substrates at different time points. The cell outline was determined with actin staining (white dashed lines). The synaptic plane is shown with stainings for lysosomes (red) and acetylated microtubules in green. (D) Quantification of lysosome accumulation on acetylated microtubule tracks from cells shown in (C). Pearson's correlation coefficient (PCC) is shown for the overlap of both stainings. (E) Representative timelapse images showing the tracking lysosomes stained with lysotracker (black) on either stiff or soft conditions control (Non treated – NT) cells and SAHA-treated cells. Lysosome tracks were followed for 5 minutes after seeding the cells for 15 minutes. Tracks in magenta represent the 15-20 minutes time frames of interaction with the different substrates. (F) Displacement and mean speed of lysosome tracks for experiments detailed in (E). Data shown considers n ≥ 30 cells pooled from N = 3 biological replicates. All scale bars are 5 µm. P values illustrated with asterisks are * < 0.05, ** < 0.01, **** <0.0001. Error bars are mean ± SEM.

ATAT1 translocates to the Cytoplasm of B cells activated on stiff surfaces.

The impact of tubulin acetylation on lysosome dynamics prompted us to investigate the regulatory mechanisms controlling this process. Tubulin acetylation is catalyzed by the acetylase enzyme ATAT1, which shuttles between the nucleus and cytoplasm (Deb Roy *et al.*, 2022). Given that tubulin acetylation is enhanced in response to substrate stiffness during B cell activation, we explored whether this was coupled to changes in the localization of ATAT1.

To address this, we seeded B cells in soft and stiff substrates and evaluated the localization of ATAT1 by confocal microscopy after different time points of activation. With increasing times of activation and stiffness, ATAT1 shifts from the nucleus to the cytoplasm, which was not observed in B cells activated on soft substrates (Fig. 4 A,B), supporting our hypothesis that BCR-mediated mechanosensing enhances tubulin acetylation by promoting the cytoplasmic localization of ATAT1.

To confirm that B cells elicit mechanosensory responses, we show that YES-associated-protein (YAP), a canonical marker of mechanosensing, is translocated to the nucleus in B cells activated on substrates with higher stiffness (Fig. 4 C,D) similarly to other cell types (Panciera *et al.*, 2017).

ATAT1 regulates lysosome dynamics.

To formally show that ATAT1-dependent microtubule acetylation regulates lysosome dynamics in B cells, we silenced ATAT1 expression using siRNA and evaluated its effect over tubulin acetylation and lysosome distribution. B cells activated on soft substrates display low levels of tubulin acetylation, therefore, to confirm the effect of ATAT1 silencing, we quantified microtubule acetylation in B cells activated on stiff substrates.

To this end, B cells were seeded over stiff plastic plates coupled to BCR^+ or BCR^- ligands for 30 minutes. As expected, levels of acetylated tubulin were dramatically reduced upon silencing of ATAT1 compared to control conditions (Fig. EV4 A-B), confirming the role of ATAT1 in this process. Interestingly, cells activated over stiff substrates exhibited greater tubulin acetylation when in contact with BCR^+ ligands than in control (BCR^-) conditions (Fig. EV4 A-B). These findings provide additional evidence for the mechanosensing role of the BCR and its link to tubulin acetylation upon its stimulation.

We next analyzed the effect of silencing ATAT1 in lysosome positioning in B cells forming an immune synapse. To this end, B cells were labeled for LAMP1 in ATAT1-silenced and control cells (Fig. 4E, Fig. EV4 C-D) and their distribution at the IS upon stimulation in stiff or soft substrates was analyzed. As anticipated, ATAT1-silenced B cells activated onto stiff substrates, were unable to accumulate lysosomes at the center of the IS after 30 minutes (Fig. 4F).

Silencing ATAT1 also decreased pFAK levels (Fig. EV4 E-F) at later time points of activation in B cells seeded onto stiff substrates, suggesting an interplay between the formation of nascent focal adhesions and tubulin acetylation, which could involve the release of actin-factors such as GEF-H1 from the lumen of microtubules when they are acetylated.

Overall, these results reveal that impairing tubulin acetylation by silencing ATAT1 results in defective lysosome positioning at the IS. Hence, ATAT1-mediated tubulin acetylation emerges as a mechanism for controlling the correct positioning and dynamics of lysosomes at the IS in response to external physical cues.

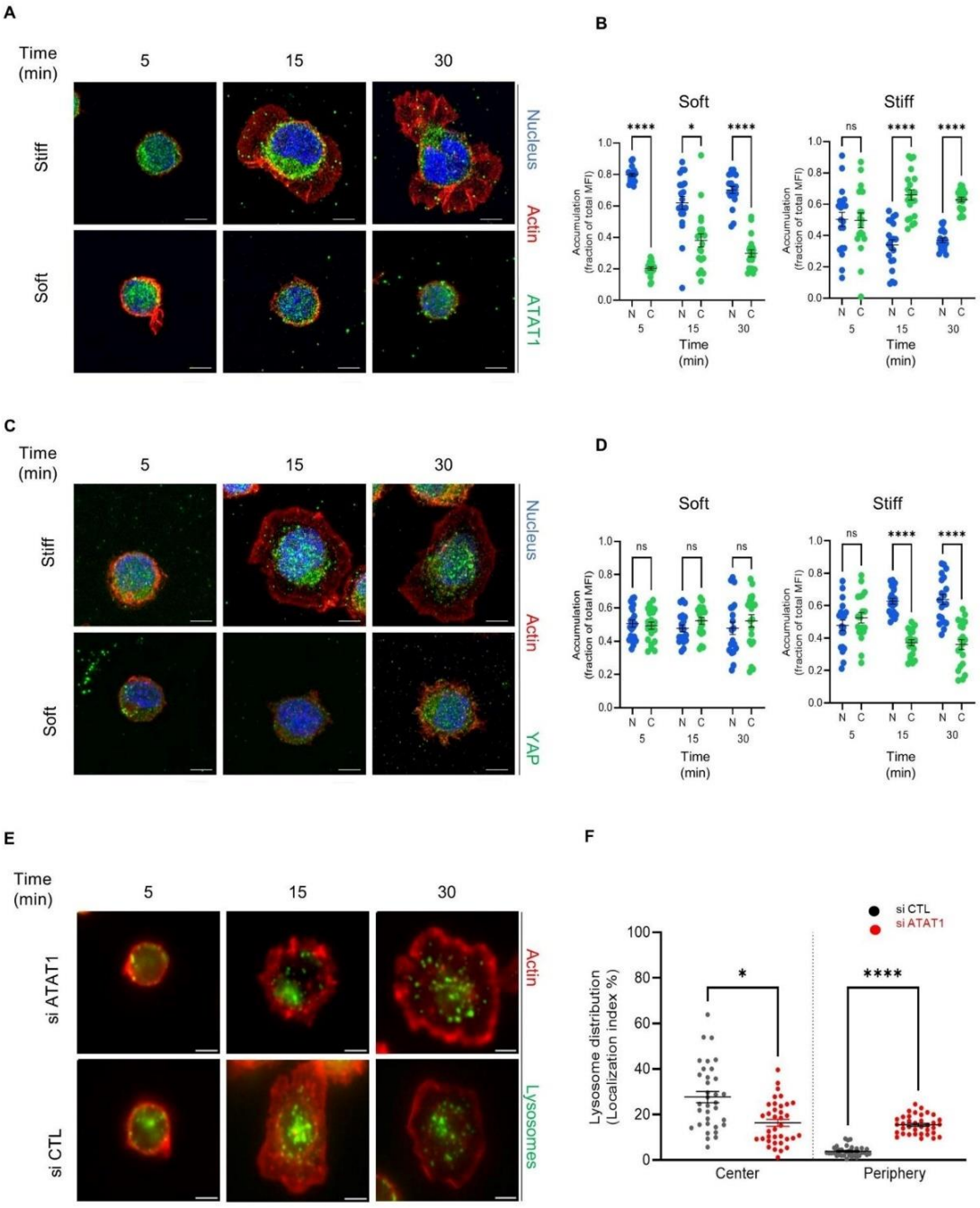

Fig.4: ATAT1 Localizes to the cytoplasm of B cells activated on stiff surfaces to promote microtubule acetylation and regulate lysosome dynamics

(A) and (C) Representative images of fixed B cells seeded over stiff or soft substrates at different activation times. ATAT1 is shown in green, the nucleus in blue (Hoechst), and the actin cytoskeleton in red, stained with Phalloidin. (B) Quantification of nuclear or cytoplasmic accumulation of ATAT1 from cells in (A). The distribution index (y-axis) indicates the fraction of ATAT1 fluorescence in the nucleus (N) or the cytoplasm (C, excluding the nucleus) with respect to the total area of the cell. (C) YAP is shown in green, the nucleus in blue (Hoechst), and the actin cytoskeleton in red, stained with Phalloidin. (D) Quantification of YAP nuclear or cytoplasmic accumulation from cells in (C) using the distribution index. (E) Images of B cells seeded over stiff substrates at different activation times in non-silenced (si CTL) or silenced for ATAT1 (si ATAT1). Lysosomes (LAMP1) are shown in green and the actin cytoskeleton in red, stained with Phalloidin. (F) Quantification of LAMP1 accumulation at the IS center or periphery from cell in (E). Shown data considers n ≥ 30 cells pooled from N = 3 biological replicates. All scale bars are 5 µm. P values illustrated with asterisks are: * < 0.05, **** <0.0001. Error bars are mean ± SEM.

The efficiency of antigen presentation by B cells depends on substrate stiffness and ATAT1.

A fundamental step in B cell activation is the capacity of these cells to present external antigens as peptides loaded on MHC class II molecules to T cells. This enables B-T cooperation and provides survival signals for B cells to sustain their maturation and differentiation into plasma cells (Akkaya, Kwak and Pierce, 2020). To directly evaluate whether physical cues regulate the capacity of B cell to extract and present antigens, B cells were seeded over substrates of different stiffness containing BCR^+ ligands together with the LACK antigen from *Leishmania major*. The ability of the cells to present MHC-II–LACK processed peptide complexes derived from the substrates to a specific T cell hybridoma that recognizes processed antigen was measured by monitoring IL-2 secretion by activated T lymphocytes. Importantly, we included a positive control for extreme stiffness (glass) coupled to BCR^+ or BCR^- ligands.

As shown in Fig.5 A, B cells seeded on immobilized antigens associated to stiffer substrates, triggered higher IL-2 production from T cells in comparison with B cells activated on soft substrates. This suggests a positive correlation between substrate stiffness, the presence of an activating BCR ligand, and the capacity of B cells to extract, process, and present antigens to T cells. Increasing levels of stiffness had no effect on the presentation of the LACK $^{156\text{-}173}$ peptide, showing that varying substrate rigidity does not significantly influence T cell responses or B-T cell interactions (Fig. 5 B).

Having shown that physical cues from the environment regulate the capacity of B cells to extract and present immobilized antigens, we next evaluated whether this relied on ATAT1-dependent microtubule acetylation. For this purpose, B cells were silenced for ATAT1 and their capacity to extract and present antigens was assessed using the aforementioned experimental setup. As shown in Fig. 4 C, the capacity to present *Lack* antigen associated to stiff substrates was lower in ATAT1-silenced B cells compared to controls cells. However, no significant differences between control and ATAT1-silenced cells were observed when activated on soft substrates.

This result is consistent with our observations showing that B cells activated on soft substrates display low levels of translocation of ATAT1 to the cytoplasm and therefore silencing of this enzyme should not have a major effect on antigen presentation. Additionally, the capacity of ATAT1-silenced B cells to present processed $LACK^{156\text{-}173}$ peptide was slightly decreased compared to control cells (Fig.5 D), suggesting that B-T cell interactions could be affected. Collectively, these results suggest that silencing ATAT1 renders B cells insensitive to substrate rigidity during activation, compromising their capacity to enhance antigen extraction and presentation.

In summary (Fig. 5 E), our results highlight how B cells couple mechanosensing pathways to control lysosome dynamics and tune their capacity to extract and present immobilized antigens. We show that B cells respond to substrate stiffness translocating ATAT1 from the nucleus to the cytoplasm, thereby increasing tubulin acetylation, which in turn promotes stable lysosome recruitment at the IS.

Notably, upon interaction of B cells with stiffer substrates, their lysosomes exhibit a more concentrated pool at the center of the immunological synapse, displaying slower speed and less displacement compared to lysosomes from B cells activated on softer substrates. These changes in lysosome dynamics correlate with the levels of tubulin acetylation, upregulated by B cells in response to substrate stiffness, where lysosomes preferentially associate to acetylated tubulin tracks in stiffer conditions.

Overall, these findings underscore the existence of a cellular pathway that connects antigen-extraction mechanisms with mechanical cues originating from APCs, which are regulated by BCR-mediated mechanosensing.

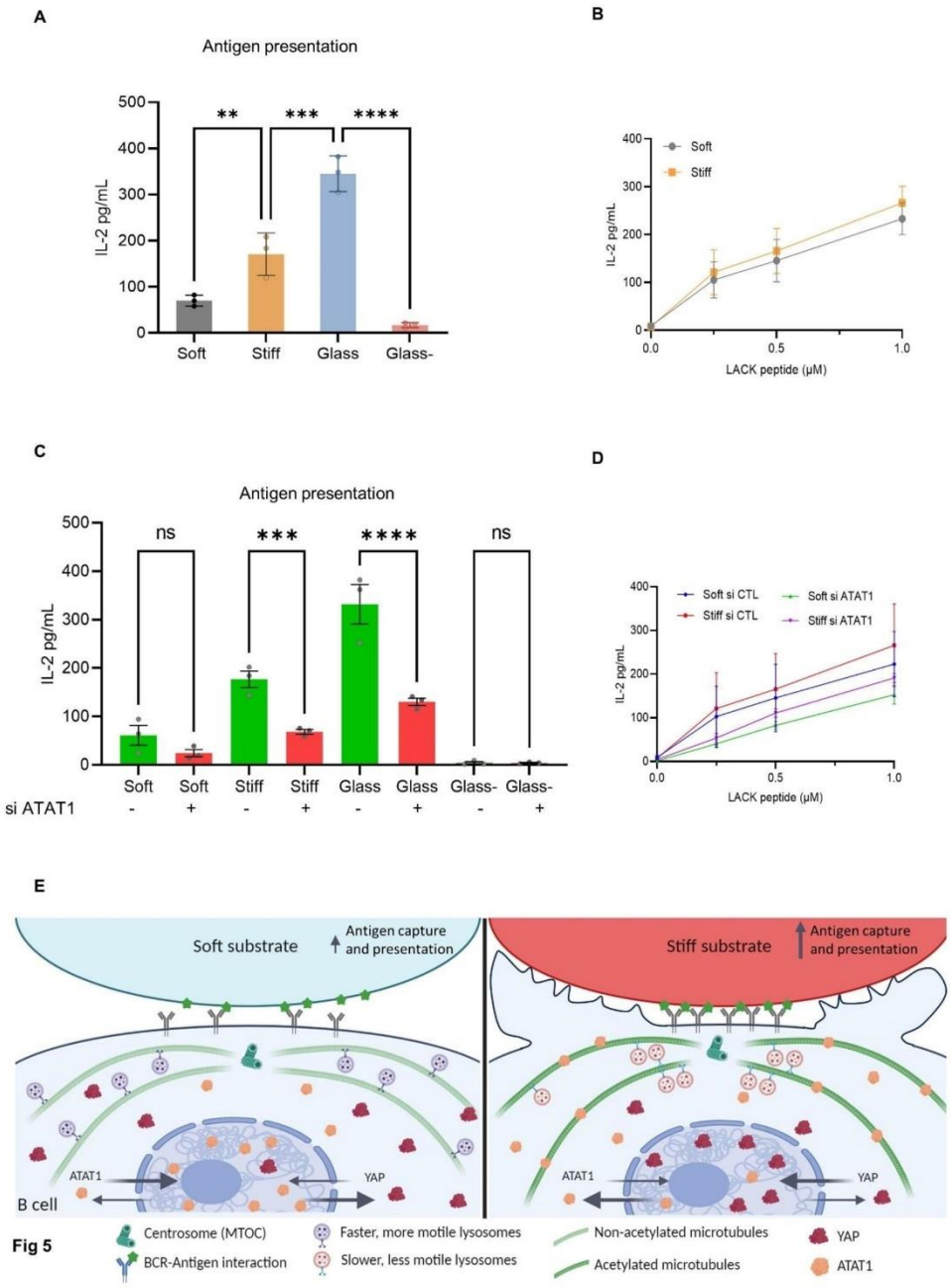

Fig.5 Antigen extraction and presentation by B cells is dependent on the substrate stiffness and ATAT1

Antigen presentation assays (A) of B cells activated on substates with different stiffness and (C) with control or ATAT1-silenced B cells. (B) and (D) Lack peptide control for the cells used. Mean amounts of IL-2 are shown for a representative of three independent experiments performed in triplicate. (E) Proposed model for B cell activation coupled to physical cues: In response to antigens associated to stiff substrates, B cells undergo enhanced spreading responses, increase the formation of actin foci and localize YAP to the nucleus, whereas the acetylase ATAT1 is translocated from the nucleus to the cytoplasm where it catalyzes tubulin acetylation. This enables the central accumulation of lysosomes that preferentially bind to acetylated microtubules at the immune synapse of B cells. These lysosomes exhibit slower speed and displacement than lysosomes from B cells activated on soft substrates. Consequently, B cells interacting with antigens coupled to stiff substrates increase their capacity to capture and present antigens to T cells which is impaired upon ATAT1 downregulation. P values illustrated with asterisks are ** < 0.01,*** <0.001, **** <0.0001. Error bars are mean ± SEM.

References

Akkaya, M., Kwak, K. and Pierce, S.K. (2020) 'B cell memory: building two walls of protection against pathogens', *Nature Reviews Immunology*, 20(4), pp. 229–238. Available at: https://doi.org/10.1038/s41577-019-0244-2.

Basu, R. *et al.* (2016) 'Cytotoxic T Cells Use Mechanical Force to Potentiate Target Cell Killing', *Cell*, 165(1), pp. 100–110. Available at: https://doi.org/10.1016/j.cell.2016.01.021.

Bhuwania, R., Castro-Castro, A. and Linder, S. (2014) 'Microtubule acetylation regulates dynamics of KIF1C-powered vesicles and contact of microtubule plus ends with podosomes', *European Journal of Cell Biology*, 93(10–12), pp. 424–437. Available at: https://doi.org/10.1016/j.ejcb.2014.07.006.

Bufi, N. *et al.* (2015) 'Human primary immune cells exhibit distinct mechanical properties that are modified by inflammation', *Biophysical Journal*, 108(9), pp. 2181–2190. Available at: https://doi.org/10.1016/j.bpj.2015.03.047.

Charrier, E.E. *et al.* (2020) 'A novel method to make viscoelastic polyacrylamide gels for cell culture and traction force microscopy', *APL Bioengineering*, 4(3). Available at: https://doi.org/10.1063/5.0002750.

Chen, Y. *et al.* (2017) 'Receptor-mediated cell mechanosensing', *Molecular Biology of the Cell*, 28(23), pp. 3134–3155. Available at: https://doi.org/10.1091/mbc.E17-04-0228.

Ciechomska, M. *et al.* (2014) 'Antigen-specific B lymphocytes acquire proteoglycan aggrecan from cartilage extracellular matrix resulting in antigen presentation and CD4+ T-cell activation', *Immunology*, 141(1), pp. 70–78. Available at: https://doi.org/10.1111/imm.12169.

Deb Roy, A. *et al.* (2022) 'Non-catalytic allostery in α-TAT1 by a phospho-switch drives dynamic microtubule acetylation', *Journal of Cell Biology*, 221(11). Available at: https://doi.org/10.1083/jcb.202202100.

Friedman, D. *et al.* (2021) 'Natural killer cell immune synapse formation and cytotoxicity are controlled by tension of the target interface', *Journal of Cell Science*, 134(7). Available at: https://doi.org/10.1242/jcs.258570.

Grune, T. *et al.* (2018) '"Cyt/Nuc," a Customizable and Documenting ImageJ Macro for Evaluation of Protein Distributions Between Cytosol and Nucleus', *Biotechnology Journal*, 13(5), p. e1700652. Available at: https://doi.org/10.1002/biot.201700652.

Hoogeboom, R. and Tolar, P. (2016) 'Molecular Mechanisms of B Cell Antigen Gathering and Endocytosis', in T. Kurosaki and J. Wienands (eds) *B Cell Receptor Signaling*. Cham: Springer International Publishing (Current Topics in Microbiology and Immunology), pp. 45–63. Available at: https://doi.org/10.1007/82_2015_476.

Ibañez-Vega, J., Del Valle Batalla, F., *et al.* (2019) 'Proteasome Dependent Actin Remodeling Facilitates Antigen Extraction at the Immune Synapse of B Cells', *Frontiers in Immunology*, 10. Available at: https://doi.org/10.3389/fimmu.2019.00225.

Ibañez-Vega, J., Fuentes, D., *et al.* (2019) 'Studying organelle dynamics in B cells during immune synapse formation', *Journal of Visualized Experiments*, 2019(148), pp. 1–13. Available at: https://doi.org/10.3791/59621.

Janke, C. and Magiera, M.M. (2020) 'The tubulin code and its role in controlling microtubule properties and functions', *Nature Reviews Molecular Cell Biology*, 21(6), pp. 307–326. Available at: https://doi.org/10.1038/s41580-020-0214-3.

Kim, T.-H. *et al.* (2019) 'Stress hormone signaling through β-adrenergic receptors regulates macrophage mechanotype and function', *The FASEB Journal*, 33(3), pp. 3997–4006. Available at: https://doi.org/10.1096/fj.201801429rr.

Lachowski, D. *et al.* (2022) 'Substrate Stiffness-Driven Membrane Tension Modulates Vesicular Trafficking via Caveolin-1', *ACS Nano*, 16(3), pp. 4322–4337. Available at: https://doi.org/10.1021/acsnano.1c10534.

Li, X. *et al.* (2023) 'Polarized focal adhesion kinase activity within a focal adhesion during cell migration', *Nature Chemical Biology*, pp. 1–11. Available at: https://doi.org/10.1038/s41589-023-01353-y.

Morelli, G. *et al.* (2018) 'p27Kip1 Modulates Axonal Transport by Regulating α-Tubulin Acetyltransferase 1 Stability', *Cell Reports*, 23(8), pp. 2429–2442. Available at: https://doi.org/10.1016/j.celrep.2018.04.083.

Núñez-Andrade, N. *et al.* (2016) 'HDAC6 regulates the dynamics of lytic granules in cytotoxic T lymphocytes', *Journal of Cell Science*, 129(7), pp. 1305–1311. Available at: https://doi.org/10.1242/JCS.180885/260299/AM/HDAC6-REGULATES-THE-DYNAMICS-OF-LYTIC-GRANULES-IN.

Obino, D. *et al.* (2017) 'Vamp-7–dependent secretion at the immune synapse regulates antigen extraction and presentation in B-lymphocytes', *Molecular Biology of the Cell*, 28(7), pp. 890–897. Available at: https://doi.org/10.1091/mbc.E16-10-0722.

Panciera, T. *et al.* (2017) 'Mechanobiology of YAP and TAZ in physiology and disease', *Nature Reviews Molecular Cell Biology*, 18(12), pp. 758–770. Available at: https://doi.org/10.1038/nrm.2017.87.

Phuyal, S. *et al.* (2022) 'Mechanical strain stimulates COPII-dependent secretory trafficking via Rac1', *The EMBO Journal*, 41(18), p. e110596. Available at: https://doi.org/10.15252/embj.2022110596.

Pu, J. *et al.* (2016) 'Mechanisms and functions of lysosome positioning', *Journal of Cell Science*, 129(23), pp. 4329–4339. Available at: https://doi.org/10.1242/jcs.196287.

Roper, S.I. *et al.* (2019) 'B cells extract antigens at Arp2/3-generated actin foci interspersed with linear filaments', *eLife*. Edited by M.L. Dustin and A. Akhmanova, 8, p. e48093. Available at: https://doi.org/10.7554/eLife.48093.

Sáez, J.J. *et al.* (2019) 'The exocyst controls lysosome secretion and antigen extraction at the immune synapse of B cells', *Journal of Cell Biology*, 218(7), pp. 2247–2264. Available at: https://doi.org/10.1083/jcb.201811131.

Schindelin, J. *et al.* (2012) 'Fiji: An open-source platform for biological-image analysis', *Nature Methods*, 9(7), pp. 676–682. Available at: https://doi.org/10.1038/nmeth.2019.

Seetharaman, S. *et al.* (2022) 'Microtubules tune mechanosensitive cell responses', *Nature Materials*, 21(3), pp. 366–377. Available at: https://doi.org/10.1038/s41563-021-01108-x.

Shaheen, S. *et al.* (2017) 'Substrate stiffness governs the initiation of b cell activation by the concerted signaling of PKCβ and focal adhesion kinase', *eLife*, 6, pp. 1–29. Available at: https://doi.org/10.7554/eLife.23060.

Shaheen, S. *et al.* (2019) *B cell mechanosensing: A mechanistic overview*, *Advances in Immunology*. Elsevier Inc. Available at: https://doi.org/10.1016/bs.ai.2019.08.003.

Wan, Z. *et al.* (2013) 'B Cell Activation Is Regulated by the Stiffness Properties of the Substrate Presenting the Antigens', *The Journal of Immunology*, 190(9), pp. 4661–4675. Available at: https://doi.org/10.4049/jimmunol.1202976.

Yuseff, M.I. *et al.* (2011) 'Polarized Secretion of Lysosomes at the B Cell Synapse Couples Antigen Extraction to Processing and Presentation', *Immunity*, 35(3), pp. 361–374. Available at: https://doi.org/10.1016/j.immuni.2011.07.008.

Yuseff, M.-I. *et al.* (2013) 'How B cells capture, process and present antigens: a crucial role for cell polarity.', *Nature reviews. Immunology*, 13(7), pp. 475–86. Available at: https://doi.org/10.1038/nri3469.

Zhu, C. *et al.* (2019) 'Mechanosensing through immunoreceptors', *Nature Immunology*, 20(October), pp. 1269–1278. Available at: https://doi.org/10.1038/s41590-019-0491-1.

Zhu, C., Chen, Y. and Ju, L.A. (2019) 'Dynamic bonds and their roles in mechanosensing', *Current Opinion in Chemical Biology*, 53, pp. 88–97. Available at: https://doi.org/10.1016/j.cbpa.2019.08.005.

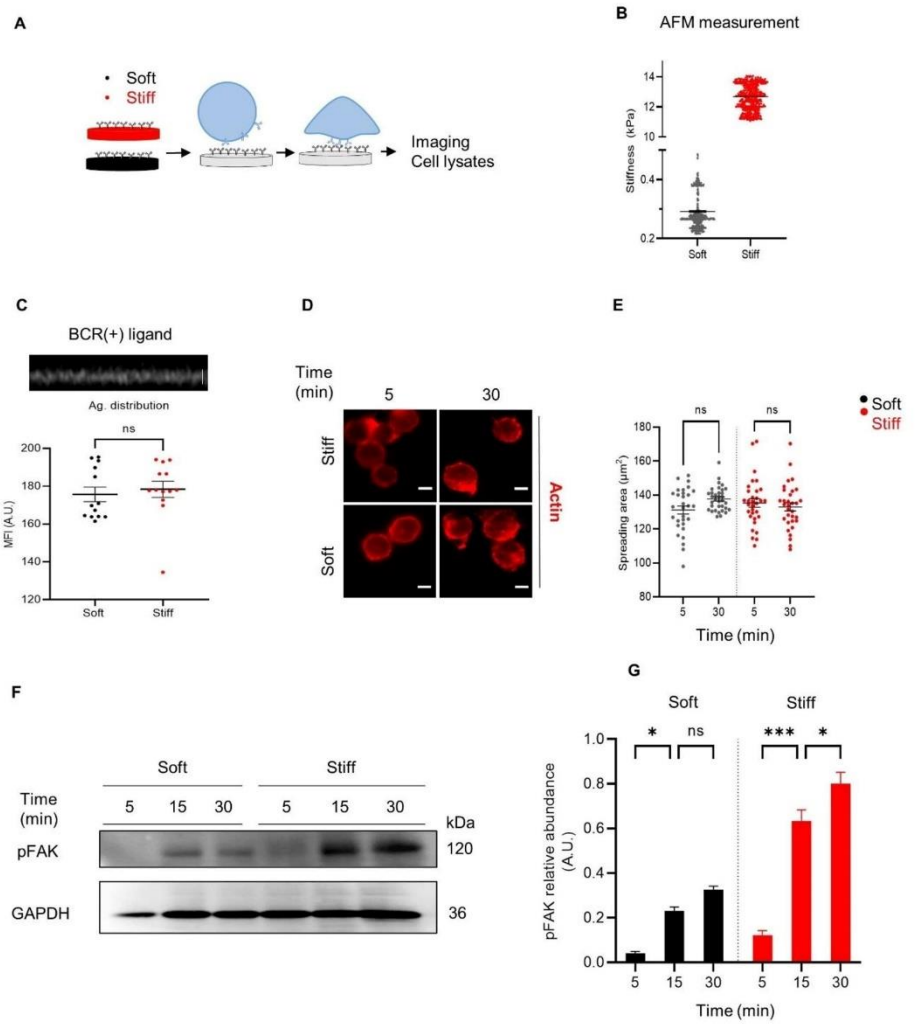

Fig EV1

(A) illustration of basic workflow with PAA gels. First, soft or stiff gels are coupled to BCR-activating ligands. Then cells are seeded for different time points, fixed and used for live imaging, or lysed for protein extraction. (B) Atomic force measurements for stiffness of the gels used in this work. Soft values are considered to be 0.3 kPa and stiff, 13 kPa. (C) representative confocal image for the Z cross-section of a PAA gel coupled to a fluorescently labeled BCR^+ ligand. Scale bar = 2μm. Bottom: analysis for antigen distribution (BCR^+ ligand) based on MFI values acquired in confocal microscopy. (D) Representative images obtained in confocal microscopy depicting the actin cytoskeleton spreading labeled with phalloidin (red) when B cells are seeded over gels coupled to a BCR^- ligand (non-activating). (E) Quantification of the spreading area from experiments depicted in (D). (F) Immunoblots for pFAK and GAPDH in cells seeded at different time points and stiffnesses. (G) Quantifications for (F) based in the relative abundance of pFAK with respect to GAPDH. Shown data considers n ≥ 30 cells pooled from N = 3 biological replicates. Scale bars are 5 μm. P values illustrated with asterisks are: * < 0.05, ** < 0.01, *** <0.001, **** <0.0001

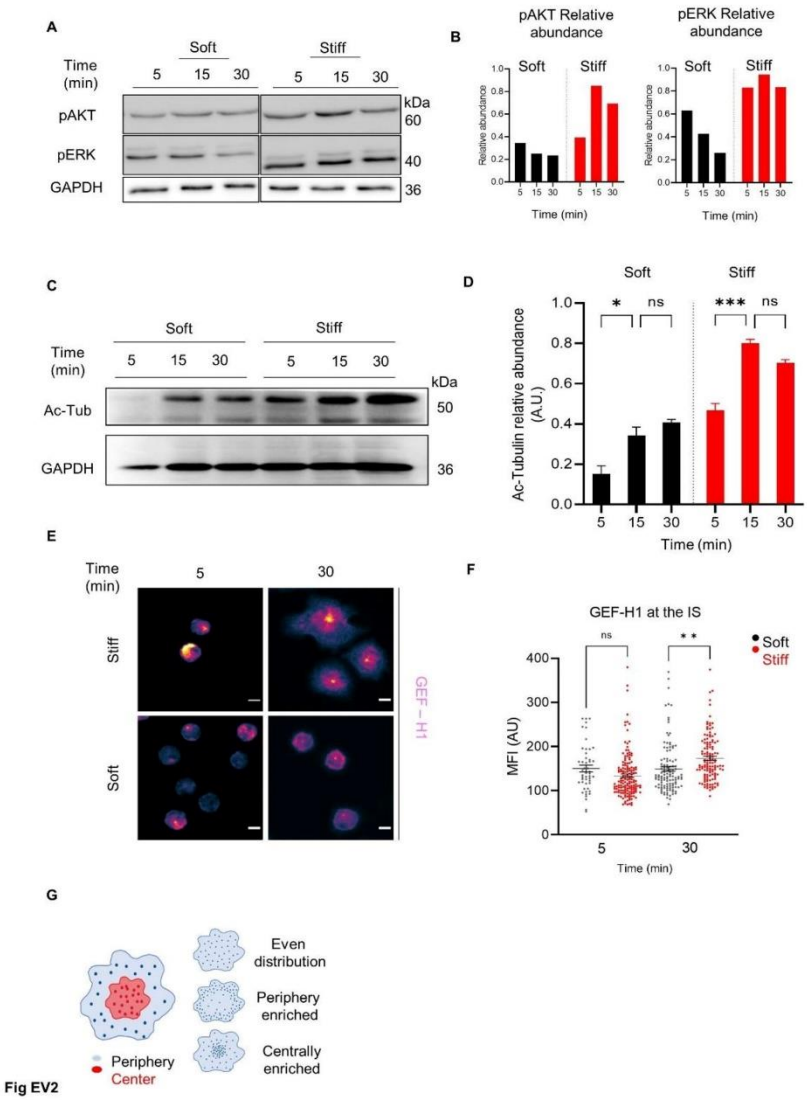

Fig EV2

Fig. EV2

(A) Immunoblot for pAKT, pERK and GAPDH in cells seeded at different time points and stiffnesses. (B) Quantifications for (A) based in the relative abundance of pAKT and pERK with respect to GAPDH. (C) Immunoblotting for Ac-Tub and GAPDH in cells seeded at different time points and stiffnesses. (D) Quantifications for (C) based in the relative abundance of Ac-Tub with respect to GAPDH. (E) Representative images of fixed cells interacting with soft or stiff substrates at different time points. GEF-H1 is shown in a gradient of magenta according to fluorescence intensity. (F) Quantification of GEFH1 intensity at the IS for the experiments represented in (E). (G) Illustration for the localization index used to determine the differential accumulation of lysosomes in each cell. Shown data considers n ≥ 30 cells pooled from N = 3 biological replicates. Scale bars are 5 µm. P values illustrated with asterisks are: * < 0.05, ** < 0.01, *** <0.001.

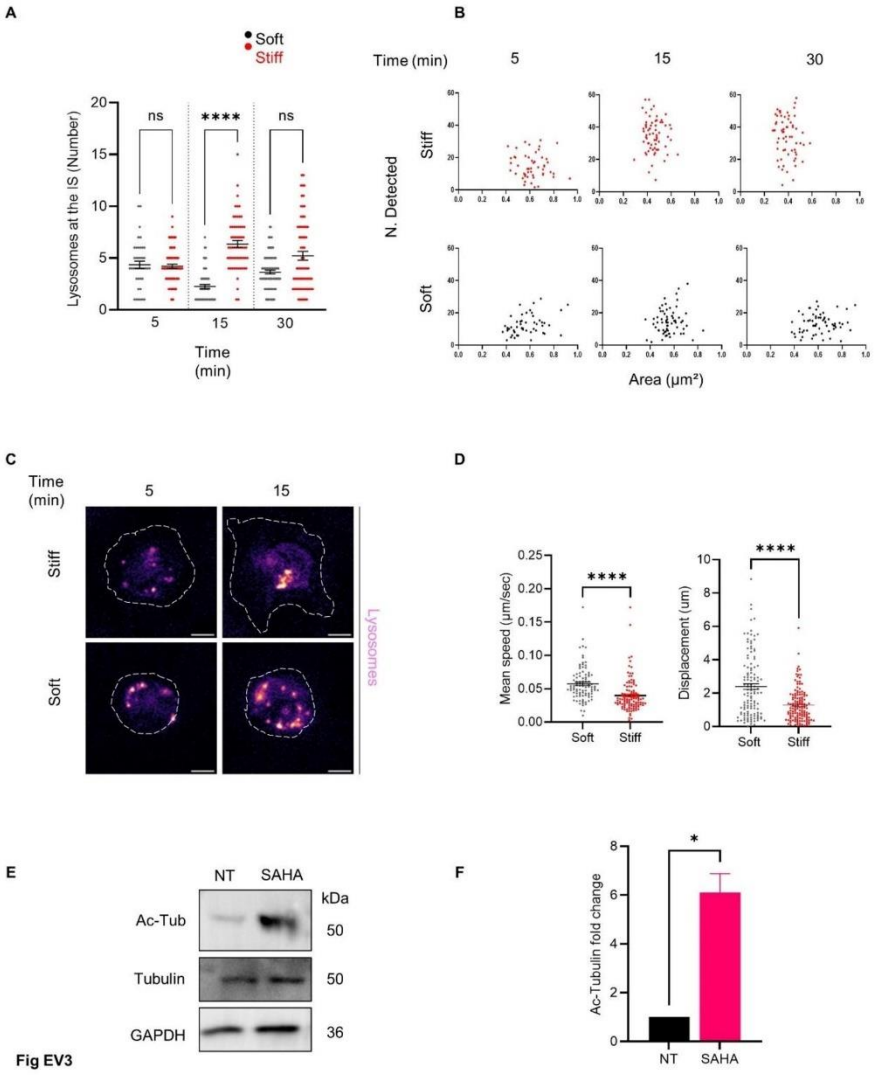

Fig EV3

Fig. EV3

(A) Quantification for LAMP1⁺ particles at the IS showing the number of particles detected at the IS in the different experimental conditions. In (B), every graph depicts summary measurements for individual cells (individual circles) considering the mean area values for segmented LAMP1 particles (x-axis) and the number of segmented particles found at the IS on that cell. (C) Representative images for lysosome tracking in B cells stained with lysotracker (magenta) and activated on either stiff or soft conditions. (D) Displacement and mean speed of lysosome tracks for experiments in (C). (E) Immunoblot to evaluate the effect of the drug SAHA on microtubule acetylation with its correspondent quantification in the fold of change for tubulin acetylation compared to non-treated cells (CTL). (F) Quantification of the effect of SAHA on Ac-tubulin fold of change with respect to total tubulin. Shown data considers n ≥ 30 cells pooled from N = 3 biological replicates. Scale bars are 5 µm. P values illustrated with asterisks are: * < 0.05, **** <0.0001

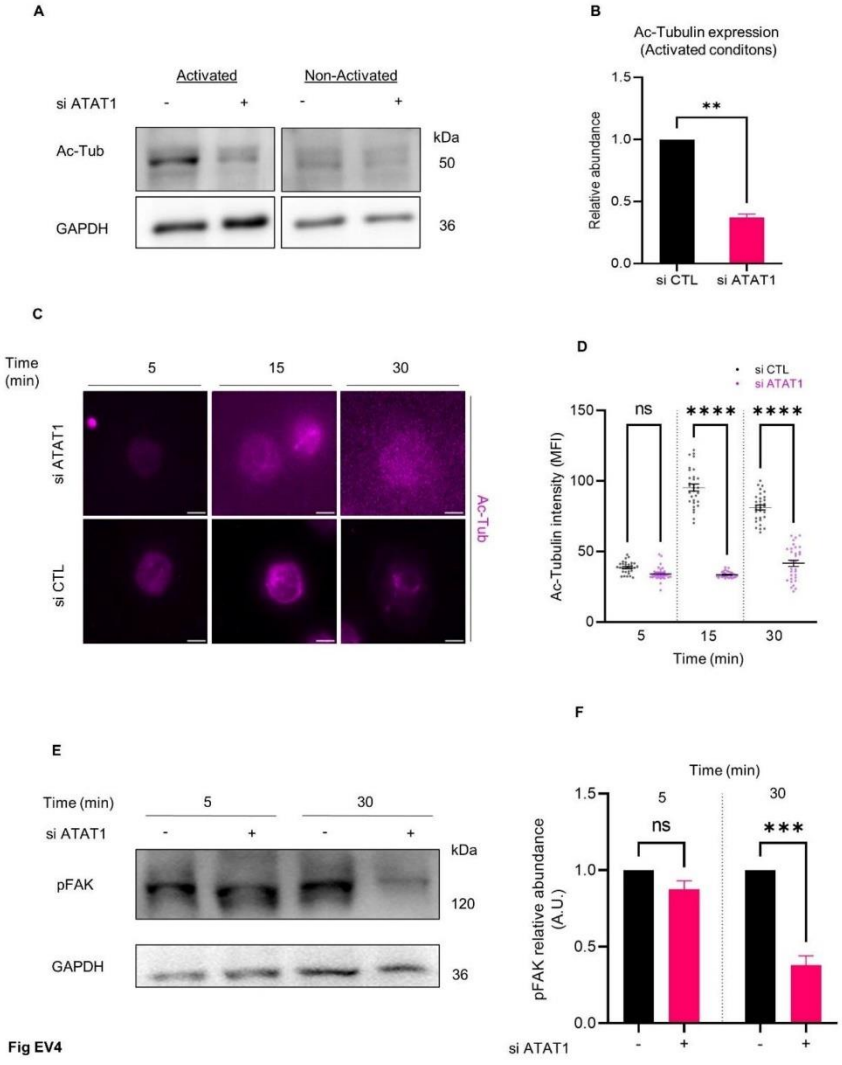

Fig EV4

Fig. EV4

(A) Immunoblot for Acetylated tubulin and GAPDH in cells seeded on stiff plastic plates for 30 minutes. Cells were treated with control or ATAT1 siRNAs. (B) Quantifications for (A) based on the relative abundance of Acetylated tubulin with respect to GAPDH. (C) Representative images of Ac-Tub in control or ATAT1-silenced B cells activated on stiff substrates. (D) Quantification of mean fluorescence intensity of Ac-Tub at the IS as shown in (C). (E) Immunoblot for pFAK and GAPDH in B cells seeded in stiff plastic plates at different time points, for control or ATAT1-silenced cells. (F) Quantifications for (E) based on the relative abundance of pFAK with respect to GAPDH for the treatments at different time points. . Shown data considers n ≥ 30 cells pooled from N = 3 biological replicates. All scale bars are 5 µm. P values illustrated with asterisks are ** < 0.01, **** <0.0001. Error bars are mean ± SEM.

Aims 1 and 2 - Manuscript 2: Quantitative analysis of the B cell immune synapse formation using imaging techniques.

The following accepted manuscript, in which I participated as a co-corresponding author, encompasses various protocols for image analysis in the context of immune synapse formation in B lymphocytes. These methods have been actively enhanced and developed with my support in the laboratory and constitute a part of the methodology used to analyze the results presented in manuscript 1.

Authors: Corrales Vázquez, Oreste[1] *., Contreras, Teemly[1] *., Alamo Rollandi, Martina[1]., Del Valle Batalla, Felipe[1]., Yuseff, Maria-Isabel[1].

(1) Laboratory of Immune Cell Biology, Department of Cellular and Molecular Biology, Pontificia Universidad Católica de Chile, Santiago 8331150, Chile

* Equal contribution

Corresponding Authors: Yuseff, María-Isabel., Del Valle Batalla, Felipe.

Abstract

This chapter presents a series of quantitative analyses that can be used to study the formation of the immune synapse (IS) in B cells. The methods described are automated, consistent, and compatible with open-source platforms. The IS is a crucial structure involved in B cell activation and function, and the spatiotemporal organization of this structure is analyzed to provide a better understanding of its mechanisms. The analyses presented here can be applied to other immune cells and are accessible to researchers of diverse fields. In addition, the raw data derived from the results can be further explored to perform quantitative measurements of protein recruitment and tracking of intracellular vesicles. These techniques have the potential to enhance not only our understanding of the IS in B cells but also in other cell models.

Quantitative analysis of the B Cell immune synapse formation using imaging technique

Oreste Corrales Vázquez, Teemly Contreras, Martina Alamo Rollandi, Felipe Del Valle Batalla, Maria-Isabel Yuseff.

Abstract

This chapter presents a series of quantitative analyses that can be used to study the formation of the immune synapse (IS) in B cells. The methods described are automated, consistent, and compatible with open-source platforms. The IS is a crucial structure involved in B cell activation and function, and the spatiotemporal organization of this structure is analyzed to provide a better understanding of its mechanisms. The analyses presented here can be applied to other immune cells and are accessible to researchers of diverse fields. In addition, the raw data derived from the results can be further explored to perform quantitative measurements of protein recruitment and tracking of intracellular vesicles. These techniques have the potential to enhance not only our understanding of the IS in B cells but also in other cell models.

1 Introduction

B cells are a crucial part of the immune response as they can differentiate into plasma cells that produce and secrete antibodies and become memory B cells that provide long-term protection against new and recurrent infections [1]. To fulfill these functions, naïve B cells must first be activated in lymphoid tissues upon interaction with antigen-presenting cells (APCs) such as macrophages or dendritic cells. This initial interaction with an APC is known as the immune synapse (IS), a highly organized structure formed between immune cells [2].

The formation of the IS involves a complex and highly regulated series of events comprising cytoskeleton rearrangement, actin remodeling, lysosome recruitment, MTOC polarization, and associated functions such as antigen extraction and changes in cell shape during the IS formation. Actin and microtubule cytoskeletons are remodeled to focus vesicle trafficking important for antigen extraction and processing, as well as to provide a platform for signaling molecules that regulate B cell activation [3].

Oreste Corrales Vázquez and Teemly Contreras contributed equally to this work.
Corresponding Authors: Yuseff, María-Isabel., Del Valle Batalla, Felipe.

To quantify and understand the mechanisms underlying the formation of the B cell IS, imaging techniques are essential. Despite recent advances in techniques and computational tools, the accurate analysis of IS formation remains a challenging task. This is due to variations in the quality and consistency of sample preparation, the heterogeneity of individual cells, and the complexity of the data obtained from imaging analysis. Nevertheless, these challenges can provide important insights and opportunities for the development of improved strategies for data analysis.

Here, we present a series of quantitative analyses of the B cell IS formation using automated and consistent workflows compatible with open-source platforms. The following methods are recommended to minimize bias and ensure reproducibility in data analysis. The use of these analyses can be extrapolated to other immune cells, such as T cells, dendritic cells, macrophages, and other cell models that exhibit polarized phenotypes under different biological contexts.

2 Materials and methods

2.1 Cells and culture

1. The mouse B lymphoma A20 cell line was used for experiments that serve as an example. These cells have the phenotype of quiescent mature B-cells expressing surface IgG2a as a BCR [4].
2. Culture and experimental medium (CLICK): RPMI 1640 supplemented with 2-10 mM glutamine, 100 U/mL penicillin, 100 µg/mL streptomycin, 50 µM 2-mercaptoethanol (2-ME), 5 mM sodium pyruvate, and 10 or 5% fetal bovine serum (FBS) for cell culture or activation experiments, respectively.

1X phosphate-buffered saline (PBS) sterile.

2.2 Antibodies and Reagents

Primary/secondary antibody	Host	Reactivity	Catalog ID	Observations
Anti-α-tubulin	Rat	Mouse	ab6160, Abcam	Labels the microtubule network. 1:500 dilution, fixation with methanol or paraformaldehyde (PFA) 3%.
Anti-Cep55	Rabbit	Mouse	ab170414, Abcam	Labels the microtubule network. 1:500 dilution, fixation with PFA 3%.
Anti-γ-tubulin	Rabbit	Mouse	ab179503, Abcam	Labels the microtubule organizing center (MTOC) or centrosome. 1:500 dilution, fixation with methanol.

Anti-pericentrin	Rabbit	Mouse	ab4448, Abcam	Labels the microtubule organizing center (MTOC) or centrosome. 1:500 dilution, fixation with methanol.
Anti-LAMP1	Rat	Mouse	553792, BD Pharmigen	Labels lysosomes. 1:200 dilution, fixation with PFA 3%.
AffiniPure F(ab')$_2$ Fragment Alexa Fluor 488, IgG (H+L)	Donkey	Rabbit	711-546-152, Jackson Immunoresearch	1:500 dilution.
AffiniPure F(ab')$_2$ Fragment Cy3, IgG (H+L)	Donkey	Rabbit	711-166-152, Jackson Immunoresearch	1:500 dilution.
AffiniPure F(ab')$_2$ Fragment Alexa Fluor 647, IgG (H+L)	Donkey	Rabbit	711-606-152, Jackson Immunoresearch	1:500 dilution.
AffiniPure F(ab')$_2$ Fragment Alexa Fluor 488, IgG (H+L)	Donkey	Rat	712-546-150, Jackson Immunoresearch	1:500 dilution.
AffiniPure F(ab')$_2$ Fragment Cy3, IgG (H+L)	Donkey	Rat	712-166-153, Jackson Immunoresearch	1:500 dilution.
AffiniPure F(ab')$_2$ Fragment Alexa Fluor 647, IgG (H+L)	Donkey	Rat	712-606-153, Jackson Immunoresearch	1:500 dilution.
Hoechst			H3570, Invitrogen	Labels the nucleus. 1:1000 dilution, fixation with PFA.
Rhodamine phalloidin			R415, Invitrogen	Labels polymerized actin. 1:400 dilution, fixation with PFA.
NH-2 Beads			Polysciences, Inc. Cat. No. 17145-5	Consider the size of the beads depending on the cell that will interact with them. In our model, we use 3 µm Micros size for beads.
Fluoromount G			Electron Microscopy Sciences, Cat No. 17984-25	Add 5 µL for 10 mm coverslips and 7 µL for 12 mm coverslips
Microscope Cover Glasses			Paul Marlenfeld Gmb H &Co Ref 0111500	If super-resolution techniques will be used, consider alternatives more suitable with the optical configuration.

For additional information about materials **see Note 1.**

2.3 Preparation of antigen-coated beads

1. To activate B cells, use NH2-beads covalently coated with antigen (antigen-coated beads), which are prepared using 50 µL (~20*106 beads) of 3 µm NH2-beads and activating (BCR-ligand+) or non-activating (BCR-ligand-) antigens.
2. For A20 B cells, which are an IgG+ FcγR-defective B cell line with the phenotype of quiescent mature B-cells, use the anti-IgG-F(ab')2 fragment as BCR-ligand+ and anti-IgM-F(ab')2 or bovine serum albumin (BSA) as BCR-ligand-. **See Note 2.**

3. To prepare antigen-coated beads, place the 50 µL of beads in a low-binding protein microcentrifuge tube containing 1 mL of 1X PBS to maximize the beads recovery during the sample manipulation, and centrifuge at 16,000 g for 5 min to wash the beads. Discard the supernatant.
4. Resuspend the beads with 500 µL of 8% glutaraldehyde to activate the NH2 groups and rotate for 4 h at room temperature (RT), protected from light.
   CAUTION: The glutaraldehyde stock solution should only be used in a chemical fume hood. Follow the instructions on the material safety data sheet (MSDS).
5. Centrifuge beads at 16,000 g for 5 min, remove the glutaraldehyde and wash the beads three times with 1 mL of 1X PBS.
   CAUTION: Glutaraldehyde solution should be discarded as hazardous chemical waste.
6. Resuspend the activated beads in 100 µL of 1X PBS. The sample can be divided into two low-protein binding microcentrifuge tubes: 50 µL for the BCR-ligand+ and 50 µL for BCR-ligand-.
7. To prepare the antigen solution use two 2 mL low-protein binding microcentrifuge tubes containing 100 µg/mL of antigen solution in 150 µL of PBS: one tube with BCR-ligand+ and the other with BCR-ligand-.
8. Add 50 µL of activated beads solution to each tube containing 150 µL of antigen solution, vortex, and rotate overnight at 4 °C.
9. Add 500 µL of 10 mg/mL BSA (in PBS 1X) to block the remaining reactive NH2 groups on the beads and rotate for 1 h at 4 °C.
10. Centrifuge the beads at 16,000 g for 5 min at 4 °C and remove the supernatant. Wash the beads with cold 1X PBS three times.
11. Resuspend activated beads in 40 µL of 1X PBS.
12. To determine the final concentration of the antigen-coated beads, dilute a small volume of beads (~1 µL) in 1X PBS (1:200) and count them using a hemocytometer. Then store at 4°C until use. **See Note 3**.

2.4 Preparation of antigen-coated coverslips

1. Prepare the antigen solution: 1x PBS containing 10 µg/mL BCR-ligand+. **See Note 4**
2. Place the 12- or 10- mm coverslip onto a 24-well plate lid covered with parafilm, add 40 µL of antigen solution onto each coverslip, and incubate in a humid chamber at 4 °C overnight. Seal the plate to avoid evaporation of antigen solution.
3. Wash the coverslips gently with with 100µL of 1X PBS using Pasteur pipettes before continuing to next steps. To prevent the coverslips from drying out, store them in 1X PBS until use.

2.5 Preparation of poly-L-lysine coverslip

1. Prepare 40 mL of 0.01 % w/v of poly-L-lysine solution. Use a 50 mL tube to immerse 10 mm coverslips into the solution and rotate overnight at RT. **See Note 4.**

2. Wash the poly-L-lysine coverslips (PLL-coverslips) with 1X PBS and leave to air dry on a 24-well plate lid covered with filter paper.

2.6 B cell activation with antigen-coated beads

1. Dilute B cells to a final concentration of 1.5*106 cells/mL in CLICK medium with 5% FBS.
2. Add 150,000 of antigen-coated beads to 100 uL of B cells (150,000) in 0.6 mL tubes to obtain a ratio of 1:1, respectively. Mix gently using a vortex and seed the 100 µL onto the PLL-coverslip. Incubate for different time points in a cell culture incubator (37 °C and 5 % CO2). The typical activating time points are 0, 30, 60, and 120 min. For time 0 min, place the PLL-coverslips into the 24-well plate lid on ice. Add the antigen-bead mixture to the cells and incubate for 5 min on ice. **See Note 5.**
3. After each time point, carefully aspirate the media off each coverslip and add 100 µL of cold 1X PBS (1 - 3 minutes) to stop the activation. Continue with the immunofluorescence protocol. See section 8.

2.7 B cell activation on antigen-coated surface

1. Dilute B cells to a final concentration of 1.0*106 cells/mL in CLICK medium with 5% FBS.
2. Add 80 µL of B cells (80,000) onto an antigen-coated coverslip (antigen-coverslip) and activate for different time points in a cell incubator at 37 °C / 5% CO2. The typical activating time points are 0, 15, 30 and 60 min. For time 0, use PLL-coverslip and add the cells. Incubate for 5 min.
3. After each time point, carefully aspirate the media off each coverslip and add 100 µL of cold 1X PBS (1 - 3 minutes) to stop the activation. Continue with the immunofluorescence protocol. See section 8.

2.8 Immunofluorescence

1. Remove the 1X PBS and proceed with the fixation of each coverslip. **See Note 6.**
2. Add 50 µL of cold 3% PFA in PBS 1X and incubate for 10 min at (RT).
   CAUTION: PFA is toxic. Please read the MSDS before working with this chemical. PFA solutions should only be prepared under a chemical fume hood wearing gloves and safety glasses. PFA solution should be discarded as hazardous chemical waste.
3. Wash three times with 1X PBS as explained in 6.3. **See Note 7.**
4. Remove 1X PBS and add 50 µL of blocking buffer (2% BSA and 0.3 M glycine in 1X PBS) onto each coverslip and incubate at RT for 10 min. Wash off the blocking buffer with 1x PBS.
5. Prepare the antibodies dilution in permeabilization buffer (0.2% BSA and 0.05% saponin in 1X PBS). Place 40 µL drops of primary antibody solution on a 24-well plate lid or a plastic petri dish lid covered with parafilm. Place the coverslips with fixed cells over each drop and incubate in a humid chamber at 4 °C overnight.

Seal the plate to avoid evaporation of antigen solution. **See Note 7 and 8.**

6. Wash the coverslips three times with permeabilization buffer.
7. Dilute the secondary antibodies or dyes in permeabilization buffer, using 40 µL per coverslip. Place the coverslips over drops of secondary antibody dilutions and incubate for 1h at RT in dark and humid chambers.
8. Wash the coverslips twice with permeabilization buffer and once with 1X PBS.
9. Remove the PBS solution from the coverslips.
10. Add 5 µL of mounting reagent to a microscope slide. Mount the coverslips onto the slide with the cell side facing down. Allow the slides to dry for 30 min at 37 °C or RT overnight protected from light. **See Note 9.**
11. Acquire fluorescence images on a confocal or widefield microscope with a 60X or 100X objective according to sample and cell size. Images acquired for bead assays were obtained in a Nikon Ti Eclipse inverted microscope with 60X/1.45NA oil objective. For spreading assays, a Zeiss LSM880 Confocal microscope (Airyscan detector) with 63X/1.4NA oil immersion lens was used. **See Note 10.**

3 Analysis of B lymphocytes activation with immobilized antigens

As mentioned above, cytoskeleton rearrangement, centrosome, and lysosome polarization to the antigen contact site are prerequisites and key hallmarks of immune synapse formation. The following protocols detail B cell activation using antigen-coated beads and surfaces with BCR+ or BCR- ligands that emulate an APC. The selection of either method of activation depends on the user needs and experimental design.

The activation of B cells with antigen-coated beads is useful to evaluate and polarization of intracellular structures (e.g. cytoskeleton, organelles) towards a particular region of the cell, in this case, a surface mimicking an Antigen presenting cell. One of the limitations of this technique is the number of beads that randomly become in contact with cells under the experimental conditions. The user should be aware that finding cells in contact with beads at shorter times of activation could be challenging. On the other hand, antigen-coated surfaces, such as coverslips are suitable for analyzing organelle distribution and dynamics at the IS in 2D and 3D, and also allows the user to employ high-resolution techniques, such as TIRF microscopy, to explore features of the synaptic plane. A caveat of this method is the limited control of the amount of ligand adsorbed and the uneven distribution on the surface. References [3] and [6] illustrate examples using Antigen-coated Beads and Antigen-coated coverslips, respectively.

We will explain the image analysis to study the recruitment of different organelles during B cell IS formation in B cells. These methods can be extrapolated to other cell models that present polarized phenotypes or differential recruitment of organelles to discrete cell regions.

3.1 Image and microscopyanalysis

It is important for the user to consider the different alternatives to perform quantitative imaging analysis when studying structural features of the immune synapse. For observations of B cell receptor distribution the most suitable approach is to use a high numerical aperture objective and TIRF illumination, which due to the short penetration depth of the evanescent field (~100 nm) improves signal-to-noise ratio for observing movement of molecules at the cell membrane. If not available, confocal microscopy can provide sufficient resolution to perform 3D imaging and determine colocalization of labels, organelle distribution and particle segmentation. For other experiments, a widefield illumination microscope is useful to quantify organelle distribution and other measurements that we show in this chapter.

After microscopy and image acquisition, we advise users to save raw images in .tif format at the highest bitrate. It is also convenient to use an output as a single file that preserves Z-slices and channels, such as hyperstacks. Fiji has a built-in macro .tif converter available in the "Process" -> "Batch" -> "Convert…" menu that works for these purposes. For convenient file handling and posterior use, we strongly suggest that files be named correctly with channel information (e.g. staining) and assigned pseudocolor. We also recommended adding a brief description of the experiment in a text file inside the image folder.

The following algorithms are described for Fiji - ImageJ software [5], which have been tested and work in versions 1.52 to 1.53t of said software. We recommend downloading the Bio-formats plugin for importing image files. No other plugins are needed for running the macros used in this chapter. However, this can be performed using equivalent software such as Napari or others if instructions are adjusted to those working environments. For R scripts, all codes were written and tested in R 4.2.2 , packages Tidyverse and Readr are needed.

The mentioned ImageJ-compatible macros and R scripts are available to download at https://github.com/YuseffLab/Image-Analysis. All codes are commented to be self-explanatory. If the user needs more details on how to use the R language, several open source projects are available for learning the fundamental concepts for use of this programming language (https://swirlstats.com/students.html , https://r4ds.had.co.nz/).

As we have done for this chapter, for statistical analysis, we recommend using 3 individual biological replicates with at least 20 cells per

experiment. It is critical to check for normality of data and remove outliers when identified by statistical tests.

Finally, for all the following Fiji instructions the user should configure the "Set measurements" menu. This can be found in the "Analyze" tab. Select all measurements except "Limit to threshold", "Invert Y coordinates", "Add to overlay", "Scientific notation" and "NaN empty cells". This will provide all of the information needed for the analyses.

4 Analysis of the distribution of organelles in B cells activated with antigen-coated beads

The next protocol details the steps to quantify the polarization of cell components to the IS. In this case, we define an arbitrary value, the polarity index, as a measure of proximity to the IS. The index ranges between -1 (anti-polarized) and 1 (fully polarized, object on the bead), as previously presented by Reversat et al [6].

4.1 Estimate the polarity index for the centrosome. See Note 11.

We use this algorithm to analyze the polarity of organelles that display a discrete point. In this case we have labeled the centrosome with α-tubulin (see table 1).

1. First, it is recommended to crop individual cells using the cell_cutter.ijm (drag and drop into Fiji main window) macros available on the GitHub repository. Instructions are available in the code.
2. Open the image and define the bead and cell areas to analyze using the circle tool selection to delimit both boundaries and save them as regions of interest (ROI) (Figure 1). If the cell has an irregular shape, the freehand tool can be used to select the area. For cell outline delimitation, both actin staining or bright field can be used.
3. Determine the cell center **(CC)** and the bead center **(BC)** by running **Analyze | Measure** on cell and bead areas, respectively. The **X and Y** values obtained from the **Results** window determine the center coordinates, as highlighted in the figure with a red dashed box (Figure 1).
4. Manually determine the center of the **centrosome** (highest intensity of the antibody staining) using the **Point tool** selection in ImageJ and run **Analyze | Measure.** The **X and Y** values obtained from the **Results** window determine the centrosome coordinates, as highlighted with a red dashed box in the figure (Figure 2).
5. Then, draw an angle from **CC to Cell structure (a)** and from **CC** to **BC (b)** using the **Angle tool** selection and run **Analyze | Measure.** The **Angle** value (highlighted with a red dashed box in the figure) in the **Results** window shows the angle **(α)** between both vectors **(a and b)** (Figure 3).

Figure 1

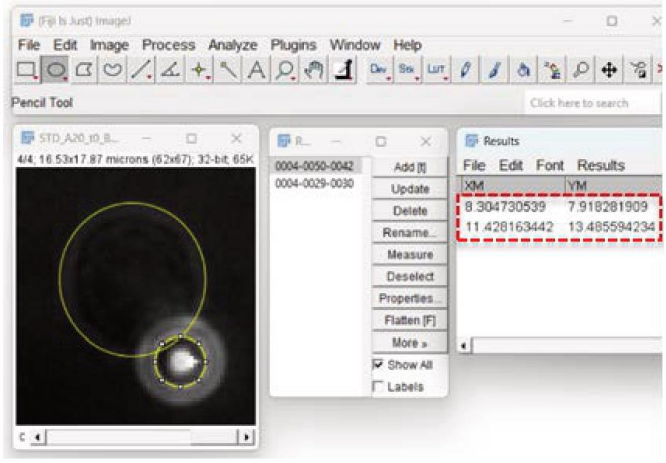

Figure 2

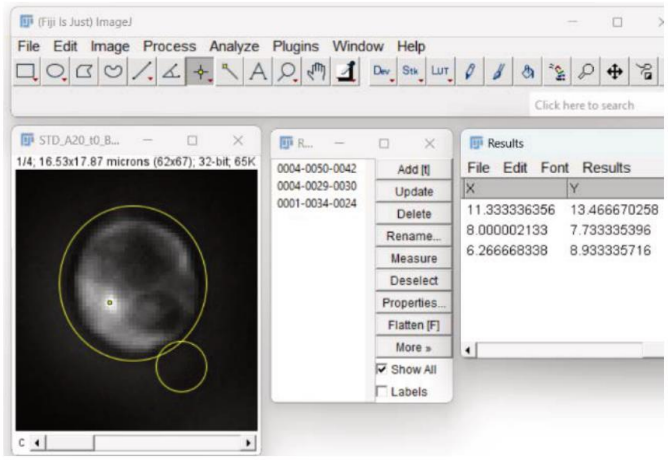

Figure 3

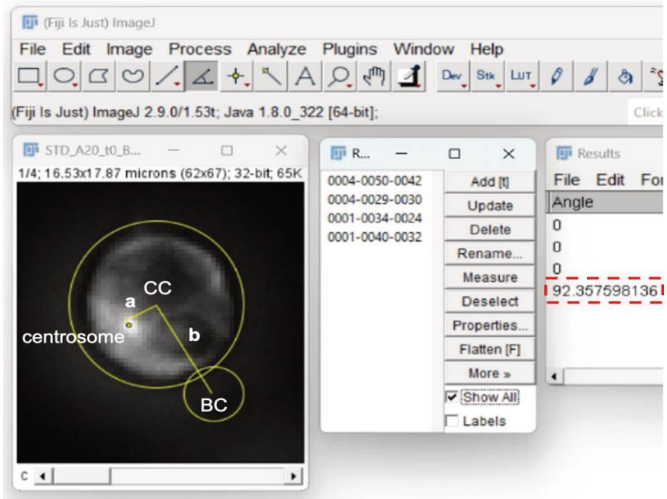

6. Calculate the **Polarity Index** using the following formula:

$$\text{Polarity Index} = a\,\frac{\cos(\alpha)}{b}$$

7. Representative Results
   The following image shows the centrosome recruitment to the IS upon B cell stimulation with antigen-coated beads over time (Figure 4).

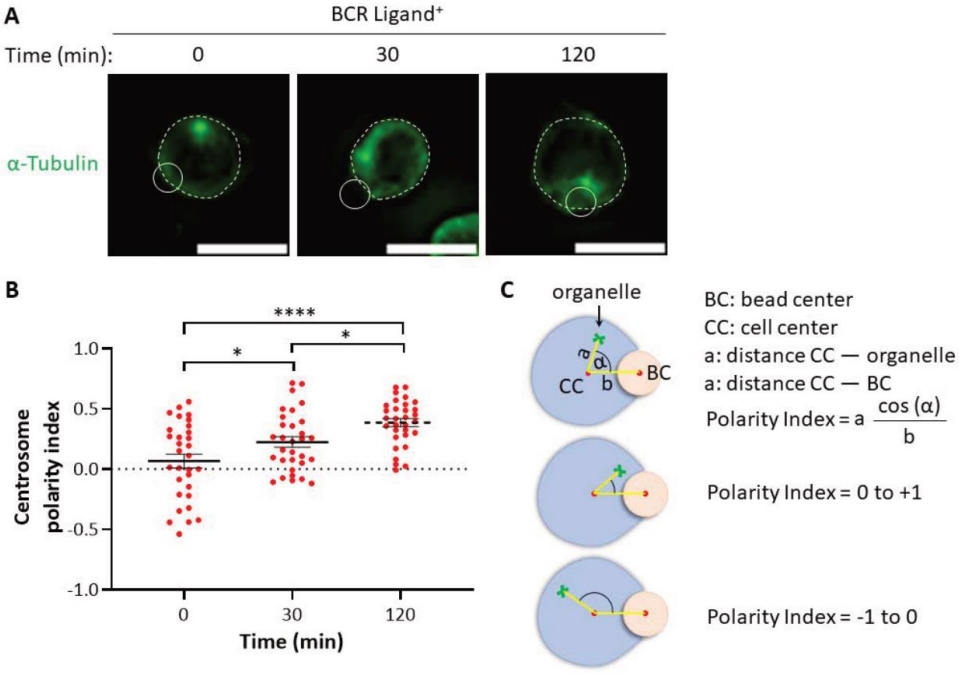

Figure 4: (A) Images of B cells stained for α-tubulin (shown in green) activated with BCR ligand–positive beads for the indicated times. Scale bar: 10 µm. **(B)** Centrosome polarity index calculated from the images in A. *, $p<0.05$; ****, $p<0.0001$; one-way ANOVA with Holm-Sidak's multiple comparison test; $n \geq 31$ cells from three independent experiments. **(C)** Scheme depicting how to calculate the polarity index of organelles (centrosome or Golgi apparatus) toward the IS. a = distance between the center of the cell **(CC)** to the organelle. b = distance from the CC and to the bead center **(BC)**.

4.1 Estimating the polarity index for lysosomes

We use this algorithm to analyze the polarity of organelles that display a more dispersed distribution. In this case we have labeled lysosomes with Lamp1 (see table 1).

1. Define the bead and cell areas to analyze, using the **Circle tool** selection to delimit both boundaries and save them as ROI (Figure 5). Once the bead and cell areas have been determined, set

the fluorescence channel and project the image into one z-stack **(Image | Stacks | Z-Project [Sum slices]),** then run **Analyze | Measure** and extract the mass center **(MC)** coordinates (**XM** and **YM**) from the Results windows, these values are highlighted with a red dashed box in the figure (Figure 6).

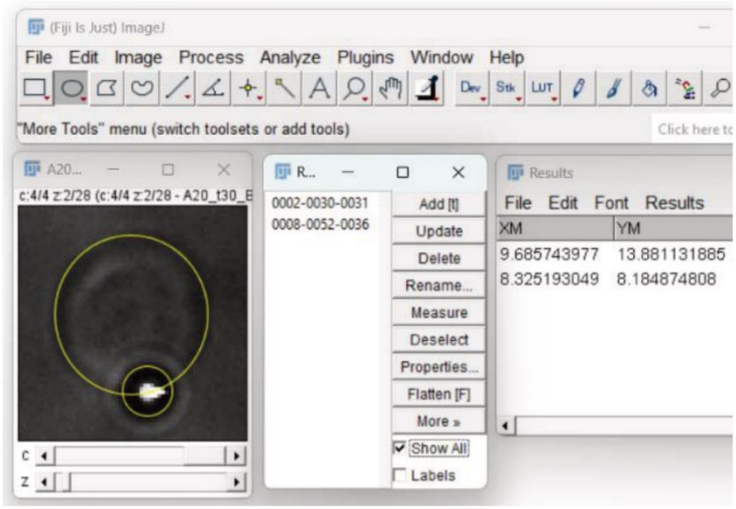

Figure 5

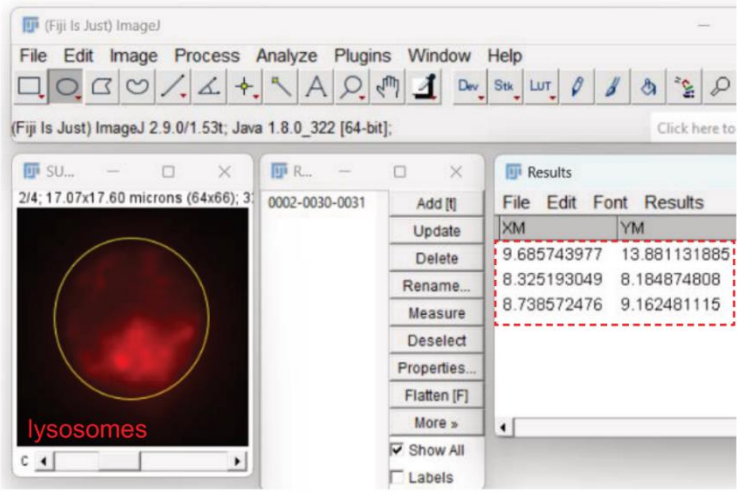

Figure 6

2. Apply the same algorithm mentioned before changing **Cell structure** for **MC**. Thus, the angle (α) is defined by CC-MC **(a)** and CC-BC **(b)**. The angle value is highlighted with a red dashed box in the figure (Figure 7).

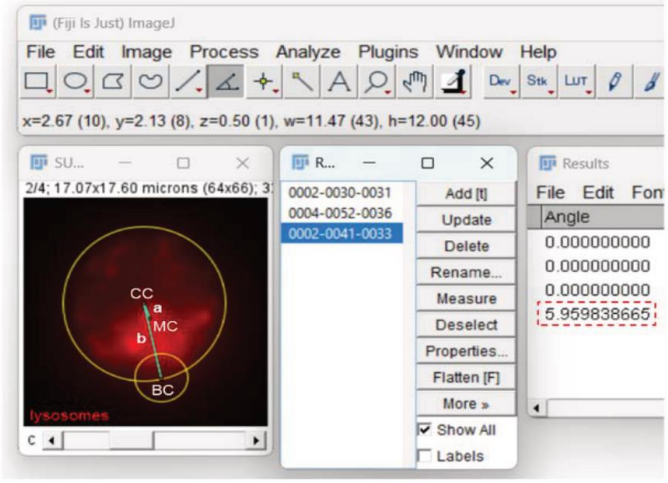

Figure 7

3. Calculate the polarity using the following formula:

$$\text{Polarity Index} = a\frac{\cos(\alpha)}{b}$$

4. Representative Results
   The following image depicts the quantification of polarized organelles that display a dispersed distribution, such as lysosomes (Figure 8). In this case, we use the lysosome center of mass coordinates (Figure 6). The images show that the polarity indexes of lysosome pools reach more positive values over time, indicating that lysosomes are being recruited to the IS during B cell activation (Figure 8).

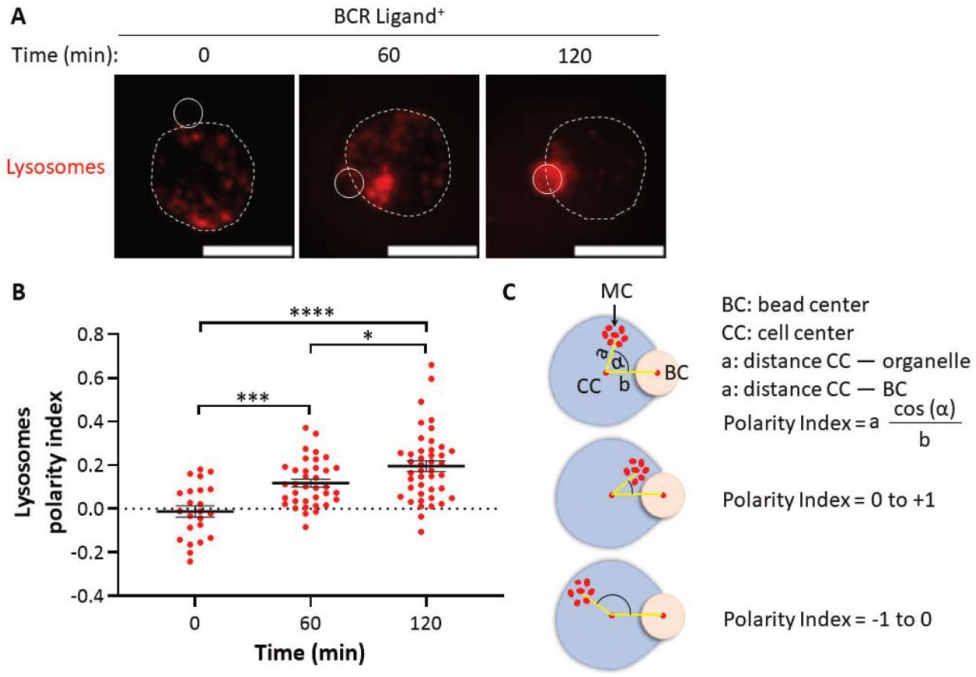

Figure 8: (A) Immunofluorescence staining of Lysosomes (LAMP1) in B cells incubated with BCR ligand+ beads for the indicated times. Scale bar: 10 µm. **(B)** Lysosomes polarity index calculated from images in A. *, $p<0.05$; ***, $p<0.001$ ****, $p<0.0001$; one-way ANOVA with Holm-Sidak's multiple comparison test; $n \geq 23$ cells from three independent experiments. **(C)** Scheme depicting how to calculate the polarity index of lysosomes toward the IS. a = distance between the center of the cell (CC) to the mass center (MC). b = distance from the CC and to the bead center (BC).

4 Characterization of the immune synapse organization of B cells activated on antigen-coated surfaces.

This analysis is used to quantify organelles that are recruited to the IS of B cells activated on an antigen-coated surface. In this example, we will quantify the lysosomes at the IS as a marker of B cell activation. This analysis could also be used to segment and quantify other discrete markers, such as Actin foci at the IS.

4.1 Measuring organelle recruitment at the IS area

1. As a requisite, you must previously cut single cells from the original images. An extra macro is provided for this task (cell_cutter.ijm in GitHub repository). **See Note 12.**
2. The macros will prompt you to select the channel of interest, in this case, we will focus on lysosomes.
3. Then, determine the contact slice between the cell and the surface (IS) and define the cell outline with a cytoskeleton marker (actin

channel in the example). You could use the freehand or circle tool selection to delimit the boundaries. (Figure 9).

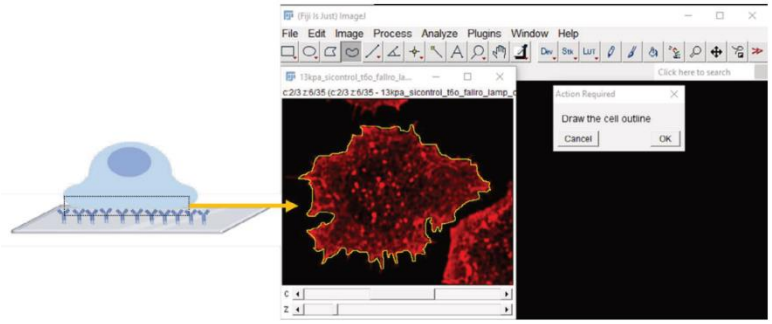

Figure 9

4. Take into consideration the Z plane of interest. The macros will ask you for this number. In this case, it is number 6 (z:6/35 in the image title). Only use entire numbers in this section.
5. Next, the macros will convert the image to 8-bit and the previously outlined cell ROI will be analyzed with "Analyze Particles". We use "size = 0.10 - 4.00 µm2" for lysosome analysis [7]. In Figure 10, LAMP1 signal and segmented particles are shown (left and right images, respectively). **See Note 13.**

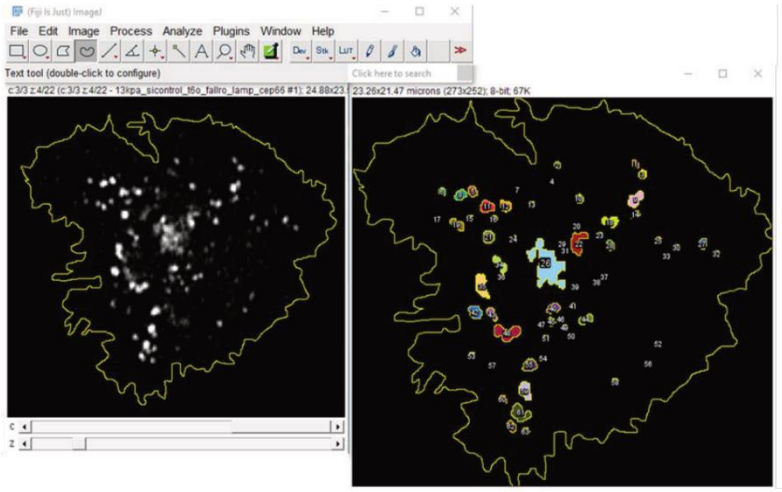

Figure 10

6. The next image in the folder will be opened automatically to proceed with the same steps as before.
7. Finally, Fiji's - imageJ "Log" shows the number and name of images, the area of the cell, the number and area of particles, and the average size of them within the cell. Save this table with results.

8. Representative Results
   The following image depicts the quantification of particles present at the IS. In this case, we measured the number of lysosomes recruited at the IS plane (Figure 11 D) and the formation of actin foci at the IS (Figure 11 B). The images show that the number of lysosome and actin foci at the IS increase over time, indicating the state of activation of the B cell (Figure 11 D and C, respectively).

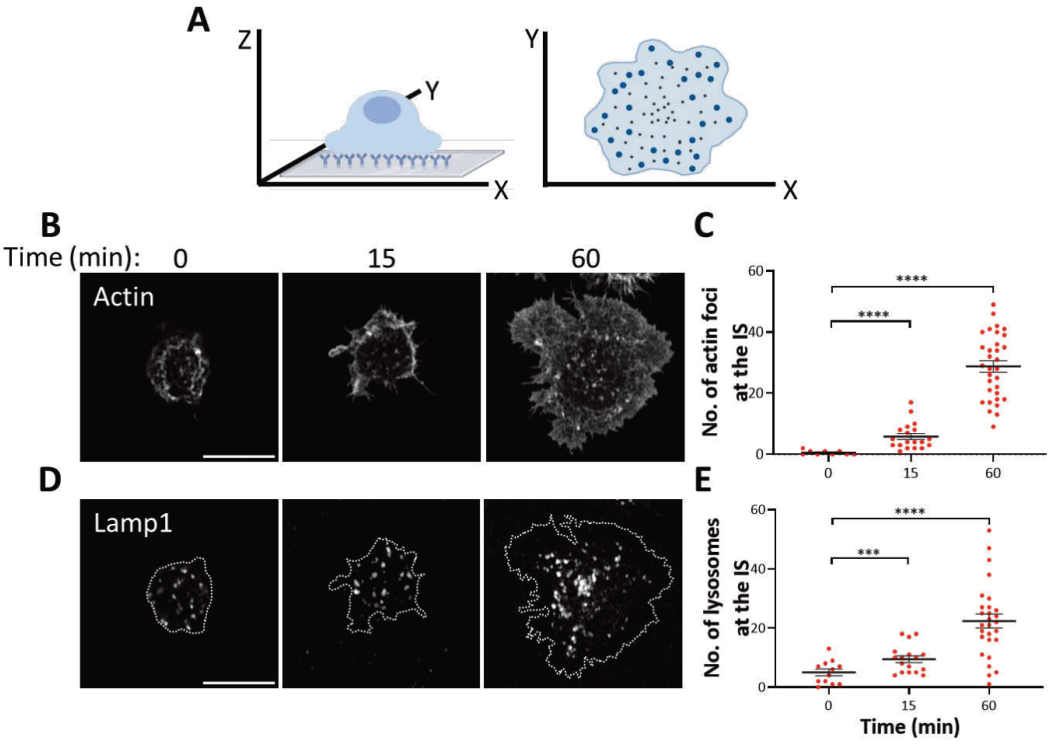

Figure 11: (A) Scheme depicting activation of B cells onto antigen-coated coverslips and representative image of YX planes. **(B-D)** Representative confocal images of actin (Phalloidin) and Lamp1 (lysosomes) in resting (0 min) and activating (15-60 min) conditions. **(C)** Quantification of the number of actin foci at the IS at different conditions. **(E)** Quantification of the number of lysosomes at the IS. N > 10 cells. P < 0.0001; One-way ANOVA with Tukey's multiple comparisons tests. Scale bar = 10 um.

4.2 Measurement of organelle distribution at the IS.

After the activation of B cells, lysosomes are preferentially found in the center of the IS. This feature is often referred to as a marker of activation in B cells, along with other organelles and structures, such as the BCR. To analyze organelle distribution at the IS, we make available the following imageJ macros (2D_distribution_analysis.ijm in the GitHub repository). The following instructions serve as a guide for using and understanding its components. Importantly, the results of these macros can be further processed with an R-language script that

will provide the user with a final .csv file containing the values of the central accumulation of a marker of interest (Rscript_2D_analysis.R in the GitHub repository).

1. Previously cut single cells from the original images. An extra macros is provided for this task (cell_cutter.ijm in the GitHub repository). In addition, generate two folders to organize the images and the results. We recommend naming them "cells" and "results".
2. Run the macros 2D_distribution_analysis.ijm. Before starting the analysis, determine the contact slice and define the cell outline, and press "Ctrl+t".
3. Automatically, the macros will modify the scale of the ROI to the factor you choose. In this example, the ROI was rescaled to 0.4 times the size of the total outline of the cell (center). The ROI will be analyzed with "Analyze Particles". **See Note 14.**

```
50  roiManager("Select", 1);
51  RoiManager.scale(0.4, 0.4, true);
52  roiManager("Select", 0);
53  roiManager("Select", newArray(0,1));
54  roiManager("XOR");
55  roiManager("Add");
56  roiManager("Select", 2);
57  roiManager("Delete");
58  roiManager("Select", newArray(0,1,2));
59  roiManager("multi measure");
```

6. Excel files will be generated for each cell analyzed and automatically saved in the results folder. The respective ROIs of each cell will also be saved.
7. Using the R-script available at the repository, you can generate a final Excel-compatible file that reports the center/periphery ratio of accumulation for each channel present on the images. Calculate the **Ratio** using the following formula:

$$Ratio\ (r) = \frac{Mean\ Fluorescent\ Intensity\ (MFI)\ center}{MFI\ periphery}$$

8. Representative Results
   The following image (Figure 12) depicts the quantification of particles distributed at the IS. In this case, we analyzed lysosome distribution in the IS plane. The images show that lysosomes are equally distributed in the IS plane at early times of activation, but after 60 minutes of B cell activation they are accumulated at the center at the IS.

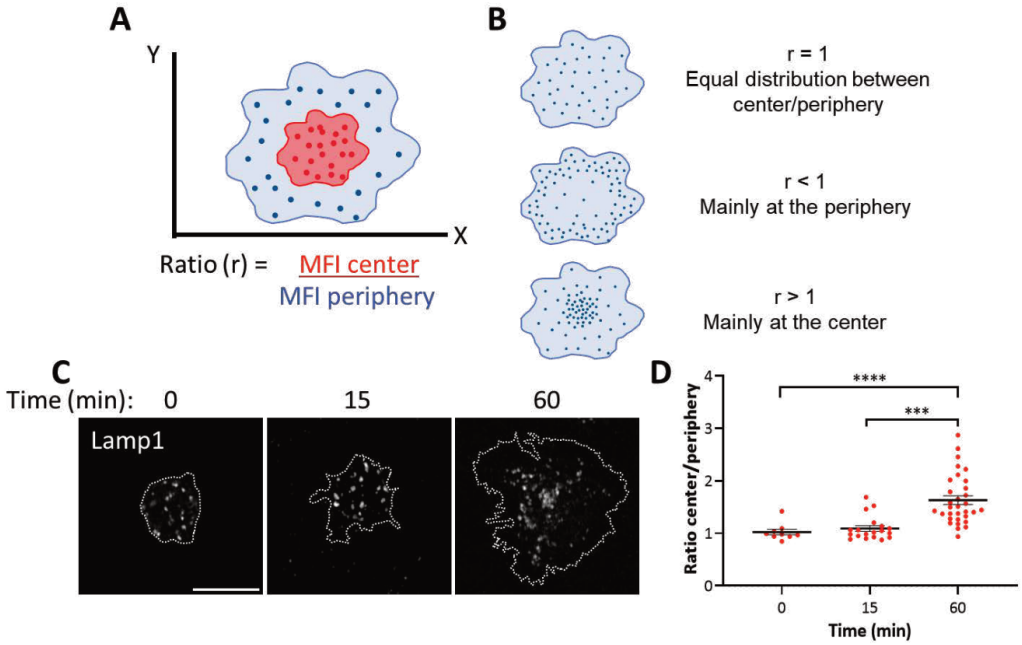

Figure 12 (A) Scheme depicting how to calculate the Ratio (r) center/periphery toward the IS. **(B)** Schematic representation of mean fluorescent intensity (MFI) distribution and r interpretation. **(C)** Representative confocal images of Lamp1 in resting (0 min) and activating (15-60 min) conditions. **(D)** The respective quantification of lysosome accumulation at the center and periphery. N > 10 cells. P < 0.0001; One-way ANOVA with Tukey's multiple comparisons tests. Scale bar = 10 um.

4.3 Measuring organelle distribution in Z planes

This analysis determines the general distribution of fluorescence intensity across the Z-slide of cells seeded over coverslips. We use this measurement to assess the organelle proximity to the immune synapse.

1. To quantify the fluorescence distribution in the Z-slides, first determine the contact slide and then the plane corresponding to the upper limit of the cell.
   Note: It is recommended to cut single-cell images from the contact plane to the top edge of the cell. You can analyze different cells in the same image if all cells are found in the same contact (lower) and upper planes.
2. Draw the cell outline at the contact plane and add the area to the ROI manager with "Ctrl+t."
3. At the ROI manager, click on "Select All" areas and analyze them with the "multi-measure" option.
4. Save the results. From the results table you can filter all measurements, in this case, the Mean intensity of fluorescence and Z-slides of the cell. You can select a channel of interest and filter the data.

5. Representative Results
The following image depicts the quantification of centrosome polarization in B cells activated on antigen-coated surfaces (Figure 12 A). By measuring the fluorescence intensity of the centrosome in all z-slices of the cell we observed that its highest peak of intensity is closer to the IS in activated B cells, while it is equally distributed among z-slices at early times of activation (Figure 12 B-C).

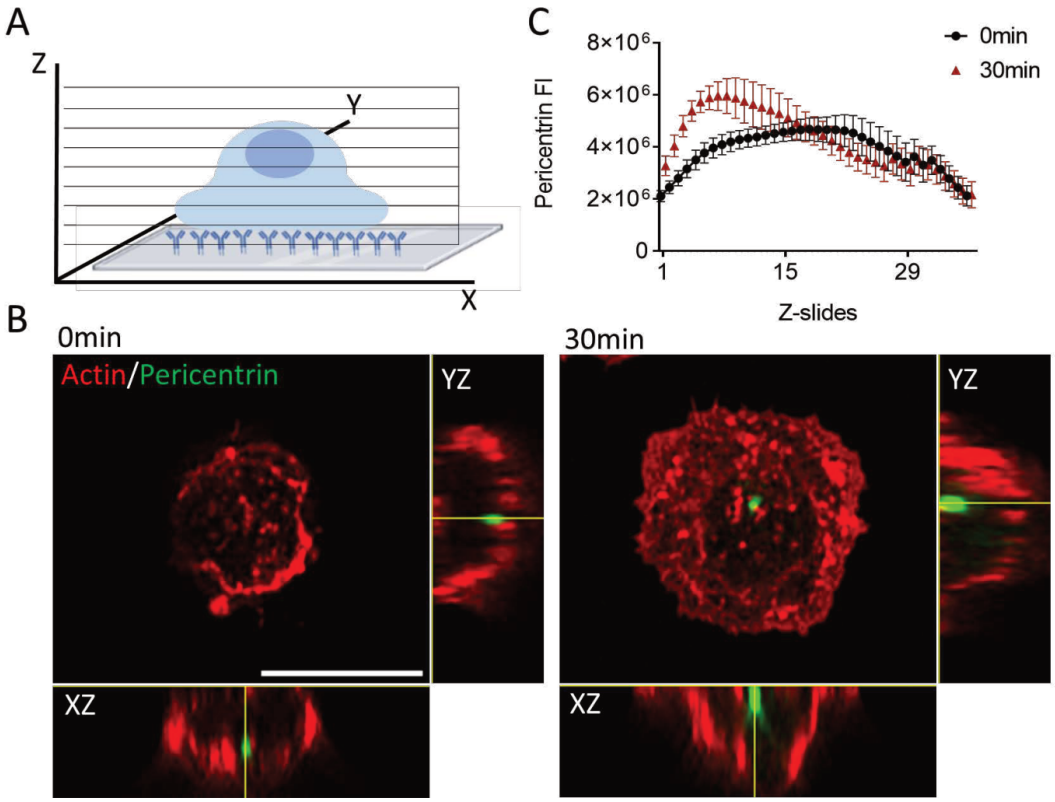

Figure 13: (A) Scheme depicting activation of B cells on antigen-coated coverslips and how to determine the distribution of the signal of interest in the Z plane, and the plot per Z fraction. **(B)** Representative confocal images of B cells labeled actin and pericentrin (centrosome) activated onto Ag-coated coverslips in different conditions, showing the YZ and XZ planes. **(C)** The distribution of pericentrin across the Z plane is represented by a line plot of the fluorescence intensity distribution versus each Z fraction. N = 5 Cells. Mean with SEM are shown.

5 Discussion and Relevance

In conclusion, the analyses presented here represent a significant advancement in analyzing the immune synapse of B cells. By providing detailed information on the spatiotemporal organization of this crucial structure, these methods allow for a better understanding of the mechanisms underlying B cell activation and provides a mean to analyze the effects of extracellular cues on B cell function

[8]. It is important to note, however, that the quality of microscopy imaging is critical to the success of these methods. Any deviation in sample preparation or imaging settings could significantly impact the results.

These methods are compatible with open-source applications, providing accessibility to researchers worldwide. In addition, the raw data derived from the results can be explored to perform further analyses that are not considered here, for example, the study of antigen extraction, processing, and presentation by quantitative measurements of protein recruitment and tracking of intracellular vesicles. Therefore, these methods have the potential to not only contribute to a deeper understanding of the immune synapse of B cells but also in other cell models.

6 Notes

1. The centrosome of B cells can be identified by transfecting cells with a centrin-GFP expression plasmid and actin cytoskeleton can be detected by transfecting cells with a LifeAct expression plasmid. Depending on the needs of the experimental setup, one can use specific antibodies such as gamma tubulin for a discrete labeling of the centrosome. If not available, one can use alpha tubulin and consider the highest intensity point as the MTOC (centrosome).
2. To avoid the binding of ligands to the Fc receptor, use F(ab') or F(ab')2 antibody fragments instead of full-length antibodies.
3. Antigen-coated beads should not be stored for more than one month.
4. Consider preparing the coverslips the day before the assay. UV lamps or plasma can be used to clean the coverslip before use. To assess the ligand activating density on a surface one could label the ligand with a fluorochrome and calculate the mean fluorescence intensity on a region (or bead, depending on the experiment) to ensure homogenous coating.
5. It is important to mix by vortex instead of pipetting up and down because this could reduce the number of beads in the sample, due to their accumulation in the plastic tip of the pipette. Use beads coated with BCR-ligand- as a negative control for each assay. We recommend starting the activation with the longest incubation time and proceeding with the following time points. For shorter times of activation (0 min) you can add thrice the cells, and thrice the amount of beads , meaning 450,000 of cells with 1,350,00 of beads to have a sufficient amount of adhering cells on the coverslip. Calculate intervals of activation for samples such that they are ready for fixation at the same time.

References

1. F. D. Batista and N. E. Harwood, "The who, how and where of antigen presentation to B cells," Nat Rev Immunol, vol. 9, no. 1, pp. 15–27, 2009, doi: 10.1038/nri2454.
2. M.-I. Yuseff, P. Pierobon, A. Reversat, and A.-M. Lennon-Duménil, "How B cells capture, process and present antigens: a crucial role for cell polarity.," Nat Rev Immunol, vol. 13, no. 7, pp. 475–86, 2013, doi: 10.1038/nri3469.
3. M. I. Yuseff et al., "Polarized Secretion of Lysosomes at the B Cell Synapse Couples Antigen Extraction to Processing and Presentation," Immunity, vol. 35, no. 3, pp. 361–374, 2011, doi: 10.1016/j.immuni.2011.07.008.
4. D. Lankar et al., "Syk Tyrosine Kinase and B Cell Antigen Receptor (BCR) Immunoglobulin-Subunit Determine BCR-mediated Major Histocompatibility Complex Class II-restricted Antigen Presentation," 1998. [Online]. Available: http://www.jem.org
5. E. T. Arena, C. T. Rueden, M. C. Hiner, S. Wang, M. Yuan, and K. W. Eliceiri, "Quantitating the cell: turning images into numbers with ImageJ," Wiley Interdiscip Rev Dev Biol, vol. 6, no. 2, 2017, doi: 10.1002/wdev.260.
6. A. Reversat et al., "Polarity protein Par3 controls B-cell receptor dynamics and antigen extraction at the immune synapse," Mol Biol Cell, vol. 26, no. 7, pp. 1273–1285, 2015, doi: 10.1091/mbc.E14-09-1373.
7. M. E. G. de Araujo, G. Liebscher, M. W. Hess, and L. A. Huber, "Lysosomal size matters," Traffic, vol. 21, no. 1. Blackwell Munksgaard, pp. 60–75, Jan. 01, 2020. doi: 10.1111/tra.12714.
8. J. Lagos et al., "Autophagy Induced by Toll-like Receptor Ligands Regulates Antigen Extraction and Presentation by B Cells," Cells, vol. 11, no. 23, Dec. 2022, doi: 10.3390/cells11233883.
9. S. I. Roper, L. Wasim, D. Malinova, M. Way, S. Cox, and P. Tolar, "B cells extract antigens at Arp2/3-generated actin foci interspersed with linear filaments," Elife, vol. 8, p. e48093, 2019, doi: 10.7554/eLife.48093.

6. To decide which fixation method to use, check the antibody/dye data sheet.
7. At this point, coverslips can be stored in 1X PBS in a humid chamber sealed at 4 °C for a maximum of three days. In the image below we illustrate two options for using and crafting the humid chamber; In (a) a drop of PBS or antibody solution lays on top of the coverslip, or, as shown in (b) the coverslip is placed on top of the drop.

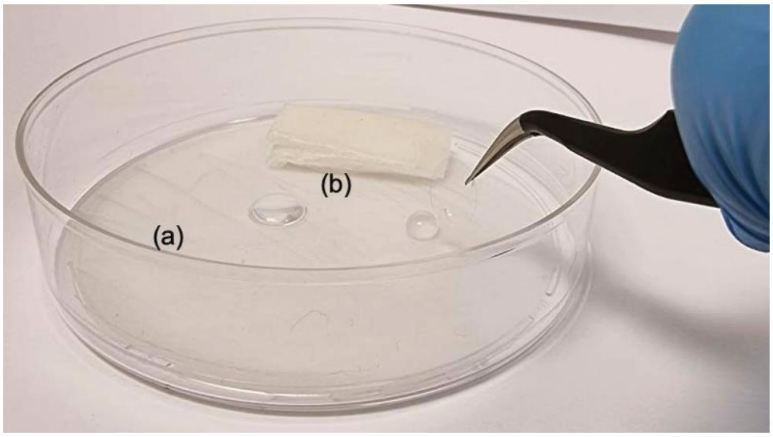

8. To avoid cross-reactivity of the secondary antibody with the B cell receptor of B cells, do not use mouse-derived primary antibodies unless they are fluorescence labeled primary antibodies.
9. Consider using an "anti-fade" mounting reagent (see the Table of Materials).
10. When using a confocal microscope, we recommend taking 0.2 µm thick stacks when acquiring three-dimensional (3D) images. This allows the analysis of the cell using z-stacks analysis This algorithm can be used for cell structures or organelles observed as discrete markers.
11. It is recommended to analyze individual cells because the plane of interest may not be the same for all cells. In the GitHub repository the user can find examples for testing the macros and scripts provided.
12. You can modify the particle size depending on your interests. For example, we use "size=0.10 - 0.50 µm2" for actin foci analysis [9].
13. You can modify the ROI scaling depending on your interests. In this case, we use the 0.4 scale factor to analyze a specific central region and to discriminate organelles separated from actin enriched areas. The previous is based in the knowledge that the immune synapse of B cells is characterized by three concentric regions: the central supramolecular activation cluster (cSMAC) in which BCRs-ligands are concentrated, the peripheral SMAC (pSMAC), which contains adhesion molecules such as LFA1, and the distal SMAC (dSMAC) in which actin is enriched.

Additional - Manuscript 3: Endolysosomal vesicles at the center of B cell activation

This manuscript, in which I participated as a co-first author, corresponds to a literature review aimed at updating and integrating knowledge about lysosomes and lysosome-related organelles in the context of immune synapse formation in B lymphocytes.

REVIEW

Endolysosomal vesicles at the center of B cell activation

Saara **Hämälistö**[1,2,3,#], *Felipe Del Valle Batalla* [4#], *María Isabel Yuseff*[4§], *Pieta K Mattila*[1,2,3§]

Endolysosomal vesicle systems maintain cellular homeostasis by processing and delivering internalized cargo to the acidic lysosome population that serves as a degradation station. However, lysosomes have also developed various additional functions which cells of the immune system exploit to carry out their specific tasks. In this review, we will discuss lysosome and lysosome-related organelle function with a special focus on B lymphocytes during their activation process, such as antigen extraction and processing. Increasing evidence shows that some vesicles are also active outside of the cell, either proteolytically or as secreted extracellular vesicles. We believe that the intricate functions of the endolysosomal vesicles in B cells, but also in other specialized cells of the immune system, pose an interesting frontier for future research.

Introduction

B cells fill a key position in the adaptive immune system: they are the only cells capable of producing high-affinity antibodies against invading pathogens [Batista and N. E. Harwood , 2009]. During their maturation, B cells migrate from the bone marrow to secondary lymphoid organs, where they await to get activated by antigens (Ag). Via their unique B Cell Antigen Receptor (BCR), B cells recognize Ag either as soluble structures, typically immune complexes, or displayed on antigen-presenting cells (APCs) such as macrophages or dendritic cells, which triggers the formation of the intricate activatory cell-cell contact called immune synapse (IS) (Kuokkanen et al., 2015; Spillane & Tolar, 2018; Yuseff et al., 2013). Engagement of the BCR triggers receptor-mediated Ag internalization, followed by intracellular processing into peptides that are loaded on major histocompatibility class II complexes (MHC-II). The subsequent presentation of antigenic peptides activates cognate T-helper cells, which, in exchange, provide signals of survival and differentiation to B cells, leading to the generation of antibody-producing plasma cells. Various specialized endolysosomal vesicles play a key role in the Ag processing but also, for example, in Ag extraction by undergoing localized exocytosis at the IS (Yuseff et al., 2011). Our understanding of the different vesicle pools, their roles, and connections, remains particularly poor in lymphocytes and studies are challenged by the small and dynamic nature of these cellular structures.

To maintain cellular homeostasis, the highly heterogeneous endolysosomal vesicles carry cargo between various cellular compartments or redirect internalized cargo to different destinations for degradation (Bonifacino & Neefjes, 2017). At the same time, lysosomes have recently been described with important signaling functions coupled to cell death and metabolism, for example (Ballabio & Bonifacino, 2020; Holland et al., 2020; Lamming & Bar-Peled, 2019; Perera & Zoncu, 2016). This represents an active and interesting research field as we are only in the beginning to gain understanding of the breadth of the lysosomal heterogeneity, and their roles in cellular signalling and communication with other organelles (Ballabio & Bonifacino, 2020). In addition to functioning as messengers inside the cell, increasing evidence shows that some endolysosomal vesicles are also active in the extracellular space. The secretion of extracellular vesicles (EVs) is often increased upon cell death or cell activation. However, their role in cellular processes and intercellular communication, in the immune system or B cells particularly, remains largely enigmatic (Buzas, 2022).

[1] Institute of Biomedicine, and MediCity Research Laboratories, University of Turku, Finland
[2] Turku Bioscience, University of Turku and Åbo Akademi University, Turku, Finland
[3] InFLAMES Research Flagship Center, University of Turku
[4] Laboratory of Immune Cell Biology, Department of Cellular and Molecular Biology, Pontificia Universidad Católica de Chile, Santiago, Chile
[#] Equal contribution
[§] Corresponding author

Corresponding authors:
Pieta Mattila: pieta.mattila@utu.fi
Maria Isabel Yuseff: myuseff@bio.puc.cl

Keywords: Adaptive immune system, B cells, antigen extraction, antigen processing, lysosomes, lysosome-related organelles, extracellular vesicles

In this review, we will cover what is currently known about the functions of lysosomal vesicles in B cells and how they are involved in Ag extraction and processing during early B cell activation, also considering their novel roles as signaling platforms related to cell homeostasis. We also discuss other emerging functions of both endolysosomal vesicles and the highly intriguing EVs.

Lysosome structure and maturation

While lysosomes are generally defined as intracellular vesicles carrying degradative acid hydrolases, recent studies promote them as a heterogeneous pool of vesicles that differ in their subcellular localization, acidity, content, and signaling function, as well as hybrid organelles forming through fusion/fission and "kiss and run" events (Bouhamdani et al., 2021). Lysosomes are found as hundreds of vesicles in all mammalian cells and their size can range between ~50 to 1000 nanometers. To this day, close to 200 different proteins are identified on the lysosomal membrane with various structural or signaling roles (Ballabio & Bonifacino, 2020). Type 1 proteins, such as lysosomal associated membrane protein-1 and -2 (LAMP-1 and LAMP-2), CD63 (LAMP-3), and LIMP-2 are the most abundant, constituting ~50% of all transmembrane (TM) proteins on lysosomes (Eskelinen, 2006; Gao et al., 2017). Owing to the transmembrane protein complexes that have accessible cytosolic domains, lysosomes act as scaffolds for transport machinery, signaling proteins, and other effector molecules (Inpanathan & Botelho, 2019). The heavily glycosylated LAMP molecules form a luminal glycocalyx structure and counteract the degradative actions of lysosomal acid hydrolases, thus helping maintain the barrier function of the membrane. Interestingly however, this robust shielding mechanism can be modulated according to altered physiological situations; in mitosis, the architecture changes so that the expression of lysosomal membrane proteins and proteolytic cathepsin enzymes are downregulated, the lysosomal pH increases and the limiting membranes become more fragile without compromising the cell homeostasis, simultaneously allowing a regulated enzymatic release to the nuclear region (Stahl-Meyer et al., 2022). This suggests that the lysosome regulation can respond to cell-intrinsic cues by tuning down protein expression and/or functions, in this case, to shield the exposed genomic content from degradative enzymes.

In general, the expression levels of the most prominent lysosomal proteins are regulated by the transcription factor EB (TFEB), which plays a critical role in boosting lysosomal biogenesis or exocytosis, which involves lysosome fusion to the plasma membrane (PM) and extracellular secretion of lysosome content into the extracellular space (Medina et al., 2011) in its inactive state, TFEB is localized on the lysosomal membrane, where it is phosphorylated by the mammalian target of rapamycin complex 1 (mTORC1) (Medina et al., 2011; Settembre et al., 2012). When cellular nutrient levels are low or upon cellular stress, mTORC1 is inhibited, leading to the dephosphorylation of TFEB and its translocation into the nucleus. There, TFEB can activate the expression of genes involved in the formation of new lysosomes, which in turn can lead to increased recruitment of lysosomes to the PM and promote Ca2+ -driven lysosomal exocytosis by activating the lysosomal Ca2+ channel mucolipin receptor MCOLN1(Kim et al., 2019).

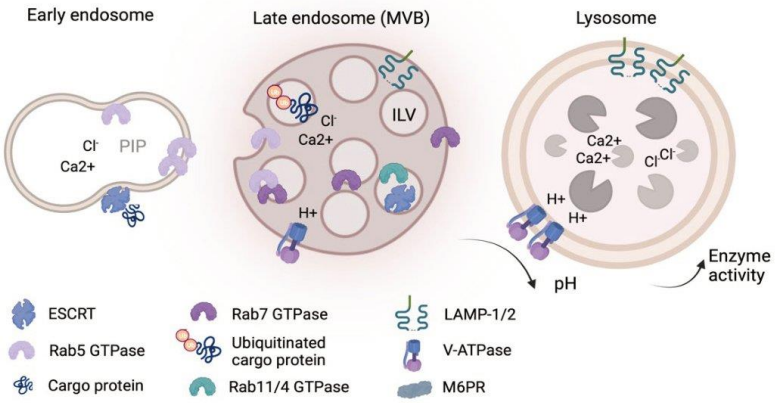

Figure 1. **The endosome maturation in a nutshell.**
During endosomal maturation, in the early endosomes (EE) the main GTPase Rab5 is replaced by Rab7 to trigger maturation into late endosomes (LE). The size of the endosomes increases which is finely balanced by e.g. phosphoinositide lipid (PIP) levels. Molecules such as LAMPs and the V-ATPase are transported from the trans-Golgi to the maturing endosomes via the mannose-6-phosphate receptor (M6PR): the V-ATPase, as the main H+ pump on the late endosomes and lysosomes, generates the acidic environment. The membrane invagination process is driven by the timely delivery of the cytoplasmic ESCRT complex proteins and clathrin to the limiting endosomal membrane (i.e., the membrane facing the cytoplasm) thereby creating intra-luminal vesicles (ILVs) inside multivesicular bodies (MVB) or late endosomes. Here, the ubiquitinated membrane proteins stemming from endocytic or Golgi membranes are sorted into the growing closed ILVs. The ILVs can be released to the extracellular space as exosomes (a subtype of extracellular vesicles) or the MVB can generate Rab4/Rab11-rich recycling endosomes or, finally, fuse with an existing lysosome to fulfill its degradative function. The ion concentration during the maturation process steadily increases and the acidic environment allows for the optimal enzyme activity inside the lysosomes.

The classical model of the endosomal maturation pathway, leading to the formation of conventional lysosomes, stems from the most studied epithelial cell types. However, endolysosomes are diverse and their maturation pathways rely on the cell type as well as internalized cargo (Huotari & Helenius, 2011). The maturation of the endocytic vesicles towards late endosomal or lysosomes involves several steps; however, the timing and sequential order of events are not still entirely clear (Podinovskaia et al., 2021). As the classical model of endolysosomal maturation has been well reviewed in the literature (Huotari & Helenius, 2011) , we will not go into the details of it here. Briefly, early endosomes (EE) mature into late endosomes (LE) upon switching the EE-specific Rab5 into LE-specific Rab7 (Rink et al., 2005) and the invagination of the EE membrane that forms intraluminal vesicles (ILVs) leading to formation of multivesicular bodies (MVB) or the late endosomal pool. This process of endosomal maturation involves dynamic and continuous rearrangements of the protein composition at the endosome limiting membranes (Bouhamdani et al., 2021). The ILVs can be destined to the recycling pathway, the limiting membrane can be fused with the PM to induce the extracellular release of ILVs (as exosomes), or the multivesicular body can fuse with an existing lysosome to convert into a classical lysosome.

Critically important for endolysosomal maturation is acidification, which gradually increases starting from the early endosomes (pH 5.9-6.8) to the late endosomes (pH 4.9-6.0) and lysosomes (pH 4.5-5) and is linked to the progression of the Rab5/7 switch (Hu et al., 2015; Podinovskaia et al., 2021). The acidic environment is generated by increasing the expression of the V-ATPase H+ pump on the endosomal membrane. From the trans-Golgi network, the transport of the V-ATPase is mediated, by the lysosome-targeting mannose 6-phosphate receptor (M6PR) (Braulke & Bonifacino, 2009 where coordinated trafficking to and from lysosomes is crucial to maintain organelle fitness (Ballabio & Bonifacino, 2020; Huotari & Helenius, 2011; Saftig & Klumperman, 2009).

The morphology of the endolysosomes undergoes major transformations during maturation. In short, the EEs elongate with tubular extensions, that are lost upon the maturation process, and the LEs and lysosomes acquire an oval-to-round morphology and grow in size (Huotari & Helenius, 2011). The lysosome size is partially maintained by lipids, such as phosphoinositide phosphates (PIPs) and both too low or too high phosphatidylinositol-3,5-biphosphate (PI(3,5)P2) levels result in swelling of the endolysosomal structures (Bouhamdani et al., 2021; Podinovskaia et al., 2021). Although vesicles at different stages may have similar protein markers and localization, the end-stage, fully mature lysosomes are distinguished by their high hydrolase content and electron-dense appearance, which sets them apart from acidic late endosomes (Huotari & Helenius, 2011).

Lysosome positioning and function

Canonically, lysosomes are associated with actin and microtubule cytoskeleton and can be found distributed across the cell depending on the homeostatic conditions (Oyarzún et al., 2019) Haga clic o pulse aquí para escribir texto.. While short distance endolysosomal vesicle mobility is typically achieved by local actin reorganization (Cordonnier 2001), for long displacements, lysosomes move along the microtubule network via the action of motor proteins such as kinesins and dyneins and their adaptors (Gennerich, 2009; Ballabio & Bonofacino 2020). Both kinesin and dynein molecular motors use ATP for their action. Kinesins move endolysosomal vesicles in an anterograde fashion toward the dynamic microtubule plus ends (Serra-Marques, 2020). Kinesin functions are mediated by the action of small GTPases that also confer molecular identity or subcellular localization to different vesicles. Conversely, dyneins move cargoes in a retrograde fashion, guiding them towards the minus ends of the microtubule network, i.e., towards the microtubule organizing center (MTOC) (Gennerich, 2009].

Interestingly, the subcellular positioning of lysosomes is also linked to their acidity and motility, where peripheral lysosomes are shown to have higher, less acidic pH than the ones residing perinuclearly (Johnson et al., 2016). Various signals or conditions affect lysosome positioning. For example, nutrient deprivation can trigger the lysosomes to accumulate in the perinuclear region whereas nutrient-rich environments promote peripheral localization (Ballabio & Bonifacino, 2020; Korolchuk et al., 2011). However, little is known about how the lysosome positioning is tuned in B cells to regulate the functional properties of these organelles upon immune response. Recently, in B cells, an autophagic regulator Atg5 was shown to promote lysosome polarization to the IS and the recruitment of Ag to MHCII vesicles (Arbogast et al., 2018). Interestingly, toll like receptor ligands, such as lipopolysaccharide (LPS), were shown to restrict lysosome repositioning to the IS of B cells by triggering autophagy-dependent degradation of GEF-H1, a Rho GTP exchange factor required for stable lysosome recruitment at the synaptic membrane (Lagos et al., 2022). The BCR activation-directed autophagic signature can also be regulated in vivo: it was recently proposed that autophagy induction is most prominent in the germinal center (GC) B cells (Martinez-Martin et al., 2017; Raza & Clarke, 2021). The autophagy machinery could thus play a central role in finetuning the specialized endolysosomal features in B cells.

Antigen processing compartments and other lysosome-related organelles

Endolysosomes within different immune cells display unique features. One such key feature is intracellular processing of extracellular-derived Ag for peptide-MHCII presentation, key to trigger generation of both B and T effector cells responsible for the adaptive immune response. This process involves specialized lysosomal Ag processing compartments equipped with carefully controlled proteolytic enzymes. While the vesicular identity and trafficking involved in Ag processing remain to be fully understood, the associated biochemical chain of events is relatively well characterized, mainly by studies in dendritic cells and macrophages. In the endoplasmic reticulum, the newly synthesized MHCII complexes with the invariant chain (Ii), which protects the peptide-binding groove

and provides targeting signals directing the complex to the Ag processing compartments (Roche & Furuta, 2015). Reported to occur in the ILVs of the MBV/LEs, the sequential proteolytic processing of Ii is initiated and finally leads into a short CLIP peptide that remains to occupy the peptide-binding groove of MHCII (Roche & Furuta, 2015). Finally, CLIP is removed by HLA-DM (H2-M in mice), or HLA-DO (H2-O in mice) in mildly acidic compartments, allowing for Ag-derived peptide binding to the MHCII and subsequent exit of the complex to the plasma membrane for peptide antigen presentation. Processing of antigens occurs essentially by the same enzymes that process the Ii, the most prominent being asparaginyl endopeptidase and cathepsins (Manoury et al., 1998; Shi et al., 1999).

With their acidic and proteolytic environment, the Ag processing compartments show clear lysosomal character, yet their key role is to generate critical protein complexes for presentation rather than simply degrade cargo. How the endolysosomal system is adopted to this function remains unclear.

The Ag processing compartments within B cells undoubtedly share similarities with those of other antigen-presenting cells. However, they are unique in their capability of presenting specific antigens, originating from the engagement of the BCR, with high efficiency, allowing very small quantities of antigen to elicit efficient immune responses (Lanzavecchia, 1985; Rastogi et al., 2022) . Interestingly, our recent studies indicate that BCR-mediated Ag processing occurs along the entire endosomal route starting with the rapid fusion of internalized Ag into peripheral acidic compartments together with plasma membrane-derived MHCII (Hernández-Pérez et al., 2020). We also observed that the EE and LE markers often overlapped in the Ag-containing compartments in B cells, which could further reflect that the immune cell endolysosomal system has adapted hybrid forms to fulfill their specialized functions in antigen processing (Hernández-Pérez et al., 2020).

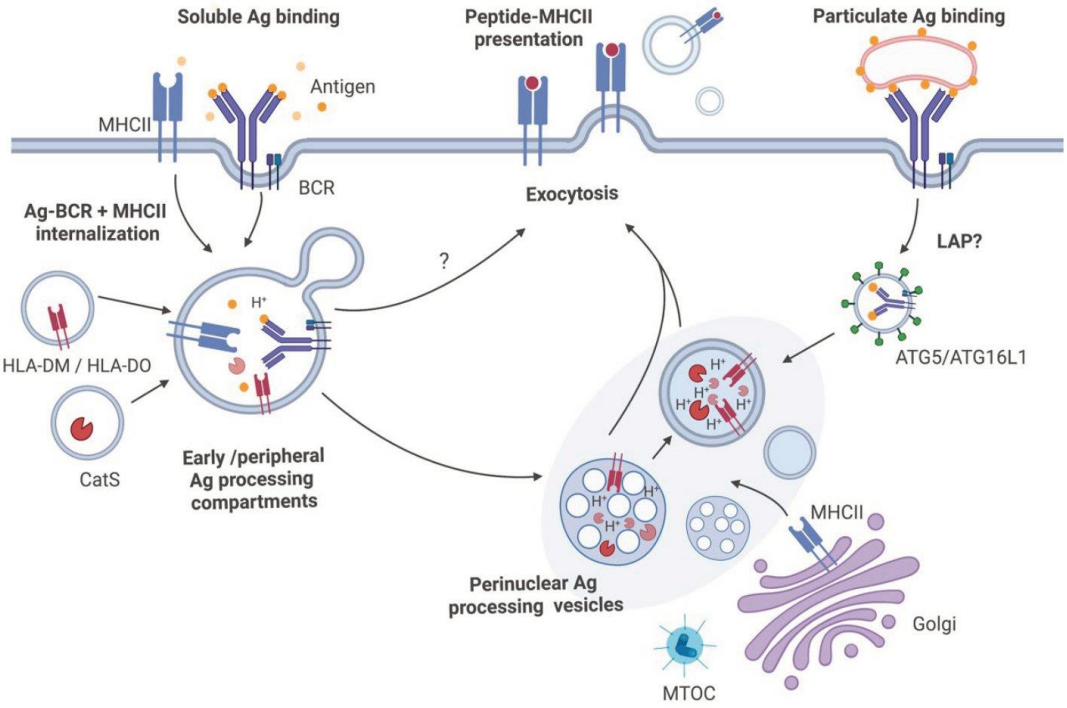

Figure 2. **Antigen processing pathways in B cells.**
Perinuclearly located MHCII$^+$ vesicles of lysosomal or multivesicular nature are considered as the main Ag processing compartments, where Ag-derived peptides, after digestion by cathepsins, are loaded on MHCII in a process tightly regulated by molecules such as the H2-M and H2-O chaperones. Peptide-MHCII complexes are then directed for cell surface presentation via exocytosis or they can also be secreted as extracellular vesicles. Two specialized pathways have been highlighted as possible routes of targeting the BCR-bound Ag to the Ag processing vesicles. For soluble Ag, simultaneous targeting of Ag-BCR and plasma membrane-derived MHCII to the peripherally located acidic early Ag processing vesicles has been shown (Hernández-Pérez et al., 2020). As these early vesicles already show the key features of Ag processing compartments, some peptide-MHCII could be directed to the cell surface already from them. Surface-bound antigens, on the other hand, have been proposed to be internalized in an ATG5-dependent process, presumably involving a form of LC3-associated phagocytosis (LAP) (Arbogast et al., 2018). Overall, it is likely that the Ag processing endolysosomes form a heterogenous gradient with varying amounts of the protein components necessary for peptide-MHCII generation. The nature of these vesicular compartments is likely to depend on the status or type of the B cell and the Ag.

Ag processing compartments are an example of various lysosome-related organelles (LROs): the LROs resemble lysosomes with their low pH and the presence of hydrolases but have additional unique characteristics (Delevoye et al., 2019; Watts, 2022). For instance, LROs in cytotoxic T cells contain a distinct pool of hydrolytic enzymes, perforin and granzyme B, which are released at the synaptic membrane after LRO fusion to the PM to kill their target cells (Catalfamo & Henkart, 2003). Another example are the secretory granules of mast cells, bearing similarity also to the granules of NK cells and platelets, that release e.g. histamine and lysosomal hydrolases to initiate an inflammatory response (Azouz et al., 2014).

As the function of immune cells is to be sensitized by pathogenic products, it is not surprising that upon exposure, lysosomes are remodeled in different ways. Various vesicle-linked proteins have been shown to alter their intracellular positioning, for instance, upon BCR engagement (Music et al., 2022; Awoniyi et al., in press). However, more efforts are required to dissect the functions of the different endosomal players in B cell activation. A proteomic analysis of isolated lysosomes shows how exposure to different pathogens to murine macrophages alters the lysosomal protein expression profile depending on the pathogen used (Gao et al., 2017). For example, the relative abundance of transmembrane proteins Lamp-1/Limp-2 or digestive hydrolases Cathepsin K or L was shown to be adjusted in a pathogen-specific manner, suggesting alternative regulatory mechanisms depending on the pathogen species and the nature of the external stimuli. Also, in macrophages and dendritic cells, activation by LPS drives microtubule-assisted lysosome tubulation and surface expression of MHCII (Saric et al., 2016) . In dendritic cells, the exclusive expression of Lamp-3 (or CD63) in the lysosomes and the cell surface promotes the delivery of peptide-MHCII+ compartments to the PM as well as dendritic cell migration to draining lymph nodes(Li et al., 2023) . Whether Lamp1 and Lamp2, typically pre-assumed to decorate the same vesicular compartments, also regulate differential endolysosomal functions, analogously to Lamp3, in immune cells, is not known.

Lysosomes facilitate antigen extraction at the IS during B cell activation

In B cells, Ag recognition also boosts lysosome exocytosis, releasing digestive hydrolases to facilitate Ag extraction from antigen presenting cell surface (Maeda et al., 2021). Here, cell signaling and Ag extraction are tightly coordinated in the synaptic structure formed between the B cell and Ag presenting surface(Batista & Harwood, 2009; M. I. Yuseff et al., 2011). During IS formation, B cells undergo rapid cytoskeletal remodeling, leading to changes in cellular morphology, and directed trafficking of polarity proteins and vesicular organelles to the IS to help extract the Ag (Bolger-Munro et al., 2019) Haga clic o pulse aquí para escribir texto.. In addition to the lamellipodia-like actin-based spreading, myosin-dependent contraction helps accumulate the BCR-bound Ag at the center of the IS for internalization (Bolger-Munro et al., 2019; Kuokkanen et al., 2015; Treanor et al., 2009) . The Ag-BCR microclusters form and accumulate in the middle of the IS within a couple of minutes upon Ag recognition (Bolger-Munro et al., 2019; Kuokkanen et al., 2015). Finally, the antigen is internalized via Clathrin-mediated endocytosis or a recently reported Fast endophilin-mediated route (McShane & Malinova, 2022; Stoddart et al., 2002) . In the case of B cell activation with soluble Ag, clathrin-mediated endocytosis is preferred.

Lysosomes have a crucial role in facilitating antigen extraction at the IS to enable efficient B cell activation, but how are the lysosomes targeted to the IS? During the first steps of IS formation, the centrosome becomes detached from the perinuclear region, in a process mediated by the depolymerization of actin and proteasome activity [Ibañez-Vega 2019, 2021]. Then, the centrosome is polarized to the Ag-BCR contact zone at the PM, guided by the activity of conserved polarity proteins, such as PAR3/aPKC/Cdc42 (M.-I. Yuseff et al., 2013). The re-orientation of the microtubule network enables the recruitment of lysosomes and other functional cellular compartments to the IS, using molecular motors such as dyneins (Reversat et al., 2015; Wang et al., 2017). After polarization to the IS, lysosomes fuse with the PM and secrete their acidic content to promote Ag extraction and presentation to T Cells (Maeda et al., 2021; M. I. Yuseff & Lennon-Duménil, 2015). Lysosomal exocytosis, mainly described to occur via LAMP-1, allows the release of vesicle content e.g. hydrolases to the extracellular space: this can be detected as an exposure of the luminal epitope of LAMP-1 at the extracellular side of the plasma membrane where the epitope is not normally detected [Andrews, 2017]. LAMP1+ endolysosomes in B cells present the V-SNARE VAMP-7 (also known as Ti-Vamp), that mediates fusion with the plasma membrane and lysosome exocytosis, and thereby facilitates antigen extraction, processing, and presentation (Obino et al., 2017) .Lysosome exocytosis in B cells has also been shown to involve permeabilization of the PM to facilitate efficient Ag extraction in a mechanism that requires BCR signaling and non-muscle myosin II activity (Maeda et al., 2021); in brief, the higher the affinity of antigen to the BCR, the more permeable the PM becomes and the higher the rates of lysosomal exocytosis are, measured by LIMP-2 at the cell surface.

Another critical component of the exocytic machinery at the IS is the Exocyst complex. This protein complex was identified by comparing the differential enrichment of centrosome-linked proteins of activated and resting B cells, where four of its 8 subunits were found to be enriched in centrosome fractions isolated from activated B lymphocytes (Sáez et al., 2019). Upon activation, B cells upregulate acetylation and stabilization of their microtubule network in the vicinity of the MTOC. This releases Exo70, a subunit of the Exocyst complex, and GEF-H1 from microtubules, which become associated with the synaptic membrane enabling successful docking of lysosomes at the IS. Cells silenced for Exo70 and GEF-H1 display defective Ag extraction, processing, and presentation (Sáez et al., 2019).

Thus, lysosomes have special roles in the IS and the subsequent B cell activation. However, more mechanistic insight on lysosome positioning and dynamics (fusion/fission) while establishing an effective IS in B cells, remains to be discovered.

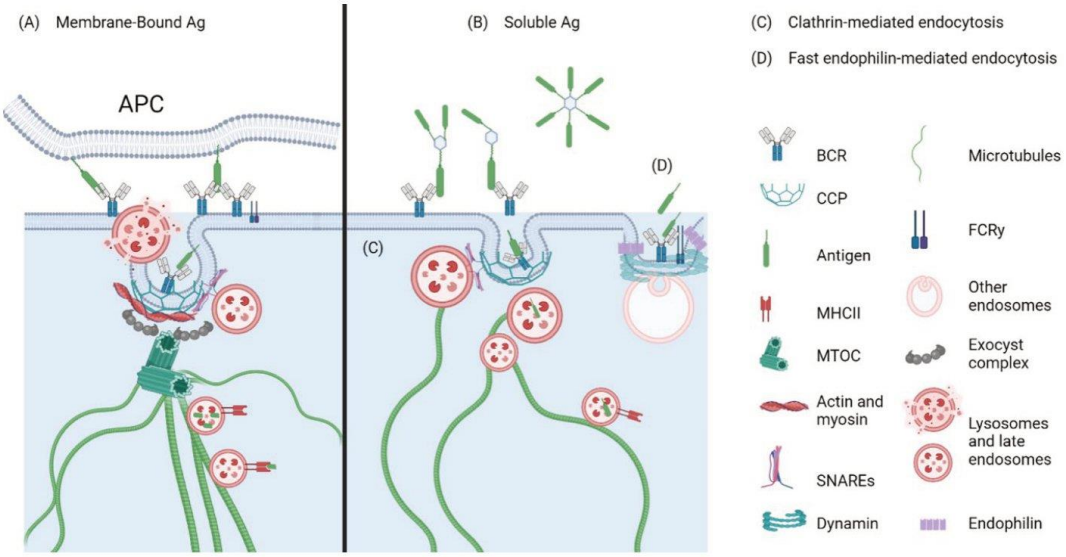

Figure 3. **Lysosome contribution to antigen extraction and internalization at the immune synapse (IS).**
When B cells encounter membrane-bound antigens **(A)**, they rely on the balanced action of actin- and myosin-mediated forces and lysosomal exocytosis to extract and internalize the Ag and establish an IS. Lysosomes move on microtubule tracks directed by the MTOC and fuse with the plasma membrane with the aid of the exocyst complex and the effective binding of SNAREs. They secrete their acidic content to the synaptic cleft promoting further internalization and processing of antigens. In soluble Ag conditions **(B)** the Ag is primarily internalized primary by clathrin-mediated endocytosis **(C)**. The binding of clathrin induces membrane curvature and the formation of clathrin-coated pits (CCPs). These CCPs invaginate and separate from the plasma membrane, forming clathrin-coated vesicles (CCVs) that contain BCR-antigen complexes. These CCVs subsequently fuse with late endosomes, enabling antigen processing and presentation to other immune cells. Alternatively, B cells employ fast endophilin-mediated endocytosis as a specialized pathway for ligand-triggered signaling receptors **(D)**. Within specific membrane patches primed by endophilin proteins, BCR-Ag binding leads to the induction of membrane curvature facilitated by endophilin proteins. Dynamin then promotes the scission of the curved membrane, resulting in the formation of an intracellular vesicle carrying the BCR-antigen complex.

Emerging roles of endolysosomal compartments in extracellular vesicle release and cellular signaling

In addition to the lysosomes secreted for antigen extraction, B cells are an intense source of EVs, the destiny and diversity of which is still to be discovered (Kato et al., 2020; Muntasell et al., 2007). EVs are often considered to originate from the late endosomal ILVs as exosomes or bud from the PM, but are also found to display lysosomal features. B cells have been shown to secrete Ag presenting exosomes containing lysosomal components such as LAMP-1, MHCI and MHCII, and costimulatory molecules, which could induce Ag-specific CD4+ T cell response or cytotoxic CD8+ T cell response (Kato et al., 2020) . EVs can mediate specific signaling functions in the immune microenvironment making cell communication via EVs an intriguing area of research that may bring forth novel therapeutic possibilities (Kugeratski & Kalluri, 2021). For instance, EVs secreted by malignant lymphoma cells Balm-3, Su-DHL-4, and OCI-Ly1 can shield the tumor cells from anti-CD20 antibody (rituximab) -mediated destruction via sequestering the antibodies on the EV-tethered CD20 (Aung et al., 2011). By silencing or inhibiting the LRO-associated ABCA3, which induces the production of EVs, the cells become more vulnerable to the rituximab treatment (Aung et al., 2011). Furthermore, the Fas ligand expressed on B cell-derived exosomes induces apoptosis in CD4+ T cells (Eberl et al., 2001). On the other hand, EVs can alter the activation status of healthy donor B cells as shown by decreased global tyrosine phosphorylation and reduced proliferation (Rincón-Arévalo et al., 2022) linkages between the endolysosomal system and the release of EVs are still very poorly understood and more studies are needed to provide insights into the signals triggering EV release.

Besides their various degradative functions, the emerging intriguing roles of lysosomes as “signaling hubs” and metabolic sensors are building up (Ballabio & Bonifacino, 2020; Perera & Zoncu, 2016). Acting as hubs, they integrate metabolic inputs and direct organellar crosstalk with emphasis on lysosome to nucleus signaling pathways mediated by e.g. mTORC1 (mammalian target of rapamycin), AMPK (AMP-activated protein kinase), and lipid metabolism. Lysosomes recruit mTORC1 or AMPK or other moieties upon unfavorable energy conditions. The mTORC1 senses the amino acid availability in the cytoplasm and can also interact with the lysosomes directly. As a result, if needed, specific lysosomal proteases will release basic amino acids e.g. arginine from the lysosomal storage as shown by yeast vacuole studies (Kitamoto et al., 1988). Also, v-ATPase can read amino acid levels inside the lysosomes and convey the information to mTORC1. The energy levels are equally monitored and here,

one major player is AMP-activated protein kinase AMPK that responds to glucose levels and binds to lysosomal membrane (Perera & Zoncu, 2016). Lipids represent a third major group of signaling molecules and the most known process is the endocytic uptake of LDL and the following breakdown of cholesteryl esters (CE) by acid lipases to generate cholesterol (Chang et al., 2006). How these signaling functions are adapted to serve B cell activation is an interesting research question, particularly considering the recently discovered metabolic rewiring of lymphocytes upon their activation and differentiation cascade (Chapman & Chi, 2022).

Discussion and future perspectives

The small and crowded cytoplasmic space challenges the studies of the complex and specialized endolysosomal features of B cells (Hernández-Pérez & Mattila, 2022) . Given this spatial restriction and high density of vesicles together with the highly specialized functional needs of B cells, it is not surprising that the organellar regulation would differ from, for example, epithelial or neuronal type of cells where the cytoplasmic space is larger and often more longitudinally organized.

Profound aspects of B cell lysosomal biology are still unexplored. Some answers to the heterogeneity, atypical features, and specific functions could arise from a better understanding of the proteins linked to vesicle identity and trafficking, such as LAMP-1 and LAMP-2 as well as many different Rab GTPases. How are these key vesicle-linked proteins altered in response to antigenic or other stimuli? What are the key factors distinguishing the Ag processing pathway from the canonical endolysosomal route, and how are these pathways coupled to lysosome exocytosis to facilitate antigen extraction?

How do perturbations in lysosome homeostasis affect B cell activation? Insight can be gained by studying rare disorders such as lysosomal storage diseases (LSDs), where mutations in genes encoding for lysosomal hydrolases, transporters, or membrane proteins result in the abnormal accumulation of macromolecules within lysosomes leading to cell death and multiple organ dysfunction (Cabrera-Reyes et al., 2021) . Most of the LSDs are associated with severe neurological defects, however immune deficiencies and autoimmunity have also been observed (Rigante et al., 2017; Simonaro, 2016) and possibly often overlooked. Few studies have addressed how B cell activation is compromised in LSDs or when defective trafficking of lysosome proteins occurs. For instance, mice deficient in the formation of M6P residues exhibit significant loss of cathepsin proteases in B cells, leading to lysosomal dysfunction with an accumulation of storage material, impaired Ag processing and presentation, and subsequent defects in B cell maturation and antibody production (Otomo et al., 2015) . Peripheral B cells isolated from patients with Niemann-Pick disease type C1 (NP-C1), a rare lysosomal storage disorder resulting from mutations in an endolysosomal cholesterol transporter display increased levels of lysosomal glycosphingolipids (Lachmann et al., 2004) and B lymphocytes treated with U18666A, an inhibitor of the lysosomal cholesterol transporter, NPC1, accumulate lysosomes in the perinuclear region, suggesting that their function might be compromised.

The study of LSDs can therefore contribute to a better understanding of how lysosome fitness can impact B cell activation and humoral responses. The knowledge obtained from such severe pathological settings can reveal critical information that could be relevant for other conditions found in the general population, such as metabolic disorders including diabetes and obesity, where impaired lysosomal function is a common hallmark (Cabrera-Reyes et al., 2021).

It is clear that more research is needed to understand the multifaceted functions of lysosomal vesicles in B cells. We expect that proteomics could be key in the quest to unravel important new insights into lysosome functions upon B cell activation. Analysis of isolated lysosomes (like in macrophages, (Gao et al., 2017) or modern proteomics tools like LysoIP (Laqtom, 2023)and proximity proteomics (similarly to Awoniyi et al., in press), combined, for example, with the information of the overall proteome recruited to the IS upon B cell activation (Cunha et al., 2023; Cunha et al., bioRxiv) hold great promise for new insights of the lysosomal heterogeneity and LRO functions. Understanding B cell activation at the molecular level would help us to decipher the pathogenesis of various autoimmune conditions or B cell lymphomas and has implications on immunotherapeutic aspects as well. The role of B cells has also emerged in tumor immunology. For example, recent studies promote B cell-rich tertiary lymphoid structures (TLS) as a positive prognostic indicator (Trüb & Zippelius, 2021). Furthermore, EVs undoubtedly generate an interesting frontier with plenty of possibilities for future diagnostics or therapies, given their signaling functions, aided by specific surface markers that distinguish B cell-derived EVs from other sources.

Acknowledgements

This work was supported by the Academy of Finland (grant ID: 339810 to P.K.M.; 337530 to InFLAMES flagship), the Sigrid Jusélius foundation (to P.K.M.), as well as Finnish Cultural foundations (to S.H.). Additionally, ANID supported MIY and FDV through FONDECYT funding (Grant ID: 1221128 to M.I.Y. and the Ph.D. national Scholarship ID 21191062 to F.D.V.)

References

Arbogast, F., Arnold, J., Hammann, P., Kuhn, L., Chicher, J., Murera, D., Weishaar, J., Muller, S., Fauny, J.-D., & Gros, F. (2018). ATG5 is required for B cell polarization and presentation of particulate antigens. Autophagy, 15(2), 1–15. https://doi.org/10.1080/15548627.2018.1516327

Aung, T., Chapuy, B., Vogel, D., Wenzel, D., Oppermann, M., Lahmann, M., Weinhage, T., Menck, K., Hupfeld, T., Koch, R., Trümper, L., & Wulf, G. G. (2011). Exosomal evasion of humoral immunotherapy in aggressive B-cell lymphoma modulated by ATP-binding cassette transporter A3. Proceedings of the National Academy of Sciences, 108(37), 15336–15341. https://doi.org/10.1073/pnas.1102855108

Azouz, N. P., Hammel, I., & Sagi-Eisenberg, R. (2014). Charac-

terization of Mast Cell Secretory Granules and Their Cell Biology. DNA and Cell Biology, 33(10), 647–651. https://doi.org/10.1089/dna.2014.2543

Ballabio, A., & Bonifacino, J. S. (2020). Lysosomes as dynamic regulators of cell and organismal homeostasis. Nature Reviews Molecular Cell Biology, 21(2), 101–118. https://doi.org/10.1038/s41580-019-0185-4

Batista, F. D., & Harwood, N. E. (2009). The who, how and where of antigen presentation to B cells. Nature Reviews Immunology, 9(1), 15–27. https://doi.org/10.1038/nri2454

Bolger-Munro, M., Choi, K., Scurll, J. M., Abraham, L., Chappell, R. S., Sheen, D., Dang-Lawson, M., Wu, X., Priatel, J. J., Coombs, D., Hammer, J. A., & Gold, M. R. (2019). Arp2/3 complex-driven spatial patterning of the BCR enhances immune synapse formation, BCR signaling and B cell activation. ELife, 8, 1–40. https://doi.org/10.7554/elife.44574

Bonifacino, J. S., & Neefjes, J. (2017). Moving and positioning the endolysosomal system. Current Opinion in Cell Biology, 47, 1–8. https://doi.org/10.1016/j.ceb.2017.01.008

Bouhamdani, N., Comeau, D., & Turcotte, S. (2021). A Compendium of Information on the Lysosome. Frontiers in Cell and Developmental Biology, 9. https://doi.org/10.3389/fcell.2021.798262

Braulke, T., & Bonifacino, J. S. (2009). Sorting of lysosomal proteins. Biochimica et Biophysica Acta (BBA) - Molecular Cell Research, 1793(4), 605–614. https://doi.org/10.1016/j.bbamcr.2008.10.016

Buzas, E. I. (2022). The roles of extracellular vesicles in the immune system. Nature Reviews Immunology 2022 23:4, 23(4), 236–250. https://doi.org/10.1038/s41577-022-00763-8

Cabrera-Reyes, F., Parra-Ruiz, C., Yuseff, M. I., & Zanlungo, S. (2021). Alterations in Lysosome Homeostasis in Lipid-Related Disorders: Impact on Metabolic Tissues and Immune Cells. Frontiers in Cell and Developmental Biology, 9. https://doi.org/10.3389/fcell.2021.790568

Catalfamo, M., & Henkart, P. A. (2003). Perforin and the granule exocytosis cytotoxicity pathway. Current Opinion in Immunology, 15(5), 522–527. https://doi.org/10.1016/S0952-7915(03)00114-6

Chang, T.-Y., Chang, C. C. Y., Ohgami, N., & Yamauchi, Y. (2006). Cholesterol Sensing, Trafficking, and Esterification. Annual Review of Cell and Developmental Biology, 22(1), 129–157. https://doi.org/10.1146/annurev.cellbio.22.010305.104656

Chapman, N. M., & Chi, H. (2022). Metabolic adaptation of lymphocytes in immunity and disease. Immunity, 55(1), 14–30. https://doi.org/10.1016/j.immuni.2021.12.012

Cordonnier, M. N., Dauzonne, D., Louvard, D., & Coudrier, E. (2001). Actin Filaments and Myosin I Alpha Cooperate with Microtubules for the Movement of Lysosomes. Molecular Biology of the Cell, 12(12), 4013. https://doi.org/10.1091/MBC.12.12.4013

Cunha, D. M., Hernández-Pérez, S., & Mattila, P. K. (2023). Isolation of the B Cell Immune Synapse for Proteomic Analysis (pp. 393–408). https://doi.org/10.1007/978-1-0716-3135-5_25

Delevoye, C., Marks, M. S., & Raposo, G. (2019). Lysosome-related organelles as functional adaptations of the endolysosomal system. Current Opinion in Cell Biology, 59, 147–158. https://doi.org/10.1016/j.ceb.2019.05.003

Eberl, G., Jiang, S., YU, Z., Schneider, P., Corradin, G., & Mach, J.-P. (2001). An anti-CD19 antibody coupled to a tetanus toxin peptide induces efficient Fas ligand (FasL)-mediated cytotoxicity of a transformed human B cell line by specific CD4+ T cells. Clinical and Experimental Immunology, 114(2), 173–178. https://doi.org/10.1046/j.1365-2249.1998.00710.x

Eskelinen, E.-L. (2006). Roles of LAMP-1 and LAMP-2 in lysosome biogenesis and autophagy. Molecular Aspects of Medicine, 27(5–6), 495–502. https://doi.org/10.1016/j.mam.2006.08.005

Gao, Y., Chen, Y., Zhan, S., Zhang, W., Xiong, F., & Ge, W. (2017). Comprehensive proteome analysis of lysosomes reveals the diverse function of macrophages in immune responses. Oncotarget, 8(5), 7420–7440. https://doi.org/10.18632/oncotarget.14558

Gennerich, A., & Vale, R. D. (2009). Walking the walk: how kinesin and dynein coordinate their steps. Current Opinion in Cell Biology, 21(1), 59–67. https://doi.org/10.1016/J.CEB.2008.12.002

Hernández-Pérez, S., & Mattila, P. K. (2022). A specific hybridisation internalisation probe (SHIP) enables precise live-cell and super-resolution imaging of internalized cargo. Scientific Reports, 12(1), 620. https://doi.org/10.1038/s41598-021-04544-6

Hernández-Pérez, S., Vainio, M., Kuokkanen, E., Šuštar, V., Petrov, P., Forstén, S., Paavola, V., Rajala, J., Awoniyi, L. O., Sarapulov, A. V., Vihinen, H., Jokitalo, E., Bruckbauer, A., & Mattila, P. K. (2020). B cells rapidly target antigen and surface-derived MHCII into peripheral degradative compartments. Journal of Cell Science, 133(5). https://doi.org/10.1242/JCS.2351912

Holland, L. K. K., Nielsen, I. Ø., Maeda, K., & Jäättelä, M. (2020). SnapShot: Lysosomal Functions. Cell, 181(3), 748-748.e1. https://doi.org/10.1016/J.CELL.2020.03.043

Hu, Y.-B., Dammer, E. B., Ren, R.-J., & Wang, G. (2015). The endosomal-lysosomal system: from acidification and cargo sorting to neurodegeneration. Translational Neurodegeneration, 4(1), 18. https://doi.org/10.1186/s40035-015-0041-1

Huotari, J., & Helenius, A. (2011). Endosome maturation. The EMBO Journal, 30(17), 3481–3500. https://doi.org/10.1038/emboj.2011.286

Ibañez-Vega, J., Batalla, F. D. V., Saez, J. J., Soza, A., & Yuseff, M.-I. (2019). Proteasome Dependent Actin Remodeling Facilitates Antigen Extraction at the Immune Synapse of B Cells. Frontiers in Immunology, 10. https://doi.org/10.3389/fimmu.2019.00225

Ibañez-Vega, J., Valle, F. del, Sáez, J. J., Guzman, F., Diaz, J., Soza, A., & Yuseff, M. I. (2021). Ecm29-Dependent Proteasome Localization Regulates Cytoskeleton Remodeling at the Immune Synapse. Frontiers in Cell and Developmental Biology, 9. https://doi.org/10.3389/fcell.2021.650817

Inpanathan, S., & Botelho, R. J. (2019). The Lysosome Signaling Platform: Adapting With the Times. Frontiers in Cell

and Developmental Biology, 7. https://doi.org/10.3389/fcell.2019.00113

Johnson, D. E., Ostrowski, P., Jaumouillé, V., & Grinstein, S. (2016). The position of lysosomes within the cell determines their luminal pH. Journal of Cell Biology, 212(6), 677–692. https://doi.org/10.1083/jcb.201507112

Kato, T., Fahrmann, J. F., Hanash, S. M., & Vykoukal, J. (2020). Extracellular Vesicles Mediate B Cell Immune Response and Are a Potential Target for Cancer Therapy. Cells, 9(6), 1518. https://doi.org/10.3390/cells9061518

Kim, M. S., Muallem, S., Kim, S. H., Kwon, K. B., & Kim, M. S. (2019). Exosomal release through TRPML1-mediated lysosomal exocytosis is required for adipogenesis. Biochemical and Biophysical Research Communications, 510(3), 409–415. https://doi.org/10.1016/j.bbrc.2019.01.115

Kitamoto, K., Yoshizawa, K., Ohsumi, Y., & Anraku, Y. (1988). Dynamic aspects of vacuolar and cytosolic amino acid pools of Saccharomyces cerevisiae. Journal of Bacteriology, 170(6), 2683–2686. https://doi.org/10.1128/jb.170.6.2683-2686.1988

Korolchuk, V. I., Saiki, S., Lichtenberg, M., Siddiqi, F. H., Roberts, E. A., Imarisio, S., Jahreiss, L., Sarkar, S., Futter, M., Menzies, F. M., O'Kane, C. J., Deretic, V., & Rubinsztein, D. C. (2011). Lysosomal positioning coordinates cellular nutrient responses. Nature Cell Biology, 13(4), 453–460. https://doi.org/10.1038/ncb2204

Kugeratski, F. G., & Kalluri, R. (2021). Exosomes as mediators of immune regulation and immunotherapy in cancer. The FEBS Journal, 288(1), 10–35. https://doi.org/10.1111/febs.15558

Kuokkanen, E., Šuštar, V., & Mattila, P. K. (2015). Molecular control of B cell activation and immunological synapse formation. Traffic, 16(4), 311–326. https://doi.org/10.1111/tra.12257

Lachmann, R. H., te Vruchte, D., Lloyd-Evans, E., Reinkensmeier, G., Sillence, D. J., Fernandez-Guillen, L., Dwek, R. A., Butters, T. D., Cox, T. M., & Platt, F. M. (2004). Treatment with miglustat reverses the lipid-trafficking defect in Niemann–Pick disease type C. Neurobiology of Disease, 16(3), 654–658. https://doi.org/10.1016/j.nbd.2004.05.002

Lagos, J., Sagadiev, S., Diaz, J., Bozo, J. P., Guzman, F., Stefani, C., Zanlungo, S., Acharya, M., & Yuseff, M. I. (2022). Autophagy Induced by Toll-like Receptor Ligands Regulates Antigen Extraction and Presentation by B Cells. Cells, 11(23). https://doi.org/10.3390/cells11233883

Lamming, D. W., & Bar-Peled, L. (2019). Lysosome: The Metabolic Signaling Hub. Traffic (Copenhagen, Denmark), 20(1), 27. https://doi.org/10.1111/TRA.12617

Lanzavecchia, A. (1985). Antigen-specific interaction between T and B cells. Nature, 314(6011), 537–539. https://doi.org/10.1038/314537a0

Laqtom, N. N. (2023). Studying lysosomal function and dysfunction using LysoIP. Nature Reviews Molecular Cell Biology. https://doi.org/10.1038/s41580-023-00619-6

Li, J., Zhou, J., Huang, H., Jiang, J., Zhang, T., & Ni, C. (2023). Mature dendritic cells enriched in immunoregulatory molecules (mregDCs): A novel population in the tumour microenvironment and immunotherapy target. Clinical and Translational Medicine, 13(2). https://doi.org/10.1002/ctm2.1199

Maeda, F. Y., van Haaren, J. J., Langley, D. B., Christ, D., Andrews, N. W., & Song, W. (2021). Surface-associated antigen induces permeabilization of primary mouse B-cells and lysosome exocytosis facilitating antigen uptake and presentation to T-cells. ELife, 10. https://doi.org/10.7554/eLife.66984

Manoury, B., Hewitt, E. W., Morrice, N., Dando, P. M., Barrett, A. J., & Watts, C. (1998). An asparaginyl endopeptidase processes a microbial antigen for class II MHC presentation. Nature, 396(6712), 695–699. https://doi.org/10.1038/25379

Martinez-Martin, N., Maldonado, P., Gasparrini, F., Frederico, B., Aggarwal, S., Gaya, M., Tsui, C., Burbage, M., Keppler, S. J., Montaner, B., Jefferies, H. B. J., Nair, U., Zhao, Y. G., Domart, M.-C., Collinson, L., Bruckbauer, A., Tooze, S. A., & Batista, F. D. (2017). A switch from canonical to noncanonical autophagy shapes B cell responses. Science, 355(6325), 641–647. https://doi.org/10.1126/science.aal3908

McShane, A. N., & Malinova, D. (2022). The Ins and Outs of Antigen Uptake in B cells. Frontiers in Immunology, 13. https://doi.org/10.3389/fimmu.2022.892169

Medina, D. L., Fraldi, A., Bouche, V., Annunziata, F., Mansueto, G., Spampanato, C., Puri, C., Pignata, A., Martina, J. A., Sardiello, M., Palmieri, M., Polishchuk, R., Puertollano, R., & Ballabio, A. (2011). Transcriptional Activation of Lysosomal Exocytosis Promotes Cellular Clearance. Developmental Cell, 21(3), 421–430. https://doi.org/10.1016/j.devcel.2011.07.016

Muntasell, A., Berger, A. C., & Roche, P. A. (2007). T cell-induced secretion of MHC class II–peptide complexes on B cell exosomes. The EMBO Journal, 26(19), 4263–4272. https://doi.org/10.1038/sj.emboj.7601842

Music, A., Tejeda-González, B., Cunha, D. M., Fischer von Mollard, G., Hernández-Pérez, S., & Mattila, P. K. (2022). The SNARE protein Vti1b is recruited to the sites of BCR activation but is redundant for antigen internalisation, processing and presentation. Frontiers in Cell and Developmental Biology, 10. https://doi.org/10.3389/fcell.2022.987148

Obino, D., Diaz, J., Sáez, J. J., Ibañez-Vega, J., Sáez, P. J., Alamo, M., Lankar, D., & Yuseff, M. I. (2017). Vamp-7-dependent secretion at the immune synapse regulates antigen extraction and presentation in B-lymphocytes. Molecular Biology of the Cell. https://doi.org/10.1091/mbc.E16-10-0722

Otomo, T., Schweizer, M., Kollmann, K., Schumacher, V., Muschol, N., Tolosa, E., Mittrücker, H.-W., & Braulke, T. (2015). Mannose 6 phosphorylation of lysosomal enzymes controls B cell functions. Journal of Cell Biology, 208(2), 171–180. https://doi.org/10.1083/jcb.201407077

Oyarzún, J. E., Lagos, J., Vázquez, M. C., Valls, C., De la Fuente, C., Yuseff, M. I., Alvarez, A. R., & Zanlungo, S. (2019). Lysosome motility and distribution: Relevance in health and disease. In Biochimica et Biophysica Acta - Molecu-

lar Basis of Disease (Vol. 1865, Issue 6, pp. 1076–1087). Elsevier B.V. https://doi.org/10.1016/j.bbadis.2019.03.009

Perera, R. M., & Zoncu, R. (2016). The Lysosome as a Regulatory Hub. Https://Doi.Org/10.1146/Annurev-Cellbio-111315-125125, 32, 223–253. https://doi.org/10.1146/ANNUREV-CELLBIO-111315-125125

Podinovskaia, M., Prescianotto-Baschong, C., Buser, D. P., & Spang, A. (2021). A novel live-cell imaging assay reveals regulation of endosome maturation. ELife, 10. https://doi.org/10.7554/eLife.70982

Rastogi, I., Jeon, D., Moseman, J. E., Muralidhar, A., Potluri, H. K., & McNeel, D. G. (2022). Role of B cells as antigen presenting cells. Frontiers in Immunology, 13. https://doi.org/10.3389/fimmu.2022.954936

Raza, I. G. A., & Clarke, A. J. (2021). B Cell Metabolism and Autophagy in Autoimmunity. Frontiers in Immunology, 12. https://doi.org/10.3389/fimmu.2021.681105

Rigante, D., Cipolla, C., Basile, U., Gulli, F., & Savastano, M. C. (2017). Overview of immune abnormalities in lysosomal storage disorders. Immunology Letters, 188, 79–85. https://doi.org/10.1016/j.imlet.2017.07.004

Rincón-Arévalo, H., Burbano, C., Atehortúa, L., Rojas, M., Vanegas-García, A., Vásquez, G., & Castaño, D. (2022). Modulation of B cell activation by extracellular vesicles and potential alteration of this pathway in patients with rheumatoid arthritis. Arthritis Research & Therapy, 24(1), 169. https://doi.org/10.1186/s13075-022-02837-3

Rink, J., Ghigo, E., Kalaidzidis, Y., & Zerial, M. (2005). Rab Conversion as a Mechanism of Progression from Early to Late Endosomes. Cell, 122(5), 735–749. https://doi.org/10.1016/j.cell.2005.06.043

Roche, P. A., & Furuta, K. (2015). The ins and outs of MHC class II-mediated antigen processing and presentation. In Nature Reviews Immunology (Vol. 15, Issue 4, pp. 203–216). Nature Publishing Group. https://doi.org/10.1038/nri3818

Sáez, J. J., Diaz, J., Ibañez, J., Bozo, J. P., Reyes, F. C., Alamo, M., Gobert, F. X., Obino, D., Bono, M. R., Lennon-Duménil, A. M., Yeaman, C., & Yuseff, M. I. (2019). The exocyst controls lysosome secretion and antigen extraction at the immune synapse of B cells. Journal of Cell Biology, 218(7), 2247–2264. https://doi.org/10.1083/jcb.201811131

Saftig, P., & Klumperman, J. (2009). Lysosome biogenesis and lysosomal membrane proteins: trafficking meets function. Nature Reviews Molecular Cell Biology, 10(9), 623–635. https://doi.org/10.1038/nrm2745

Saric, A., Hipolito, V. E. B., Kay, J. G., Canton, J., Antonescu, C. N., & Botelho, R. J. (2016). mTOR controls lysosome tubulation and antigen presentation in macrophages and dendritic cells. Molecular Biology of the Cell, 27(2), 321–333. https://doi.org/10.1091/mbc.e15-05-0272

Serra-Marques, A., Martin, M., Katrukha, E. A., Grigoriev, I., Peeters, C. A. E., Liu, Q., Hooikaas, P. J., Yao, Y., Solianova, V., Smal, I., Pedersen, L. B., Meijering, E., Kapitein, L. C., & Akhmanova, A. (2020). Concerted action of kinesins kif5b and kif13b promotes efficient secretory vesicle transport to microtubule plus ends. ELife, 9, 1–37. https://doi.org/10.7554/eLife.61302

Settembre, C., Zoncu, R., Medina, D. L., Vetrini, F., Erdin, S., Erdin, S., Huynh, T., Ferron, M., Karsenty, G., Vellard, M. C., Facchinetti, V., Sabatini, D. M., & Ballabio, A. (2012). A lysosome-to-nucleus signalling mechanism senses and regulates the lysosome via mTOR and TFEB. The EMBO Journal, 31(5), 1095–1108. https://doi.org/10.1038/emboj.2012.32

Shi, G.-P., Villadangos, J. A., Dranoff, G., Small, C., Gu, L., Haley, K. J., Riese, R., Ploegh, H. L., & Chapman, H. A. (1999). Cathepsin S Required for Normal MHC Class II Peptide Loading and Germinal Center Development. Immunity, 10(2), 197–206. https://doi.org/10.1016/S1074-7613(00)80020-5

Simonaro, C. M. (2016). Lysosomes, Lysosomal Storage Diseases, and Inflammation. Journal of Inborn Errors of Metabolism and Screening, 4, 232640981665046. https://doi.org/10.1177/2326409816650465

Spillane, K. M., & Tolar, P. (2018). Mechanics of antigen extraction in the B cell synapse. Molecular Immunology, 101(March), 319–328. https://doi.org/10.1016/j.molimm.2018.07.018

Stahl-Meyer, J., Holland, L. K. K., Liu, B., Maeda, K., & Jäättelä, M. (2022). Lysosomal Changes in Mitosis. Cells, 11(5), 875. https://doi.org/10.3390/cells11050875

Stoddart, A., Dykstra, M. L., Brown, B. K., Song, W., Pierce, S. K., & Brodsky, F. M. (2002). Lipid Rafts Unite Signaling Cascades with Clathrin to Regulate BCR Internalization. Immunity, 17(4), 451–462. https://doi.org/10.1016/S1074-7613(02)00416-8

Treanor, B., Depoil, D., Gonzalez-Granja, A., Barral, P., Weber, M., Dushek, O., Bruckbauer, A., & Batista, F. D. (2009). The Membrane Skeleton Controls Diffusion Dynamics and Signaling through the B Cell Receptor. Immunity, 32, 187–199. https://doi.org/10.1016/j.immuni.2009.12.005

Trüb, M., & Zippelius, A. (2021). Tertiary Lymphoid Structures as a Predictive Biomarker of Response to Cancer Immunotherapies. Frontiers in Immunology, 12. https://doi.org/10.3389/fimmu.2021.674565

Watts, C. (2022). Lysosomes and lysosome-related organelles in immune responses. FEBS Open Bio, 12(4), 678–693. https://doi.org/10.1002/2211-5463.13388

Yuseff, M. I., & Lennon-Duménil, A. M. (2015). B cells use conserved polarity cues to regulate their antigen processing and presentation functions. In Frontiers in Immunology (Vol. 6, Issue MAY, pp. 1–7). https://doi.org/10.3389/fimmu.2015.00251

Yuseff, M. I., Reversat, A., Lankar, D., Diaz, J., Fanget, I., Pierobon, P., Randrian, V., Larochette, N., Vascotto, F., Desdouets, C., Jauffred, B., Bellaiche, Y., Gasman, S., Darchen, F., Desnos, C., & Lennon-Duménil, A. M. (2011). Polarized Secretion of Lysosomes at the B Cell Synapse Couples Antigen Extraction to Processing and Presentation. Immunity, 35(3), 361–374. https://doi.org/10.1016/j.immuni.2011.07.008

Yuseff, M.-I., Pierobon, P., Reversat, A., & Lennon-Duménil, A.-M. (2013). How B cells capture, process and present antigens: a crucial role for cell polarity. Nature Reviews. Immunology, 13(7), 475–486. https://doi.org/10.1038/nri3469

5. DISCUSSION

The results shown in manuscripts 1, 2, and 3 will be discussed in the following section. For reference to the figures in each manuscript, the notation (Fig. ***X***, M. ***Y***) will be used, with '***X***' being the figure number of manuscript 'M' (***Y*** = 1, 2 or 3).

1 – B cell cytoskeleton remodeling in response to varying rigidities of antigen presenting surfaces.

Upon interaction with surface-tethered antigens B cell spreading, and subsequent contraction of their actin cytoskeleton is a hallmark response for the effective establishment of an immune synapse. This allows BCR and antigen clustering at the center of the IS and the formation of specialized actin structures that assist with Ag extraction and internalization (74). However, BCR-mediated mechanosensing responses as an independent phenomenon from the classical integrin mechano-transduction pathways, have not been sufficiently explored in the context of IS formation and function. Despite previous studies using tunable stiffness to understand B cell mechanobiology, these usually implement rigidities that are far from physiological stiffness values for APCs (0.1-0.5 kPa), using surfaces of ~2 kPa as "soft"- healthy substrates (55).

In this work, by employing tunable stiffness PAA gels, we could emulate the stiffness of unstimulated APCs (0.3 kPa) in conditions we consider "soft" and 13 kPa, as "stiff" comparable to scenarios in which APCs increase their membrane stiffness by inflammatory or mechanical cues. We believe that the conditions used in our study contribute to the current knowledge on how B cells respond to soft and stiff Ag. bound surfaces during the IS, as they represent values closer to physiological and pathological conditions. Our results provide insight on how mechanical cues shape the IS formation, antigen capture and overall B cell activation.

PAA gels constructed for this work are functional in terms of triggering a spreading response in B cells in increasing times of activation when coupled to BCR^+ ligands without the presence of integrin-binding molecules. Importantly, as we evaluated short incubation times, no significant cell death was triggered when using these substrates. Few studies have data on the malignancy of prolonged cell culture on PAA Gels, but this effect should be noticeable in a period of days (86). Noticeably, as shown in (Fig.1 M.1) only stiff substates coupled to BCR^+ ligands cause increasing spreading responses while soft ones maintain B cells in a non-spreading state, suggesting that BCR-mediated signaling is responsible for cytoskeleton remodeling in the range of the presented stiffnesses. Our experimental setup provided additional information on the presence of secondary actin structures that are related to enhanced states of B cell activation, such as actin foci.

Inside-out activation of the BCR (43) following antigen interaction is sufficient to promote focal adhesion, integrin clustering and actin foci formation. The latter are sites where antigen is concentrated and acquired (75). Actin foci number and lamellipodia area counts were enhanced when B cells interacted with stiff substrates compared to softer ones in a time-dependent manner. It is possible that increasing stiffnesses promote the formation of actin structures to stabilize the IS process, as other actin structures including actin arcs have been described in experimental setups of higher stiffness (glass) (22) to prompt increased levels of overall antigen capture and B cell activation. These data suggest that BCR signaling is sufficient to trigger a spreading response and initial activation markers in conditions that have not been previously reported within this range of rigidities.

In line with the previous observations, we decided to evaluate other mechanosensing responses downstream BCR activation that directly affect the cytoskeleton and integrin adhesions such as the focal adhesion kinase (FAK). FAK is activated via phosphorylation (pFAK) by PKCB after the

initiation of the IS signaling cascade, accumulating in nascent focal adhesions, thereby promoting integrin function (56).

In this work, we could find single pFAK spots that correlate more accurately with their distribution and features in migrating cells, thus improving the previously characterized responses of this signaling pathway. pFAK regulation over integrins should sustain a more stable IS by producing mechanical forces derived from local tensions. On the other hand, dysfunctional mechano-responses associated to pFAK deficiencies could be detrimental to the formation of a functional IS. For instance, in patients with rheumatoid arthritis (RA), increased cartilage stiffness leads to auto-antigen-presenting B cells, which subsequently causes the production of auto-antibodies (76).

When exploring other markers of BCR downstream signaling, we analyzed kinases that are activated early on following antigen interaction. We were able to verify for the first time that both pERK and pAKT are increased proportionally to substrate stiffness and activation times (Fig. EV2. M1) It is known that both ERK and AKT kinases are regulators of actin dynamics, enhancing migration and branching of F-Actin (77–79) which ultimately supports BCR-Ag endocytosis. Therefore, our findings provide new mechanistic insight underlying how BCR mechanosensing can tune early cellular responses, independently of integrin function, during the formation of the immune synapse.
Importantly, the limitations of the PAA gels system cannot be neglected.

Their main disadvantage is the incompatibility with total internal reflection microscopy (TIRFM), which is helpful when examining the IS (22). TIRFM only works when the refraction indexes are corresponding with the total internal reflection phenomena, and PAA gels do not fulfil this requirement. Experiments related to nascent focal adhesions, and organelle positioning (as lysosomes, that will be discussed later) can be performed with silicone-based substrates, but due to limitations of

reagents and time this was not explored in this project. Noteworthy, the possibility of performing classic biochemical experiments such as immunoblot were recently published to be compatible with this method (71) and posed a relevant challenge when obtaining proteins from cell lysates for western blot analysis. Alternatives to PAA gels are plasma membrane sheets, synthetic lipid bilayers, PDMS surfaces and alginate beads, but some of them cannot be tuned to a specific stiffness with such ease as PAA gels (80).

2 – Tubulin acetylation at the B cell immune synapse as a mechanosensory response

Tubulin acetylation is enhanced when cells engage in traction forces (67) due to the direct link between microtubules and the actin cytoskeleton, through actin foci. As contractility forces occur during the immune synapse formation, we investigated the impact of different stiffnesses on the microtubule network during B cell activation. Importantly, tubulin PTMs can shape the dynamics and affinity of vesicle trafficking, as evidenced in other immune cells. For example, in T lymphocytes, higher levels of acetylated tubulin regulate MTOC positioning and promote vesicle exocytosis during the formation of the cytotoxic synapse (81).

We found that in fixed cells stained for non-acetylated tubulin (aTub) and Ac-Tub, the abundance of Ac-Tub and its ratio of accumulation compared to aTub was increasingly higher in stiffer substrates and later time points of activation. These results represent new data in the field of B cell mechanosensing. Considering the signaling cascade of the BCR, it is possible that other PTMs of tubulin are enhanced during B cell activation in response to stiffness, such as tubulin tyrosination, glutamylation and phosphorylation. All those PTMs can also influence organelle distribution and function. These were not evaluated in this project but represent interesting targets to study how other organelles and vesicle trafficking are affected in their distribution and dynamics in response to mechanosensing.

As the previously mentioned Ac-Tub - GEF-H1 interplay is present in other cell models, we evaluated the mechanical response of GEF-H1 as shown in (Fig. EV2, M1). Our results support the notion that in B cells, GEF-H1 at the IS increases with substrate stiffness concomitantly with acetylated microtubules. This response is likely coupled to a mechanosensing axis directed by the BCR. Based on the available literature, as tubulin acetylation increases, GEF-H1 is released from the lumen of microtubules. Released GEF-H1 molecules then can act as a Rho-GEFs promoting contractibility and formation of focal adhesions and, in parallel, work as a key component for the correct assembly of the exocyst complex which helps with lysosome tethering at the IS promoting efficient antigen extraction (32).

The feedback mechanism between focal adhesion formation, tubulin acetylation and GEF-H1 release could also have major implications in B cell migration as it has been shown in other cell models. For example, GEF-H1 depletion reduces directional migration in HeLa cells. This deficiency in GEF-H1 is associated with altered leading edge actin dynamics and extended focal adhesion lifetimes (82). Furthermore, diminished tyrosine phosphorylation of FAK and paxillin, critical for focal adhesion regulation, occurs in the absence of GEF-H1/RhoA signaling.

Finally, in a complementary study (83), mice lacking GEF-H1 exhibit limited neutrophil migration and recruitment to inflamed tissues. GEF-H1−/− leukocytes demonstrate deficiencies in *in vivo* crawling and TEM within postcapillary venules. This research identifies GEF-H1 as a fundamental component of the shear stress, also a mechanical cue, critically required for a robust immune response.

3 – Substrate stiffness controls lysosome positioning and dynamics at the immune synapse of B cells

In past publications, our group has shown that upon interaction with stiff substrates such as latex beads or glass coverslips coupled to BCR^+ ligands, lysosomes are recruited preferentially to a central cluster at the IS where they secrete their acidic content and promote antigen extraction. Considering this, it is critical to understand the implications of MT network modifications in the regulation of vesicle and lysosome trafficking during B cell activation. The elevated levels of Ac-Tub in increasing stiffnesses of antigen-presenting substrates might represent a novel regulatory mechanism for lysosome positioning and function.

After evaluating whether stiffness could regulate lysosome positioning, our findings indicate that stiffer substrates promote an increased, persistent and faster accumulation of lysosomes at the center of the IS, which is correlated with higher levels of B cell activation. Conversely, in soft substrates, lysosomes maintained a peripheral distribution suggesting that their trafficking might be affected by the physical cues of the substrate. Interestingly, the number and mean area of lysosomes that arrived at the IS was also considerably different between stiffnesses. More and smaller lysosomes were found in stiffer substrates at increasing time points of activation. This could be related with evidence showing that acetylated microtubule tracks are needed to promote events lysosome fission, resulting in populations of smaller lysosomes (70).

In addition, we analyzed the co-localization of lysosomes with acetylated microtubule tracks when cells were seeded over stiff or soft substrates. As expected, lysosomes were preferentially associated with Ac-Tubulin structures at the IS when interacting with stiff substrates and increasing time points of activation. This goes in line with previous knowledge in other polarized cell models but had not been demonstrated before for B cells. However, motor proteins responsible for this association which

are most likely KIF family members, were not explored in our study. Considering the literature, KIF1 and KIF5 are the most suitable candidates, as they promote more efficient and selective binding of lysosomes to acetylated microtubules or MT presenting other PTM (58,62,84). The previous could also lead to changes in their dynamics in response to substrate stiffness.

When we explored lysosome dynamics by live cell microscopy (Fig.3, M1) we found that in non-treated control conditions, lysosomes changed their mean speed and displacement in response to substrate rigidity, exhibiting lower values for both measurements in stiffer conditions. This is consistent the previous results where Ac-Tubulin levels increased proportionally to substrate stiffness at the IS; and as mentioned before, this PTM dictates the affinity and dynamics of molecular motors that are related to lysosome transport in other cell models.

As we enhanced tubulin acetylation via the inhibition of the deacetylase HDAC6 with the microtubule stabilizing agent SAHA, we noted that treated cells seeded over soft substrates exhibited the same behavior as those in non-treated conditions in stiff substrates. For stiff conditions, there were no significant changes between treated and non-treated cells in either speed or displacement of lysosomes. The previous observation allowed us to hypothesize that there is a “acetylation threshold” which is insensitive to stiffnesses over 13 kPa and serves to fine tune lysosome dynamics at the IS. Therefore, we propose that acetylation of tubulin serves a cue for lysosomes to become more stable at the IS, and possibly, help with Ag extraction when mechanical extraction is not sufficient.

4 – The acetylase ATAT1 is translocated to the cytoplasm upon B cell activation in increasing substrate stiffness

In search of a mechanism that could explain how tubulin acetylation is enhanced upon B cell stimulation in increasing stiffnesses, we evaluated the role of ATAT1. This is the only known enzyme to catalyze tubulin acetylation (85,86), and recently was shown to shuttle between the nucleus and the cytoplasm, where its action is performed on available entrance sites in tubulin lattices.

After stimulating B cells over substrates with different stiffnesses and quantifying the localization of ATAT1, we found that in increasing activation times and stiffness ATAT1 progressively shifted its localization from the nucleus to the cytoplasm (Fig.4, M1). To further confirm that this could be related with canonical pathways of mechanotransduction, we evaluated YAP localization. The YAP-TAZ complex is translocated to the nucleus as classical response to increasing stiffnesses in various cell types, it is a key regulator of mechanosensing and promotes a series of changes in cellular signaling and adaptation. In agreement with our hypothesis, YAP switched its accumulation from the cytoplasm to the nucleus, opposed to ATAT1.

How mechanical cues regulate the trafficking of ATAT1 between the nucleus and cytoplasm in B cells remains to be explored. However, a possible explanation is supported by evidence showing that the LINC complex mediates the opening of nuclear pores in response to stiffness, as it connects integrin signaling and mechanosensing with the architecture of the nuclear envelope (87,88). Importantly, the LINC complex fulfils a crucial role in B cells, by promoting nuclear and MTOC reorientation at the IS (89). Possibly, mechanical cues originating from increasing stiffness promote the opening of the nuclear pore and allow ATAT1 to shift from its nuclear location to the cytoplasm where, upon BCR stimulation and microtubule breakage induced by local traction forces, should promote tubulin acetylation as shown in the results of our work.

Importantly, ATAT1 could also regulate B cell migration, of key importance when these cells are searching for antigens and could signify an additional layer of regulation by this enzyme on other events that lead to antigen capture. In a study involving primary astrocytes, ATAT1-mediated microtubule acetylation was observed to increase in proximity to focal adhesions, promoting cell migration (64).

Additionally, ATAT1 was found to enhance focal adhesion turnover by facilitating Rab6-positive vesicle fusion at these sites. Other evidence shows that control of microtubule acetylation is attributed to clathrin-coated pits (CCPs), where a direct interaction between ATAT1 and the clathrin adaptor AP2 was identified (90). Notably, the polarized orientation of acetylated microtubules in migrating cells corresponded with CCP accumulation at the leading edge, underscoring the requirement for ATAT1 interaction with AP2 in directional cell migration.

5 – ATAT1 coordinates efficient lysosome positioning at the immune synapse of B cells and regulates antigen capture and presentation

As tubulin acetylation and lysosome positioning at the IS are controlled by varying rigidities of antigen-presenting surfaces, we considered the action of ATAT1 to be fundamental to this process due to the observations of its variable nuclear-to-cytoplasmic translocation in response to stiffness when B cells are activated. After silencing ATAT1 (figs) and showing that the characteristic central clustering of lysosomes at the IS was lost (Fig) in stiff substrates at 30 minutes, we analyzed the effect of this enzyme in controlling antigen extraction and presentation when B cells face different stiffnesses.

After activating B cells in different stiffnesses and the subsequent co-culture with T-Cells we found that levels of IL-2 incremented with cells exposed to higher substrate stiffness. We included extreme stiffness substrates as glass coupled to either BCR^+ or BCR^- ligands to distinguish whether mechanotransduction through BCR signaling is intrinsically coupled to activating ligands or substrate stiffness alone. Importantly, only cells activated in BCR^+ conditions on the highest stiffness promoted higher levels of IL-2, reinforcing the notion of BCR-mediated mechanosensing in our model. Increasing levels of stiffness had no effect on the presentation of the LACK 156-173 peptide, showing that varying substrate rigidity does not significantly influence T cell responses or B-T cell interactions.

These results indicate that for control conditions, B cells seeded on stiffer substrates are capable of extracting and presenting antigens more efficiently than in soft surfaces, eliciting enhanced activation of T cells through B-T Cooperation. To our knowledge, this is the first evidence showing that substrate stiffness regulates antigen capture and presentation to T cells, a key step in B cell activation and maturation.

Finally, after silencing ATAT1 in experiments of antigen capture and presentation we found that for stiffer substrates, cells silenced for ATAT1 showed less capacity to extract and present antigens to T cells than those in control conditions for construct expression. Interestingly, in soft conditions no significant differences of IL-2 production were evidenced. This correlates with the previous result on stiffness-dependent ATAT1 translocation to the cytoplasm. It is possible that soft substrates do not promote sufficient localization of ATAT1 at the cytoplasm, and therefore, its silencing does not show a difference in functional outcomes. Conversely, when facing increasing stiffnesses ATAT1-silenced cells show a dramatic decrease in their antigen capture and presentation competence.

6. CONCLUSIONS, PROJECTIONS AND PROPOSED WORKING MODEL

Considering the results presented in this thesis, the following conclusions can be stated.

1. B cells remodel their actin cytoskeleton in response to substrate stiffness upon BCR stimulation without the need of integrin ligands.
2. Tubulin acetylation is enhanced proportionally to increasing rigidities when B cells form an immune synapse
3. At the immune synapse, lysosomes display a central distribution and associate preferentially with acetylated microtubules when B cells interact with stiff substrates.
4. The stiffness of the antigen-presenting surface dictates lysosome motility and distribution.
5. The microtubule acetylase ATAT1 controls lysosome positioning at increasing stiffnesses, maintaining the characteristic central accumulation of lysosomes at the immune synapse.
6. The translocation from the nucleus to the cytoplasm of ATAT1 is enhanced by increasing stiffnesses upon B cell activation.
7. The capacity of B cells to extract and present antigens is regulated by the rigidity of the antigen-presenting surfaces and increases with stiffer substrates.
8. ATAT1 controls the capacity of B cells to extract and present antigens at higher stiffnesses.

The projections arising from this doctoral thesis mainly relate to establishing precedents from cellular biology that can support potential research and development of devices or therapies aimed at the treatment of autoimmune diseases, or cancer. For instance, novel drug delivery strategies can be developed by utilizing particles with varying levels of rigidity.

Lipid nanoparticles (LNPs), play a crucial role in the formulation of mRNA vaccines, such as the Pfizer-BioNTech and Moderna COVID-19 vaccines. These lipid shells serve as protective carriers for the fragile messenger RNA (mRNA) molecules used in these vaccines. Such structures could be engineered to work as artificial APCs with varying stiffnesses and tune immune responses in sites of inflammation or in the vicinity of secondary lymphoid organs.

Furthermore, taking advantage of the recent and promising work with CAR-T Cells, *ex-vivo* conditioning and priming of B cells in environments where they encounter mechanical challenges tailored to promote or diminish antigen extraction and presentation, can be explored. Additionally, therapies that target the B cell's own stiffness could have effect on interactions with other immune cells, such as T cells.

Lastly, an interesting scenario would be the development of precision therapies aimed at regulating enzymes related with tubulin acetylation, such as HDAC6 or ATAT1, which have already undergone testing in various disease models, including cancer.

Based on the discussion and conclusions of this thesis, the following working model is proposed (Fig 10).

In response to antigens presented on stiff substrates, B cells respond by promoting increased spreading responses, actin foci formation and translocating the acetyltransferase ATAT1 from the nucleus to the cytoplasm. Conversely, YAP is translocated to the nucleus in a manner consistent with its mechanosensitive function.

ATAT1, responsible for catalyzing tubulin acetylation, modifies the mechanical properties of microtubules. This alteration in tubulin acetylation has downstream effects on lysosome dynamics. On stiffer substrates, lysosomes are concentrated at the center of the IS. This is accompanied by a reduction in their speed and displacement compared to lysosomes in B cells activated on softer substrates. Additionally, lysosomes show a preference for associating with acetylated microtubules under stiffer conditions. This preference underscores the existence of a cellular pathway that connects antigen-extraction mechanisms with the mechanical cues originating from APCs.

The functional consequence of these mechanosensing mechanism is an enhancement in the capacity of B cells to capture and present antigens to T cells in increasing stiffnesses. Notably, when ATAT1 is downregulated, this enhanced antigen presentation is impaired, highlighting the critical role of ATAT1-mediated tubulin acetylation in this process.

In summary, the response of B cells to antigens presented on stiff substrates involves a sophisticated interplay of mechanosensitive signaling, tubulin acetylation, and lysosome dynamics. This cascade of events enhances B cells' capacity to capture and present antigens, ultimately contributing to the orchestration of immune responses.

These findings offer valuable insights into the intersection of molecular and mechanical aspects of immunology, shedding light on the role of BCR-mediated mechanosensing in antigen presentation.

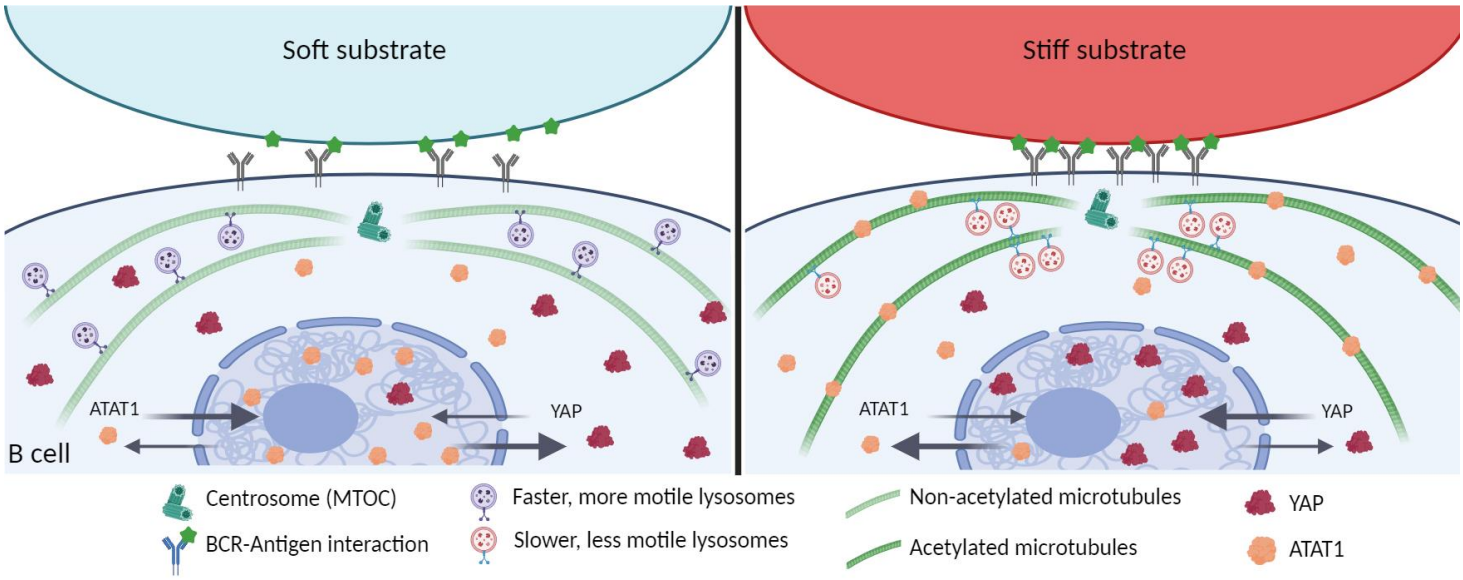

Figure 10: Working model

REFERENCES

1. Mauri C, Bosma A. Immune Regulatory Function of B Cells. *Annu Rev Immunol* (2012) 30:221–241. doi: 10.1146/annurev-immunol-020711-074934

2. Victora GD, Nussenzweig MC. Germinal Centers. *Annu Rev Immunol* (2012) 30:429–457. doi: 10.1146/annurev-immunol-020711-075032

3. Berthelot J-M, Jamin C, Amrouche K, Le Goff B, Maugars Y, Youinou P. Regulatory B cells play a key role in immune system balance. *Joint Bone Spine* (2013) 80:18–22. doi: 10.1016/j.jbspin.2012.04.010

4. Burger JA, Wiestner A. Targeting B cell receptor signalling in cancer: preclinical and clinical advances. *Nat Rev Cancer* (2018) 18:148–167. doi: 10.1038/nrc.2017.121

5. Pillai S, Mattoo H, Cariappa A. B cells and autoimmunity. *Curr Opin Immunol* (2011) 23:721–731. doi: 10.1016/j.coi.2011.10.007

6. Rawlings DJ, Metzler G, Wray-Dutra M, Jackson SW. Altered B cell signalling in autoimmunity. *Nat Rev Immunol* (2017) doi: 10.1038/nri.2017.24

7. Lee S, Ko Y, Kim TJ. Homeostasis and regulation of autoreactive B cells. *Cell Mol Immunol* (2020) 17:561–569. doi: 10.1038/s41423-020-0445-4

8. Nemazee D. Mechanisms of central tolerance for B cells. *Nat Rev Immunol* (2017) 17:281–294. doi: 10.1038/nri.2017.19

9. Corneth OBJ, Neys SFH, Hendriks RW. Aberrant B Cell Signaling in Autoimmune Diseases. *Cells* (2022) 11:3391. doi: 10.3390/cells11213391

10. Oleinika K, Mauri C, Blair PA. “Chapter 9 - B Cell Activation and B Cell Tolerance.,” In: Rose NR, Mackay IR, editors. *The Autoimmune Diseases (Sixth Edition)*. Academic Press (2020). p. 171–187 doi: 10.1016/B978-0-12-812102-3.00009-9

11. Batista FD, Harwood NE. The who, how and where of antigen presentation to B cells. *Nat Rev Immunol* (2009) doi: 10.1038/nri2454

12. Yuseff M-I, Pierobon P, Reversat A, Lennon-Duménil A-M. How B cells capture, process and present antigens: a crucial role for cell polarity. *Nat Rev Immunol* (2013) 13:475–86. doi: 10.1038/nri3469

13. Kuokkanen E, Šuštar V, Mattila PK. Molecular control of B cell activation and immunological synapse formation. *Traffic* (2015) 16:311–326. doi: 10.1111/tra.12257

14. Hao JJ, Carey GB, Zhan X. Syk-mediated tyrosine phosphorylation is required for the association of hematopoietic lineage cell-specific protein 1 with lipid rafts and B cell antigen receptor signalosome complex. *J Biol Chem* (2004) 279:33413–33420. doi: 10.1074/jbc.M313564200

15. Kläsener K, Maity PC, Hobeika E, Yang J, Reth M. B cell activation involves nanoscale receptor reorganizations and inside-out signaling by Syk. *eLife* (2014) 2014:e02069. doi: 10.7554/eLife.02069.001

16. Lankar D, Briken V, Adler K, Weiser P, Cassard S, Blank U, Viguier M, Bonnerot C. Syk Tyrosine Kinase and B Cell Antigen Receptor (BCR) Immunoglobulin-Subunit Determine BCR-mediated Major Histocompatibility Complex Class II-restricted Antigen Presentation. (1998). http://www.jem.org

17. Bolger-Munro M, Choi K, Scurll JM, Abraham L, Chappell RS, Sheen D, Dang-Lawson M, Wu X, Priatel JJ, Coombs D, et al. Arp2/3 complex-driven spatial patterning of the BCR enhances immune synapse formation, BCR signaling and B cell activation. *eLife* (2019) 8:1–40. doi: 10.7554/elife.44574

18. Yuseff M-I, Lankar D, Lennon-Duménil A-M. Dynamics of Membrane Trafficking Downstream of B and T Cell Receptor Engagement: Impact on Immune Synapses. *Traffic* (2009) 10:629–636. doi: 10.1111/j.1600-0854.2009.00913.x

19. Bolger-Munro M. The Wdr1-LIMK-Cofilin Axis Controls B Cell Antigen Receptor-Induced Actin Remodeling and Signaling at the Immune Synapse. *Front Cell Dev Biol* (2021) 9:1–22. doi: 10.3389/fcell.2021.649433

20. Tolar P. Cytoskeletal control of B cell responses to antigens. *Nat Rev Immunol* (2017) doi: 10.1038/nri.2017.67

21. Harwood NE, Batista FD. Early Events in B Cell Activation. *Annu Rev Immunol* (2010) 28:185–210. doi: 10.1146/annurev-immunol-030409-101216

22. Wang JC, Yim Y-I, Wu X, Jaumouille V, Cameron A, Waterman CM, Kehrl JH, Hammer JA. A B-cell actomyosin arc network couples integrin co-stimulation to mechanical force-dependent immune synapse formation. *eLife* (2022) 11:e72805. doi: 10.7554/eLife.72805

23. Reversat A, Yuseff M-I, Lankar D, Malbec O, Obino D, Maurin M, Penmatcha NVG, Amoroso A, Sengmanivong L, Gundersen GG, et al. Polarity protein Par3 controls B-cell receptor dynamics and antigen extraction at the immune synapse. *Mol Biol Cell* (2015) 26:1273–1285. doi: 10.1091/mbc.E14-09-1373

24. Farina F, Gaillard J, Guérin C, Couté Y, Sillibourne J, Blanchoin L, Théry M. The centrosome is an actin-organizing centre. *Nat Cell Biol* (2016) 18:65–75. doi: 10.1038/ncb3285

25. Stinchcombe JC, Griffiths GM. Communication, the centrosome and the immunological synapse. *Philos Trans R Soc B Biol Sci* (2014) 369:20130463. doi: 10.1098/rstb.2013.0463

26. Ibañez-Vega J, Del Valle Batalla F, Saez JJ, Soza A, Yuseff M-I. Proteasome Dependent Actin Remodeling Facilitates Antigen Extraction at the Immune Synapse of B Cells. *Front Immunol* (2019) 10: doi: 10.3389/fimmu.2019.00225

27. Ibañez-Vega J, Del Valle F, Sáez JJ, Guzman F, Diaz J, Soza A, Yuseff MI. Ecm29-Dependent Proteasome Localization Regulates Cytoskeleton Remodeling at the Immune Synapse. *Front Cell Dev Biol* (2021) 9: doi: 10.3389/fcell.2021.650817

28. Bouhamdani N, Comeau D, Turcotte S. A Compendium of Information on the Lysosome. *Front Cell Dev Biol* (2021) 9: doi: 10.3389/fcell.2021.798262

29. Ballabio A, Bonifacino JS. Lysosomes as dynamic regulators of cell and organismal homeostasis. *Nat Rev Mol Cell Biol* (2020) 21:101–118. doi: 10.1038/s41580-019-0185-4

30. Hernández-Pérez S, Vainio M, Kuokkanen E, Šuštar V, Petrov P, Forstén S, Paavola V, Rajala J, Awoniyi LO, Sarapulov AV, et al. B cells rapidly target antigen and surface-derived MHCII into peripheral degradative compartments. *J Cell Sci* (2020) 133: doi: 10.1242/JCS.235192

31. Yuseff MI, Reversat A, Lankar D, Diaz J, Fanget I, Pierobon P, Randrian V, Larochette N, Vascotto F, Desdouets C, et al. Polarized Secretion of Lysosomes at the B Cell Synapse Couples Antigen Extraction to Processing and Presentation. *Immunity* (2011) 35:361–374. doi: 10.1016/j.immuni.2011.07.008

32. Sáez JJ, Diaz J, Ibañez J, Bozo JP, Reyes FC, Alamo M, Gobert FX, Obino D, Bono MR, Lennon-Duménil AM, et al. The exocyst controls lysosome secretion and antigen extraction at the immune synapse of B cells. *J Cell Biol* (2019) 218:2247–2264. doi: 10.1083/jcb.201811131

33. Andrews NW. Detection of Lysosomal Exocytosis by Surface Exposure of Lamp1 Luminal Epitopes. *Methods Mol Biol Clifton NJ* (2017) 1594:205–211. doi: 10.1007/978-1-4939-6934-0_13

34. Maeda FY, van Haaren JJ, Langley DB, Christ D, Andrews NW, Song W. Surface-associated antigen induces permeabilization of primary mouse B-cells and lysosome exocytosis facilitating antigen uptake and presentation to T-cells. *eLife* (2021) 10: doi: 10.7554/eLife.66984

35. Ibañez-Vega J, Fuentes D, Lagos J, Cancino J, Yuseff MI. Studying organelle dynamics in B cells during immune synapse formation. *J Vis Exp* (2019) 2019:1–13. doi: 10.3791/59621

36. Spillane KM, Tolar P. DNA-based probes for measuring mechanical forces in cell-cell contacts: Application to B cell antigen extraction from immune synapses. *Methods Mol Biol* (2018) 1707:69–80. doi: 10.1007/978-1-4939-7474-0_5

37. Carrasco YR, Fleire SJ, Cameron T, Dustin ML, Batista FD. LFA-1/ICAM-1 Interaction Lowers the Threshold of B Cell Activation by Facilitating B Cell Adhesion and Synapse Formation. (2004). http://www.immunity.com/cgi/content/full/20/5/589/

38. Baldari CT, Dustin ML. The Immune Synapse Methods and Protocols Methods in Molecular Biology 1584. http://www.springer.com/series/7651

39. Natkanski E, Lee WY, Mistry B, Casal A, Molloy JE, Tolar P. B cells use mechanical energy to discriminate antigen affinities. *Science* (2013) doi: 10.1126/science.1237572

40. Obino D, Fetler L, Soza A, Malbec O, Saez JJ, Labarca M, Oyanadel C, Del Valle Batalla F, Goles N, Chikina A, et al. Galectin-8 Favors the Presentation of Surface-Tethered Antigens by Stabilizing the B Cell Immune Synapse. *Cell Rep* (2018) 25:3110-3122.e6. doi: 10.1016/j.celrep.2018.11.052

41. Trubelja A, Bao G. Molecular mechanisms of mechanosensing and mechanotransduction in living cells. *Extreme Mech Lett* (2018) 20:91–98. doi: 10.1016/j.eml.2018.01.011

42. Luo T, Mohan K, Iglesias PA, Robinson DN. Molecular mechanisms of cellular mechanosensing. *Nat Mater* (2013) 12:1064–1071.

43. Shaheen S, Wan Z, Haneef K, Zeng Y, Jing W, Liu W. *B cell mechanosensing: A mechanistic overview*. Elsevier Inc. (2019). 23–63 p. doi: 10.1016/bs.ai.2019.08.003

44. Jiang G, Monkley SJ, Cai Y, Zhang X, Sheetz MP, Critchley DR. Talin depletion reveals independence of initial cell spreading from integrin activation and traction. *Nat Cell Biol* (2008) 10:1062–1068. doi: 10.1038/ncb1765

45. Guilluy C, Swaminathan V, Garcia-Mata R, O'Brien ET, Superfine R, Burridge K. The Rho GEFs LARG and GEF-H1 regulate the mechanical response to force on integrins. *Nat Cell Biol* (2011) 13:722–728. doi: 10.1038/ncb2254

46. Comrie WA, Burkhardt JK. Action and traction: Cytoskeletal control of receptor triggering at the immunological synapse. *Front Immunol* (2016) 7:1–25. doi: 10.3389/fimmu.2016.00068

47. Brockman JM, Salaita K. Mechanical proofreading: A general mechanism to enhance the fidelity of information transfer between cells. *Front Phys* (2019) 7: doi: 10.3389/fphy.2019.00014

48. Zhu C, Chen W, Lou J, Rittase W, Li K. Mechanosensing through immunoreceptors. *Nat Immunol* (2019) 20:1269–1278. doi: 10.1038/s41590-019-0491-1

49. Pontes B, Monzo P, Gauthier NC. Membrane tension: A challenging but universal physical parameter in cell biology. *Semin Cell Dev Biol* (2017) 71:30–41. doi: 10.1016/j.semcdb.2017.08.030

50. Kim T-H, Ly C, Christodoulides A, Nowell CJ, Gunning PW, Sloan EK, Rowat AC. Stress hormone signaling through β-adrenergic receptors regulates macrophage mechanotype and function. *FASEB J* (2019) 33:3997–4006. doi: 10.1096/fj.201801429rr

51. Bufi N, Saitakis M, Dogniaux S, Buschinger O, Bohineust A, Richert A, Maurin M, Hivroz C, Asnacios A. Human primary immune cells exhibit distinct mechanical properties that are modified by inflammation. *Biophys J* (2015) 108:2181–2190. doi: 10.1016/j.bpj.2015.03.047

52. Judokusumo E, Tabdanov E, Kumari S, Dustin ML, Kam LC. Mechanosensing in T Lymphocyte Activation. *Biophys J* (2012) 102:L5–L7. doi: 10.1016/j.bpj.2011.12.011

53. Jones GW, Hill DG, Jones SA. Understanding immune cells in tertiary lymphoid organ development: It is all starting to come together. *Front Immunol* (2016) 7:1–13. doi: 10.3389/fimmu.2016.00401

54. Pitzalis C, Jones GW, Bombardieri M, Jones SA. Ectopic lymphoid-like structures in infection, cancer and autoimmunity. *Nat Rev Immunol* (2014) doi: 10.1038/nri3700

55. Wan Z, Zhang S, Fan Y, Liu K, Du F, Davey AM, Zhang H, Han W, Xiong C, Liu W. B Cell Activation Is Regulated by the Stiffness Properties of the Substrate Presenting the Antigens. *J Immunol* (2013) 190:4661–4675. doi: 10.4049/jimmunol.1202976

56. Shaheen S, Wan Z, Li Z, Chau A, Li X, Zhang S, Liu Y, Yi J, Zeng Y, Wang J, et al. Substrate stiffness governs the initiation of b cell activation by the concerted signaling of PKCβ and focal adhesion kinase. *eLife* (2017) 6:1–29. doi: 10.7554/eLife.23060

57. Nasrin SR, Afrin T, Kabir AMR, Inoue D, Torisawa T, Oiwa K, Sada K, Kakugo A. Regulation of Biomolecular-Motor-Driven Cargo Transport by Microtubules under Mechanical Stress. *ACS Appl Mater Interfaces* (2020) doi: 10.1021/acsabm.9b01010

58. Bhuwania R, Castro-Castro A, Linder S. Microtubule acetylation regulates dynamics of KIF1C-powered vesicles and contact of microtubule plus ends with podosomes. *Eur J Cell Biol* (2014) 93:424–437. doi: 10.1016/j.ejcb.2014.07.006

59. Wang G, Nola Ss, Bovio S, Coppey-Moisan M, Lafont F, Galli T. Biomechanical Control of Lysosomal Secretion Via the VAMP7 Hub: A Tug-of-War Mechanism Between VARP and LRRK1. *SSRN Electron J* (2018)127–143. doi: 10.2139/ssrn.3155729

60. Obino D, Diaz J, Sáez JJ, Ibañez-Vega J, Sáez PJ, Alamo M, Lankar D, Yuseff M-I. Vamp-7–dependent secretion at the immune synapse regulates antigen extraction and presentation in B-lymphocytes. *Mol Biol Cell* (2017) 28:890–897. doi: 10.1091/mbc.E16-10-0722

61. Liao YC, Fernandopulle MS, Wang G, Choi H, Hao L, Drerup CM, Patel R, Qamar S, Nixon-Abell J, Shen Y, et al. RNA Granules Hitchhike on Lysosomes for Long-Distance Transport, Using Annexin A11 as a Molecular Tether. *Cell* (2019) 179:147-164.e20. doi: 10.1016/j.cell.2019.08.050

62. Serra-Marques A, Martin M, Katrukha EA, Grigoriev I, Peeters CAE, Liu Q, Hooikaas PJ, Yao Y, Solianova V, Smal I, et al. Concerted action of kinesins kif5b and kif13b promotes efficient secretory vesicle transport to microtubule plus ends. *eLife* (2020) 9:1–37. doi: 10.7554/eLife.61302

63. Song Y, Brady S. Posttranslational Modifications of Tubulin: Pathways to Functional Diversity of Microtubules. *Trends Cell Biol* (2014) 25: doi: 10.1016/j.tcb.2014.10.004

64. Bance B, Seetharaman S, Leduc C, Boeda B, Etienne-Manneville S. Microtubule acetylation but not detyrosination promotes focal adhesion dynamics and astrocyte migration. *J Cell Sci* (2019) 132: doi: 10.1242/jcs.225805

65. Li L, Yang X-J. Tubulin acetylation: responsible enzymes, biological functions and human diseases. *Cell Mol Life Sci CMLS* (2015) 72:4237–4255. doi: 10.1007/s00018-015-2000-5

66. Janke C, Magiera MM. The tubulin code and its role in controlling microtubule properties and functions. *Nat Rev Mol Cell Biol* (2020) 21:307–326. doi: 10.1038/s41580-020-0214-3

67. Collins C, Kim SK, Ventrella R, Carruzzo HM, Wortman JC, Han H, Suva EE, Mitchell JW, Yu CC, Mitchell BJ. Tubulin acetylation promotes penetrative capacity of cells undergoing radial intercalation. *Cell Rep* (2021) 36:109556. doi: 10.1016/j.celrep.2021.109556

68. Xu Z, Schaedel L, Portran D, Aguilar A, Gaillard J, Marinkovich MP, Théry M, Nachury MV. Microtubules acquire resistance from mechanical breakage through intralumenal acetylation. *Science* (2017) 356:328–332. doi: 10.1126/science.aai8764

69. Nekooki-Machida Y, Hagiwara H. Role of tubulin acetylation in cellular functions and diseases. *Med Mol Morphol* (2020) 53:191–197. doi: 10.1007/s00795-020-00260-8

70. Xie R, Nguyen S, McKeehan WL, Liu L. Acetylated microtubules are required for fusion of autophagosomes with lysosomes. *BMC Cell Biol* (2010) 11:89. doi: 10.1186/1471-2121-11-89

71. Seetharaman S, Vianay B, Roca V, Farrugia AJ, De Pascalis C, Boëda B, Dingli F, Loew D, Vassilopoulos S, Bershadsky A, et al. Microtubules tune mechanosensitive cell responses. *Nat Mater* (2022) 21:366–377. doi: 10.1038/s41563-021-01108-x

72. Holla P, Saniee A, Lu J, Xie H, Tolar P, Pierce SK, Xu C, Kwak K, Manzella-Lapeira J, Spillane KM, et al. Intrinsic properties of human germinal center B cells set antigen affinity thresholds. *Sci Immunol* (2018) 3:eaau6598. doi: 10.1126/sciimmunol.aau6598

73. Nardone G, Oliver-De La Cruz J, Vrbsky J, Martini C, Pribyl J, Skládal P, Pešl M, Caluori G, Pagliari S, Martino F, et al. YAP regulates cell mechanics by controlling focal adhesion assembly. *Nat Commun* (2017) 8:15321. doi: 10.1038/ncomms15321

74. Carrasco YR. Building the synapse engine to drive B lymphocyte function. *Immunol Lett* (2023) 260:68–72. doi: 10.1016/j.imlet.2023.06.010

75. Roper SI, Wasim L, Malinova D, Way M, Cox S, Tolar P. B cells extract antigens at Arp2/3-generated actin foci interspersed with linear filaments. *eLife* (2019) 8:e48093. doi: 10.7554/eLife.48093

76. Mauri C, Ehrenstein MR. Cells of the synovium in rheumatoid arthritis. B cells. *Arthritis Res Ther* (2007) 9:205. doi: 10.1186/ar2125

77. Adlung L, Kar S, Wagner M, She B, Chakraborty S, Bao J, Lattermann S, Boerries M, Busch H, Wuchter P, et al. Protein abundance of AKT and ERK pathway components governs cell type-specific regulation of proliferation. *Mol Syst Biol* (2017) 13:904. doi: 10.15252/msb.20167258

78. Chaturvedi A, Martz R, Dorward D, Waisberg M, Pierce SK. Endocytosed BCRs sequentially regulate MAPK and Akt signaling pathways from intracellular compartments. *Nat Immunol* (2011) 12:1119–1126. doi: 10.1038/ni.2116

79. Enomoto A, Murakami H, Asai N, Morone N, Watanabe T, Kawai K, Murakumo Y, Usukura J, Kaibuchi K, Takahashi M. Akt/PKB Regulates Actin Organization and Cell Motility via Girdin/APE. *Dev Cell* (2005) 9:389–402. doi: 10.1016/j.devcel.2005.08.001

80. Denisin AK, Pruitt BL. Tuning the Range of Polyacrylamide Gel Stiffness for Mechanobiology Applications. *ACS Appl Mater Interfaces* (2016) 8:21893–21902. doi: 10.1021/acsami.5b09344

81. Núñez-Andrade N, Iborra S, Trullo A, Moreno-Gonzalo O, Calvo E, Catalán E, Menasche G, Sancho D, Vázquez J, Yao TP, et al. HDAC6 regulates the dynamics of lytic granules in cytotoxic T lymphocytes. *J Cell Sci* (2016) 129:1305–1311. doi: 10.1242/JCS.180885/260299/AM/HDAC6-REGULATES-THE-DYNAMICS-OF-LYTIC-GRANULES-IN

82. Nalbant P, Chang Y-C, Birkenfeld J, Chang Z-F, Bokoch GM. Guanine Nucleotide Exchange Factor-H1 Regulates Cell Migration via Localized Activation of RhoA at the Leading Edge. *Mol Biol Cell* (2009) 20:4070–4082. doi: 10.1091/mbc.e09-01-0041

83. Fine N, Dimitriou ID, Rullo J, Sandí MJ, Petri B, Haitsma J, Ibrahim H, La Rose J, Glogauer M, Kubes P, et al. GEF-H1 is necessary for neutrophil shear stress–induced migration during inflammation. *J Cell Biol* (2016) 215:107–119. doi: 10.1083/jcb.201603109

84. Dunn S, Morisson EE, Liverpool TB, Molina-París C, Cross RA, Alonso MC, Peckham M. Differential trafficking of Kif5c on tyrosinated and detyrosinated microtubules in live cells. *J Cell Sci* (2008) 121:1085–1095. doi: 10.1242/jcs.026492

85. Deb Roy A, Gross EG, Pillai GS, Seetharaman S, Etienne-Manneville S, Inoue T. Non-catalytic allostery in α-TAT1 by a phospho-switch drives dynamic microtubule acetylation. *J Cell Biol* (2022) 221: doi: 10.1083/jcb.202202100

86. Even A, Morelli G, Broix L, Scaramuzzino C, Turchetto S, Gladwyn-Ng I, Le Bail R, Shilian M, Freeman S, Magiera MM, et al. ATAT1-enriched vesicles promote microtubule acetylation via axonal transport. *Sci Adv* (2019) 5:eaax2705. doi: 10.1126/sciadv.aax2705

87. Takata T, Matsumura M. "The LINC Complex Assists the Nuclear Import of Mechanosensitive Transcriptional Regulators.," In: Kloc M, Kubiak JZ, editors. *Nuclear, Chromosomal, and Genomic Architecture in Biology and Medicine*. Results and Problems in Cell Differentiation. Cham: Springer International Publishing (2022). p. 315–337 doi: 10.1007/978-3-031-06573-6_11

88. Bouzid T, Kim E, Riehl BD, Esfahani AM, Rosenbohm J, Yang R, Duan B, Lim JY. The LINC complex, mechanotransduction, and mesenchymal stem cell function and fate. *J Biol Eng* (2019) 13:68. doi: 10.1186/s13036-019-0197-9

89. Ulloa R, Corrales O, Cabrera-Reyes F, Jara-Wilde J, Saez JJ, Rivas C, Lagos J, Härtel S, Quiroga C, Yuseff MI, et al. B Cells Adapt Their Nuclear Morphology to Organize the Immune Synapse and Facilitate Antigen Extraction. *Front Immunol* (2022) 12: doi: 10.3389/fimmu.2021.801164

90. Montagnac G, Meas-Yedid V, Irondelle M, Castro-Castro A, Franco M, Shida T, Nachury MV, Benmerah A, Olivo-Marin J-C, Chavrier P. αTAT1 catalyses microtubule acetylation at clathrin-coated pits. *Nature* (2013) 502:567–570. doi: 10.1038/nature12571